

Disorder in Multi-Channel Luttinger Liquids

by

Maximilian Jones



A thesis submitted to
The University of Birmingham
for the degree of
DOCTOR OF PHILOSOPHY

Theoretical Physics Group
School of Physics and Astronomy
The University of Birmingham

September 2017

UNIVERSITY OF
BIRMINGHAM

University of Birmingham Research Archive

e-theses repository

This unpublished thesis/dissertation is copyright of the author and/or third parties. The intellectual property rights of the author or third parties in respect of this work are as defined by The Copyright Designs and Patents Act 1988 or as modified by any successor legislation.

Any use made of information contained in this thesis/dissertation must be in accordance with that legislation and must be properly acknowledged. Further distribution or reproduction in any format is prohibited without the permission of the copyright holder.

Abstract

This thesis examines the effects of disorder upon a bundle of coupled one dimensional (1D) systems. Each 1D system is described as a Luttinger liquid, and the coupling between channels is weak enough such that this description remains valid. The coupling can be of either a density-density or current-current type. We consider continuous disorder in each channel, and derive renormalisation group (RG) equations governing the strength of the disorder. We analyse the effects of disorder in two specific examples: a lattice of identical channels, and two distinct channels. In both cases, close to the simultaneous metal-insulator transition, we arrive at coupled Berezinskii–Kosterlitz–Thouless (BKT) equations. Away from the simultaneous transition we analyse the RG equations numerically. Inter-channel interactions are found to shift the metal-insulator boundary, and destroy the mixed insulator-conductor phase close to the simultaneous transition.

Acknowledgements

I would like to acknowledge the support of my supervisors, Igor Lerner and Igor Yurkevich, as well as Martin Long, Rob Smith and Mike Gunn for many helpful discussions. I am also grateful to my office compeers, Matt Robson, Matt Hunt, Andy Lateif and Jack Gartlan for much the same reason, with a special mention to Matt Hunt for his useful advice.

To Heinz

Contents

1	Introduction	1
1.1	The Reality of One Dimensional Systems	1
1.2	Outline	3
2	Interacting Fermions in One Dimension	5
2.1	Fermi Liquids	6
2.2	The Failure of Fermi Liquid Theory in 1D	8
2.3	The Luttinger Liquid	15
2.3.1	Functional Bosonisation	19
2.3.2	Correlations and Physical Properties	24
2.4	Impurities in One Dimension	31
2.4.1	Single Impurity Problem	33
2.4.2	Many Impurity Problem	38
2.5	Concluding Remarks	46
3	Multi-Channel Luttinger Liquids	51
3.1	What is a Multi-Channel Luttinger Liquid System?	52
3.2	The Luttinger Matrix	53
3.3	Two-Channel Luttinger Liquids	58

3.4	Multi-Channel Disorder	64
3.4.1	Lattice of Identical Channels	68
3.4.2	Two Disordered Channels	72
4	Conclusions	97
	Appendices	101
A	Jacobian	103
B	List of Correlations	107

List of Figures

2.1	Occupancy of the Fermi Liquid	7
2.2	Interacting particles in 2D versus 1D	10
2.3	Fermi surface nesting in 2D versus 1D	12
2.4	Domain Walls in 1D	13
2.5	Particle-hole spectrum in 2D versus 1D	14
2.6	Interaction Processes: g_1, g_2 and g_4	17
2.7	Luttinger Liquid Phase Diagram	28
2.8	Single Impurity RG Flow	36
2.9	Momentum-Shell RG	40
2.10	Kosterlitz-Thouless RG Flow	47
3.1	Modified Luttinger parameters in the presence of inter-channel interactions 1	62
3.2	Modified Luttinger parameters in the presence of inter-channel interactions 2	63
3.3	Full RG disorder stability diagram: identical non-interacting channels	77

3.4	Full RG disorder stability diagram: distinct non-interacting channels	78
3.5	Full RG disorder stability diagram: Unbalanced disorder in identical non-interacting channels	79
3.6	Full RG disorder stability diagram: identical density-density interacting channels	80
3.7	Full RG disorder stability diagram: identical current-current interacting channels	81
3.8	Full RG disorder stability diagram: both types of interaction . .	82
3.9	Full RG disorder stability diagram: competing interactions . . .	83
3.10	Full RG disorder stability diagram: competing interactions . . .	84
3.11	Two-channel disorder RG trajectories: Insulating	92
3.12	Two-channel disorder RG trajectories: naively conducting	93
3.13	Two-channel disorder RG trajectories: destruction of the mixed phase	94

Chapter 1

Introduction

1.1 The Reality of One Dimensional Systems

The title of this thesis is “Disorder in Multi-Channel Luttinger Liquids”; Luttinger liquid theory provides a description unique to one dimensional (1D) physics. One might wonder why it is we are interested in the physics of one spatial dimension when the world is patently (at least) three dimensional. Is one dimension simply a theoretical refuge in the face the overwhelming complexity of many-body systems? In a word – partly.

The mathematical simplifications endemic to one dimension certainly do help in the consideration of strongly correlated systems, as seen in section 2.3, however one dimensional systems are becoming increasingly accessible experimentally.

Perhaps the most famous example of a one dimensional system is the carbon nanotube, specifically the single walled carbon nanotube (SWNT), which has been shown to be experimentally consistent with the one dimensional Luttinger

liquid (LL) [10, 32]. The carbon nanotube is, however, just one type of nano-wire, and by no means the most simple. Carbon nanotubes are comprised of a hexagonal lattice of carbon atoms, just as with a sheet of graphene, which has been wrapped around into a long cylindrical geometry. The hexagonal lattice has two inequivalent sites, and as a consequence behaves like two one dimensional systems[11]. This is where the ‘multi-channel’ part of the title comes to bear. We are interested in what happens when 1D systems are brought into contact with each other, the SWNT being a particularly simple realisation of this.

We are by no means limited to nano-wires; we would be highly remiss not to mention cold atomic systems[9]. Such systems are comprised of neutral atoms, which can be either fermionic or bosonic in nature, in an optical lattice which is highly tunable[23]. Interactions between atoms are controlled via the Feshbach resonance [13, 31]. The highly tunable nature of cold atomic systems enables one to experimentally test even the most esoteric theoretical models, including one dimensional ones.

Another experimental avenue is in the field of organic conductors. Bechgaard salts[35, 33, 34] are a class of organic conductor which have been shown to exhibit 1D behaviour consistent with that of a Luttinger liquid[59]. Such systems are chemically synthesised and are comprised of chains. The electronic hopping between chains is highly anisotropic: $t \sim 3000K$ along the easy axis of the chain, but between chains the coupling is much lower $t \sim 300K$ [21]. Thus provided the temperature is high enough the system will only take advantage of the one dimensional hopping yielding Luttinger liquid behaviour.

One can also touch upon the subject of topological insulators. When two

insulators with topologically distinct Hamiltonians come into contact, a robust conducting edge state necessarily exists on the interface[30]. If these materials are two dimensional, then the edge states must necessarily be one dimensional. These states may manifest themselves as quantum hall states, whereby a magnetic field creates a quantised current around the edge of a material; quantum spin hall states where electrons with different spins have currents going in opposite directions[41]; or something more exotic. An example of an experimentally verified two dimensional topological insulator is found in mercury telluride quantum wells[8].

One dimensional systems are therefore experimentally testable in a wide variety of contexts. The relative simplicity of 1D models, combined with some of the more bizarre phenomena unique to 1D systems gives rise to a wealth of interesting physics. This thesis aims to investigate the situation where many 1D systems are coupled weakly to one another, in the context of disorder.

Disorder is an interesting avenue to explore multi-channel Luttinger liquids (MLL). For a single channel of interacting electrons continuous disorder will lead to localisation of the electronic states resulting in a metal-insulator phase transition. If more channels are introduced the interactions between the channels may stop this localisation from occurring.

1.2 Outline

The thesis will start proper in chapter 2 which will go over some of the peculiarities of 1D fermions, in particular the breakdown of Landau's Fermi liquid theory in section 2.1 and the introduction of the Luttinger liquid in section 2.3.

We will then go over some of the general properties of the Luttinger liquid in section 2.3.2.

The subject of this thesis is the role of disorder in Luttinger liquids. We will cover the effect of a single impurity in section 2.4.1 before moving to continuous disorder proper in section 2.4.2. Chapter 2 is the main background chapter, introducing all the concepts and key results necessary for the main results in chapter 3 where we cover multi-channel Luttinger liquids.

The many possible physical realisations of a multi-channel Luttinger liquid (MLL) are discussed in section 3.1, before constructing the mathematical framework in section 3.2. We put special emphasis on two-channel Luttinger liquids in section 3.3 due to their relative simplicity. Disorder in the context of MLLs is then discussed in section 3.4, where explicit renormalisation group (RG) equations are constructed for a generic MLL. These equations are then analysed in two realisations: a lattice of identical channels; and two distinct channels. These results make up the original contributions to the thesis, and can be found in [36].

Everything is concluded in chapter 4, and future directions of research are discussed. There are two appendices, appendix A contains the calculation of the Jacobian necessary to arrive at the standard Luttinger liquid description, and appendix B contains a list of some of the building block correlation functions of a Luttinger liquid.

Chapter 2

Interacting Fermions in One Dimension

The purpose of this second chapter is twofold; the first task is to set our one dimensional scene by contrasting it to the more conventional three dimensional case described in section 2.1. The second order of business is to introduce the ideas and formalisms pertinent to one dimensional condensed matter physics, specifically the Luttinger liquid and its key properties in section 2.3 with special emphasis on the role of impurities in section 2.4. The role of this chapter is thus to provide all the background necessary for subsequent chapters.

This chapter assumes a working knowledge of quantum field theory, specifically the coherent state path integral. Background regarding quantum field theory can be found in refs. [3, 38, 53, 1].

2.1 Fermi Liquids

The paradigm for studying interacting electrons in two and three dimensions is the well known Fermi liquid theory developed by Landau in the 1950s [46, 47, 48]. If one were to look at the characteristic Coulomb energy versus the typical kinetic energy in a condensed matter system one would see that they were comparable. This implies that any sort of perturbation theory in the interaction would be futile and that the interactions themselves play a key role in determining the properties of electrons in solids. This may, however, be contrasted with the empirical success of non-interacting theories such as the Drude model, which characterises the linear dependence of current on electric field. We are hence in a situation where the back of the envelope calculation is contradicted by the experimental evidence. The beauty of Landau's Fermi liquid theory is its ability to reconcile this apparent contradiction.

In a Fermi liquid the bulk properties are, by and large, described by non-interacting particles, it just so happens these particles are not conventional electrons. Landau introduced the crucial idea of a quasi-particle: rather than being a 'true' particle a quasi-particle is the result of collective behaviour involving many particles. By choosing to describe a system in terms of quasi-particles we can arrive at a much more convenient description of the low energy physics. The Fermi liquid is a quasi-particle description of the Coulomb gas, whereby the quasi-particles are electrons *dressed* by particle-hole excitations arising from the Coulomb interaction.

The effective low energy excitations of the Coulomb gas are still fermions, hence we can expect typical fermionic features such as the ubiquitous Fermi surface. There is a crucial difference here, as shown in fig. 2.1, whereby the

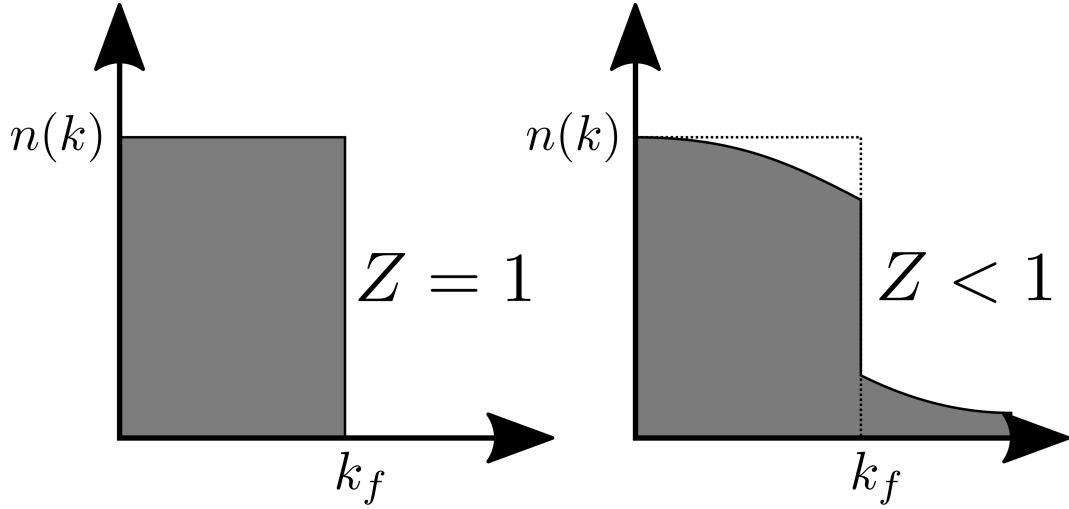


Figure 2.1: Left: Fermi-Dirac distribution at zero temperature showing occupancy against momentum. There is a discontinuity of size $Z = 1$ at the Fermi momentum. Right: Occupancy of a Fermi-Liquid at zero temperature, the discontinuity remains but with a reduced size $Z < 1$. Even in the presence of interaction we still have the concept of a Fermi surface.

zero temperature discontinuity in the single-particle occupation at the Fermi momentum is no longer unity, but of height $Z < 1$. It is also important to remember that the quasi-particles are not eigenstates of the system and hence there is a spectral width to these excitations due to their finite lifetime. As one gets closer and closer to the Fermi surface this lifetime gets longer and longer which causes the excitation to become more sharply defined against the interaction-induced background. Indeed the reduced discontinuity Z at the Fermi surface can be thought of as representing how much of the electron goes into the quasi-particle state versus this incoherent background.

As we are restricted to being close to the Fermi surface one can and should linearise the dispersion of the quasi-particles about the Fermi momentum, as seen in eq. (2.1).

$$E(k) \approx E(k_f) + \frac{k_f}{m^*}(k - k_f) \quad (2.1)$$

Here we use units such that $\hbar = 1$. Note the introduction of the effective mass m^* , for a non-interacting system this would simply be the bare mass of the electron. We can therefore see that the behaviour of the Fermi liquid is not so different from a non-interacting Fermi gas: we still have a Fermi surface, and the dispersion of the quasi-particles is of exactly the same form as that of a non-interacting Fermi gas but with a new effective mass.

At no point does this argument rely on weak interactions, only that we are dealing with physics close to the Fermi level. Hence it is no wonder that non-interacting models can be accurate, the behaviour of their interacting counterparts are practically identical. The take away message here is that although the system is created out of interacting electrons, the most convenient description for the low energy behaviour is through electron like quasi-particles which are essentially non-interacting, and crucially still fermionic. Further details may be found in various standard textbooks [1, 53], although the above precis is sufficient for our purposes.

2.2 The Failure of Fermi Liquid Theory in 1D

As may be garnered from the title of this chapter, one dimensional systems behave in a fashion distinct from that of higher dimensional systems. As such the validity of the Fermi liquid description does not persist into one dimensional physics [28], and a new paradigm is required.

It is not hard to see why the Fermi liquid fails to capture one dimensional behaviour. If one were to imagine a single electron moving in a 3D (or equally 2D) cloud of electrons as in fig. 2.2, one can see that the other electrons are

able to move out of the way, indeed the repulsive Coulomb interaction will push them out of the way. This is the picture of the Fermi liquid; through the interaction between electrons the free fermion behaviour gets ‘dressed’ by collective excitations. The fundamental picture is largely independent of the interaction, we still have fermions running around they simply have slightly different parameters to the bare electrons. Now if one considers the analogous 1D situation, the picture is rather different. Any fermion moving on the 1D line necessarily pushes up against its neighbour, which pushes up against its neighbour and so on. No particle is able to get out of the way of any other particle and any motion would have a striking resemblance to longitudinal density waves, as one would observe oscillating a metal spring backwards and forwards. All motion in 1D is wholly collective, the fermions are so thoroughly dressed by the interaction that they cease to be recognizable as fermions at all. In the Fermi liquid language the step $Z \rightarrow 0$, and the quasi-particles are no longer fermionic.

The inadequacy of Fermi liquid theory in one dimension is rooted in more than just the above ‘hand wavy’ arguments. One dimensional Fermi surfaces are unusual in that they always have the nesting property. Fermi surface nesting occurs when there exists a wave vector \vec{Q} which connects two large pieces of Fermi surface. One of the consequences of nesting is a divergence in the static particle-hole susceptibility, $\chi(\vec{q}, \omega)$. The particle-hole susceptibility is defined as the linear response to an external field, $H_{ext} = \int d\vec{r} V(\vec{r}, t) \bar{\psi}(\vec{r}, t) \psi(\vec{r}, t)$, where V is the external potential[53]. In this case it is given by the retarded Green’s function of the density operator.

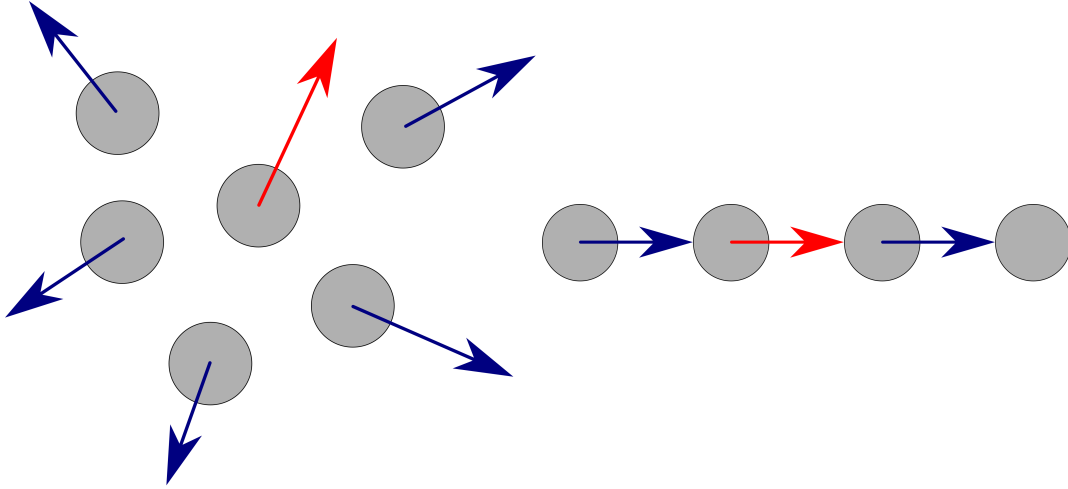


Figure 2.2: Left: A 2D system of interacting fermions (repulsive), if any one particle moves (red arrow) it is able to push past its neighbours. Right: A 1D system of interacting fermions (repulsive), if any one particle moves it has no choice but to push up against its neighbour, it cannot move past it and the resulting motion will be a density wave.

$$\chi_{ph}(\vec{q}, \omega = 0) = \frac{1}{V} \sum_{\vec{k}} \frac{f_F(\epsilon_{\vec{k}}) - f_F(\epsilon_{\vec{k}+\vec{q}})}{\epsilon_{\vec{k}} - \epsilon_{\vec{k}+\vec{q}} + i\delta} \quad (2.2)$$

Here eq. (2.2) gives the particle-hole susceptibility as a function of the momentum difference between the particle and hole, \vec{q} , at zero frequency $\omega = 0$, the $i\delta$ is simply there to ensure convergence and is treated as infinitesimal. The nesting condition is $\epsilon_{\vec{k}+\vec{Q}} = -\epsilon_{\vec{k}}$ for a portion of reciprocal space, this will lead to a logarithmic divergence of the static susceptibility at the nesting wave vector. This can be readily seen by considering an infinite volume system, and only looking at the part of the sum where the nesting condition is satisfied.

$$\text{Re}(\chi(\vec{Q}, \omega = 0)) = - \int d\epsilon N(\epsilon) \frac{\tanh(\frac{\epsilon}{2T})}{2\epsilon} \quad (2.3)$$

Where T is the temperature and $N(\epsilon)$ is the density of states. Close to the

Fermi energy, $\epsilon = 0$, the density of states is constant, leading to logarithmic behaviour[20].

$$\chi(\vec{Q}, \omega = 0) \sim N(\epsilon = 0) \log\left(\frac{E}{T}\right) \quad (2.4)$$

Where E is an ultraviolet cut-off determined by the energy range over which the nesting property is satisfied. A divergence in the linear response means the original description of the system without the external field no longer holds true, and as such implies some sort of ordering at that wave vector. Indeed Fermi surface nesting does explain phenomena such as spin density wave and charge density wave order. One can see that the nesting condition will always be true in one dimension, as can be seen in fig. 2.3.

$$\epsilon(k) \approx \begin{cases} v_f(k - k_f), & k \sim k_f \\ -v_f(k + k_f), & k \sim -k_f \end{cases} \quad (2.5)$$

$$\epsilon(k + 2k_f) = -\epsilon(k) \quad (2.6)$$

One might therefore expect 1D systems to have some sort of charge-density wave order, with $Q = 2k_f$, however it is known that we cannot have long range order in one spatial dimension[49]. In one dimension entropy always trumps energy; it is always favourable to have domain walls as there are more possible configurations and hence more entropy. This is due to the energetic cost of a domain being independent of its size in 1D (see fig. 2.4). The picture to have in mind is a system perpetually on the verge of ordering but never quite managing to make it, and hence 1D systems will behave very much like higher

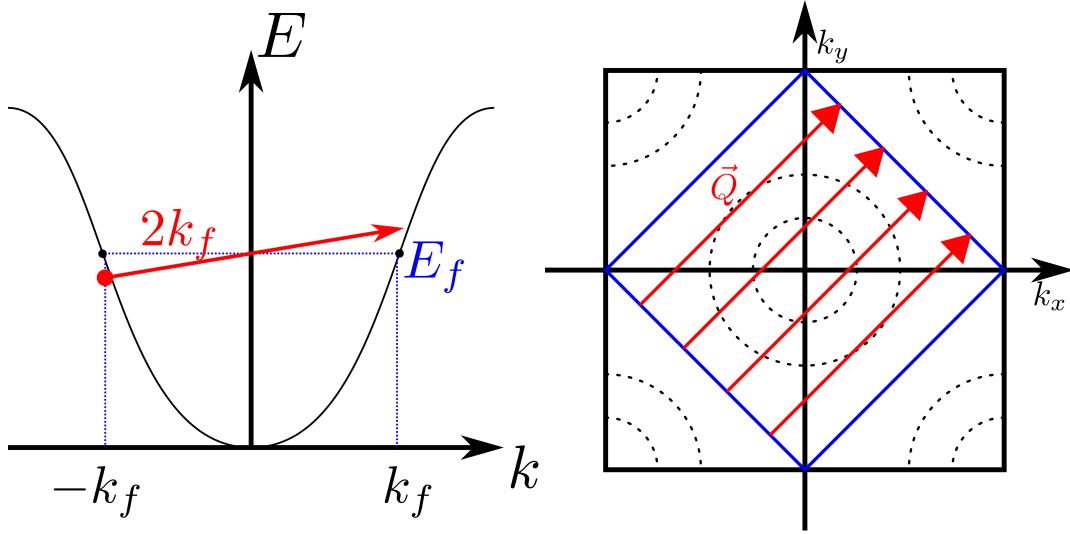


Figure 2.3: Left: Graph of a 1D band structure, the Fermi surface is reduced to just two points and hence the nesting property is always satisfied close to the Fermi surface irrespective of the dispersion. Right: A sketch of the Fermi surface of the 2D square lattice at half filling. Nesting in higher dimensions requires parallel sections of Fermi surface, in this case if the filling were less than half there would be no nesting vector.

dimensional systems close to criticality[20].

In a Fermi liquid the quasi-particles are fermions dressed by particle-hole excitations arising from the interactions, which ultimately behave in a fermionic fashion. In one dimension the quasi-particles lose their fermionic characteristics, and all that is left is the particle-hole ‘dressing’. In order to flesh out this description it is instructive to consider the distinction between the particle-hole spectra in 1D and higher dimensions, as sketched in fig. 2.5.

A particle-hole excitation is created by destroying a particle below the Fermi surface with momentum \vec{k} , leaving a hole, and creating a particle above the Fermi surface with momentum $\vec{k} + \vec{q}$. In general the energy of the pair would be dependent on both \vec{k} and \vec{q} , and indeed by fiddling with the angle between the two momenta it is possible to achieve the same energy for a wide

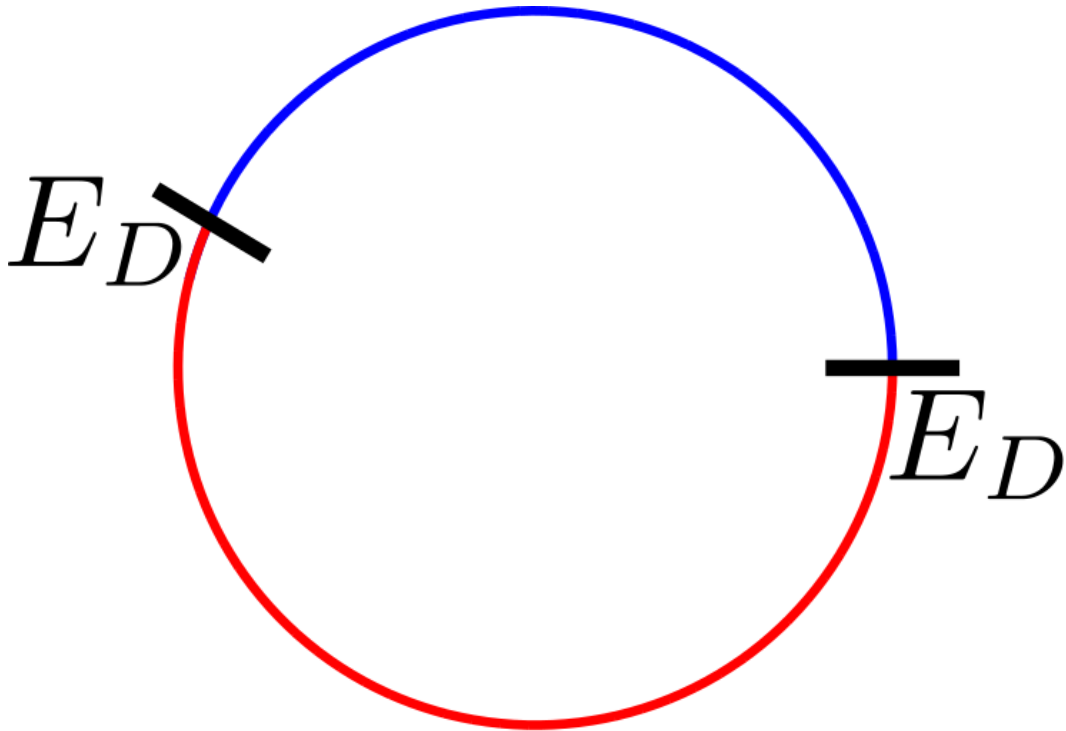


Figure 2.4: Above we have a 1D periodic system of length L with two domains. In 1D the energy cost of have a domain wall is independent of the size of the domain, denoted here as E_D . The configurational entropy gained from having two domains is $S = k_B \log(N(N - 1))$ when N is the number of sites. At a finite temperature a system seeks to minimise its free energy $F = E - TS$, and so for a large system we have the finite a energy penalty competing with the logarithmically diverging entropy gained by having a domain wall. Hence the entropy will always win at finite temperature and there can be no long range order in 1D. In higher dimensions the energetic cost of a domain will depend upon the size of the domain.

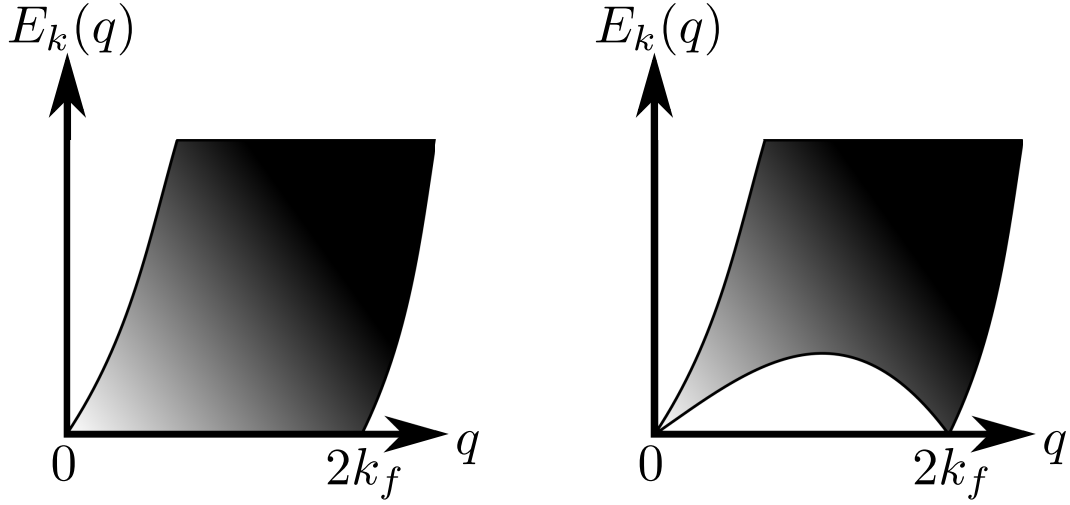


Figure 2.5: Left: Particle-hole spectrum in higher dimensions, even at low energies particle-hole pairs do not have a well defined momentum. Right: Particle-hole spectrum in 1D, particle-hole excitations close to the Fermi surface can only have two possible momenta and hence are well defined quasi-particles.

range of possible momenta. In one dimension there are no angles, and hence the degeneracy of possible momentum differences is greatly reduced.

Provided we are close to the Fermi level, i.e. $q \ll k_f$, the single particle energy spectrum may be safely expanded as a power series.

$$\epsilon(k) = v_f(k - k_f) + \frac{\lambda}{2}(k - k_f)^2 \quad (2.7)$$

$$E_{p-h}(q, k) = \epsilon(k + q) - \epsilon(k) \quad (2.8)$$

$$\frac{1}{q} \int_{k_f - q}^{k_f} dk E_{p-h}(q, k) = v_f q \quad (2.9)$$

Here eq. (2.7) gives the power series expansion, eq. (2.8) the particle-hole energy and eq. (2.9) the average energy of a particle-hole excitation. The remarkable thing about eq. (2.9) is that it only depends upon the momentum difference between the particle and the hole, which would not be true in higher

dimensions. In fact the width of possible energies shrinks faster than the average energy of such an excitation, leading to the situation where a particle-hole excitation behaves like a well defined quasi-particle. Such a quasi-particle would be bosonic as it is made up of two fermions, hence the well defined quasi particles of a Fermi system are in fact bosons.

In summary one dimensional behaviour is markedly different from that of the higher dimensional Fermi liquid theory. The guaranteed presence of nesting combined with the inability of 1D systems to support long range order on entropic grounds means 1D fermionic systems behave as if always on the verge of a phase transition. The notion of a fermionic quasi-particle is also thrown out of the window due to the necessity of collective motion. There is however a glimmer of light, particle-hole excitations which merely modify the original fermions in a Fermi liquid are themselves well defined quasi-particles. Note this point did not rely upon the presence of an interaction between particles, in 1D the low energy behaviour of fermions can, in general, be perfectly well described purely in terms of bosonic particle-hole excitations. This detail will be laboured more heavily in section 2.3 where the replacement of Fermi liquid theory for one dimension will manifest itself.

2.3 The Luttinger Liquid

There exists an exactly soluble model of interacting fermions in one dimension, this model is the ‘Tomonaga-Luttinger model’ or simply the ‘Luttinger model’. The history of this model is somewhat involved: Tomonaga first showed how to map interacting 1D fermions onto 1D bosons[61] in 1950, this was then

rediscovered in 1963 by Luttinger[52], with certain technical points corrected by Mattis and Lieb[54].

If we consider the standard description of one dimensional free fermions we arrive at the Lagrangian density as in eq. (2.10). Here ψ are anti-commuting Grassmann fields which denote the fermions. As we are interested in the low energy physics only, one seeks to linearise around the Fermi surface, or rather the Fermi points as we are in 1D. As such we introduce two new slowly varying fermionic fields as in eq. (2.11).

$$\mathcal{L}_0 = \bar{\psi} \left(i\partial_t + \frac{\partial_x^2}{2m} + \varepsilon_f \right) \psi \quad (2.10)$$

$$\psi(\xi) = \psi_R(\xi)e^{ik_f x} + \psi_L(\xi)e^{-ik_f x} \quad (2.11)$$

Here we are using the shorthand $\xi = (x, t)$. We now have separate fields for the fermions moving to the left, with $k \sim -k_f$, and those moving to the right, with $k \sim k_f$, which will be henceforth referred to as left and right movers. Inserting this transformation into eq. (2.10) and removing all the fast oscillating terms leads to the Tomonaga-Luttinger model, whose Lagrangian density is given in eq. (2.15). It describes two species of fermion each with a strictly linear dispersion, whose fields are denoted by ψ_R, ψ_L .

$$\mathcal{L}_0 = \bar{\psi}_R (i\partial_t + iv_f \partial_x) \psi_R + \bar{\psi}_L (i\partial_t - iv_f \partial_x) \psi_L \quad (2.12)$$

$$= \sum_{\eta} \bar{\psi}_{\eta} i \partial_{\eta} \psi_{\eta} \quad (2.13)$$

Here we used the shorthand $\eta = \{R, L\} = \{+1, -1\}$, $\partial_{\eta} = \partial_t + \eta v_f \partial_x$ and denote the chiral densities as $\rho_{\eta} = \bar{\psi}_{\eta} \psi_{\eta}$. In order to keep things simple

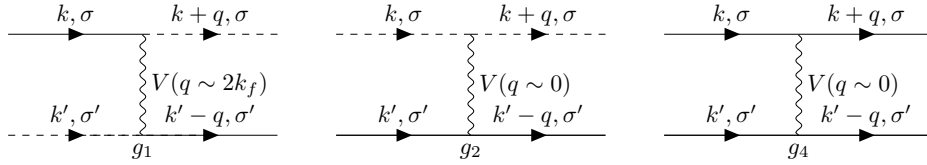


Figure 2.6: Diagrammatic representation of the g_1, g_2 and g_4 processes from left to right. The solid lines represent fermions of one specific chirality, e.g. left or right movers, the dashed lines represent fermions of the opposite chirality, and the wavy line is the interaction. Both the g_2 and g_4 processes involve interactions which carry next to no momentum, whereas the g_1 process carries a momentum close to $2k_f$ as it is a backscattering process.

we will consider the interactions in the so called ‘g-ology’ formalism where we break the interaction down into four different types of contact interaction. The different interactions are back scattering, two types of forward scattering and Umklapp scattering, as seen in fig. 2.6.

$$\mathcal{L}_{int} = \frac{1}{2} (\rho_R^2 + \rho_L^2) g_4 + \rho_R \rho_L g_2 \quad (2.14)$$

$$\mathcal{L}_{LM} = \mathcal{L}_0 + \mathcal{L}_{int} \quad (2.15)$$

Here we will ignore backscattering processes, $g_1 = 0$, as they lead to complications, however their effect is completely superseded by the introduction of impurities considered later in sections 2.4 and 2.4.2. Umklapp processes correspond to scattering events whereby a particle is scattered into a different Brillouin zone, and hence only appear in systems where there is a lattice. On a lattice the momentum conservation law is now $k_1 + k_2 - k_3 - k_4 = Q$ where Q is a reciprocal lattice vector and in 1D an integer multiple of 2π (after scaling out the lattice constant). In 1D the Fermi surface is just two points and scat-

tering events close to the Fermi surface with a finite Q would have to satisfy $4k_f = 2n\pi$, where n is an integer. Umklapp processes are therefore discarded as they are only relevant for specific lattice fillings[20], $k_f = \frac{\pi}{2}$ corresponding to half filling. Forward scattering processes are fair game, and we will happily deal with their consequences.

Although this model is somewhat specific, one can draw conclusions which reach far beyond the model's limits. The term Luttinger liquid (also Tomonaga-Luttinger liquid) was first coined by Haldane[27, 28, 29] to be evocative of the Fermi liquid. By utilising the methodology of the solution of the Tomonaga-Luttinger model one can arrive at a generic description of the low energy behaviour of one dimensional systems in general. Hence just as Fermi liquid theory describes a broad class of three dimensional systems, the Luttinger liquid is the paradigm in one dimension.

The nub of why the Luttinger liquid is such a pervasive concept is bosonisation. A one dimensional Fock space, that is to say the space of states spanned by the operators c_k , has the special property that it can be decomposed into the direct sum of Hilbert spaces with different fixed particle number. These Hilbert spaces are described entirely in terms of particle-hole excitations, which are necessarily bosonic[63]. It is important to stress that this is an extremely general property, and utterly independent of Hamiltonian, or even whether the original Fock space is fermionic or bosonic. Interactions between particles are typically of a particle-hole nature, and hence the bosonised description is a natural one allowing analytic progress to be forthcoming.

2.3.1 Functional Bosonisation

This section gets into the detail of how one bosonises in the formalism pertinent to the main calculations in this thesis: functional bosonisation. The end product of this will be the standard Lagrangian for the Luttinger liquid. One stresses that this is not the only route available, rather than proceed in the language of path integrals one can develop a series of rigorous operator identities. Operator bosonisation has many advantages over its functional counter-part, although brevity is not among them, however all subsequent calculations are done in the functional language so as to avoid methodological discontinuities. The following derivations are modified from refs. [66, 51, 24, 18, 17], a similar derivation is also available which utilizes the Keldysh technique[42, 38] for non-equilibrium field theory in ref.[26].

If we consider the expectation value of a generic observable O with respect to the Luttinger model, as defined in eq. (2.15) we must consider the following functional integral.

$$\langle O \rangle = \frac{1}{Z} \int \mathcal{D} [\bar{\psi}, \psi] O e^{i \int dx dt \mathcal{L}_{LM}} \quad (2.16)$$

$$Z = \int \mathcal{D} [\bar{\psi}, \psi] e^{i \int dx dt \mathcal{L}_{LM}} \quad (2.17)$$

As the model contains quartic terms we cannot evaluate the integrals non-perturbatively as things stand. The idea then, is to introduce auxiliary bosonic fields in which the model becomes quadratic and thus integrable. The first step is to introduce a bosonic gauge field θ_η for each fermionic species.

$$\psi_\eta(\xi) \rightarrow F_\eta(\xi) e^{i\theta_\eta(\xi)} \quad (2.18)$$

This transformation ostensibly leaves the interaction term alone, as beforehand it was quartic in the grassman fields ψ and afterwards it is still quartic in the grassman fields F . It does however modify the quadratic part and as with any change of variables there is an associated Jacobian.

$$\langle O \rangle = \frac{1}{Z} \int \mathcal{D} [\bar{F}, F] J [\theta] O e^{i \int dx dt \sum_{\eta} \bar{F}_{\eta} (i\partial_{\eta} - \partial_{\eta} \theta_{\eta}) F_{\eta} + S_{int}} \quad (2.19)$$

$$= \frac{1}{Z} \int \mathcal{D} [\bar{F}, F, \theta] J [\theta] e^{iS[\bar{F}, F, \theta]} \quad (2.20)$$

In the second line we utilised that the observable cannot depend upon a choice of gauge allowing us to integrate over the bosonic fields[43]. The details of calculating the Jacobian are left to appendix A.

$$\log(J_0) = -\frac{i}{2} \sum_{\eta} \int d\xi \partial_{\eta} \theta_{\eta} \frac{\eta}{2\pi} \partial_x \theta_{\eta} \quad (2.21)$$

$$\bar{\psi}_{\eta} \psi_{\eta} \rightarrow \bar{F}_{\eta} F_{\eta} + \frac{\eta}{2\pi} \partial_x \theta_{\eta} \quad (2.22)$$

Where J_0 is the part of the Jacobian coming from the quadratic part, and eq. (2.22) shows how the chiral densities, and thus the interaction term, transform. Now that we are equipped with how the action behaves under eq. (2.18), we are free to choose a particularly convenient representation, where the remaining fermionic fields $F_{\eta}(\xi)$ are utterly featureless and all the interesting phenomena are in the bosonic gauge fields.

$$F_{\eta}(\xi) \rightarrow F \quad (2.23)$$

This has the effect of completely removing any reference to the fermionic fields

in the action, and hence we arrive at a purely bosonic description. To relate this to the operator bosonisation formalism, we can identify our vestigial fermionic field F as a Klein factor. Earlier we mentioned that a one dimensional Fock space could be decomposed into the sum of fixed particle number subspaces which are described in terms of particle-hole excitations, the role of a Klein factor is to jump between such fixed number subspaces. We thus arrive at a fully bosonic description of our fermionic system, and what is more is the bosonic representation is fully quadratic.

$$S = -\frac{1}{2} \int d\xi \sum_{\eta} \partial_{\eta} \theta_{\eta} \frac{\eta}{2\pi} \partial_x \theta_{\eta} - \frac{1}{2} \int d\xi \left(\frac{g_4 + g_2}{2\pi^2} \right) (\partial_x \theta_R + \partial_x \theta_L)^2 + \left(\frac{g_4 - g_2}{2\pi^2} \right) (\partial_x \theta_R - \partial_x \theta_L)^2 \quad (2.24)$$

$$= \int d\xi \frac{1}{2\pi} \begin{pmatrix} \theta & \phi \end{pmatrix} \left\{ \begin{pmatrix} 0 & 1 \\ 1 & 0 \end{pmatrix} \partial_t + \begin{pmatrix} v_f + \frac{g_4 + g_2}{\pi} & 0 \\ 0 & v_f + \frac{g_4 - g_2}{\pi} \end{pmatrix} \partial_x \right\} \partial_x \begin{pmatrix} \theta \\ \phi \end{pmatrix} \quad (2.25)$$

$$= \int d\xi \frac{1}{2\pi} \begin{pmatrix} \theta & \phi \end{pmatrix} \left\{ \begin{pmatrix} 0 & 1 \\ 1 & 0 \end{pmatrix} \partial_t + \begin{pmatrix} \frac{v}{K} & 0 \\ 0 & vK \end{pmatrix} \partial_x \right\} \partial_x \begin{pmatrix} \theta \\ \phi \end{pmatrix} \quad (2.26)$$

$$\theta = \frac{1}{2}(\theta_R - \theta_L) \quad \phi = \frac{1}{2}(\theta_R + \theta_L) \quad (2.27)$$

Here we introduced the fields θ, ϕ related to the original chiral fields via eq. (2.27). These fields have a particularly convenient physical interpretation. The gradient of the θ field gives the density fluctuations in the liquid,

and the gradient of the ϕ field the current in the liquid. This can be seen by considering how the chiral densities transform in eq. (2.22), for instance $\rho_R - \rho_L \rightarrow \frac{1}{2\pi} (\partial_x \theta_R + \partial_x \theta_L) = \frac{1}{\pi} \partial_x \phi$ which is clearly related to the current.

We also introduced two new parameters, the new excitation velocity v and the Luttinger parameter K . The Luttinger parameter is what effectively controls the role of the interactions.

$$v = v_f \sqrt{\left(1 + \frac{g_4 + g_2}{\pi v_f}\right) \left(1 + \frac{g_4 - g_2}{\pi v_f}\right)} \quad (2.28)$$

$$K = \sqrt{\frac{1 + \frac{g_4 - g_2}{\pi v_f}}{1 + \frac{g_4 + g_2}{\pi v_f}}} \quad (2.29)$$

We can see from eq. (2.29) that for repulsive interactions, $g_4 > 0, g_2 > 0$, then $K < 1$. Whereas attractive interactions, $g_4 < 0, g_2 < 0$, lead to $K > 1$, with $K = 1$ as the non-interacting value.

Typically we only deal with observables which are exclusively in terms of the density field or the current field, as such it is prudent to integrate out the redundant degree of freedom. As the action is quadratic in both fields, this process is simply completing the square and shifting the fields to separate the two degrees of freedom. This will give us an action in terms of a single bosonic field, which is purely quadratic.

$$S[\theta] = \int d\xi \frac{1}{2\pi v K} [(\partial_t \theta)^2 - v^2 (\partial_x \theta)^2] \quad (2.30)$$

$$S[\phi] = \int d\xi \frac{K}{2\pi v} [(\partial_t \phi)^2 - v^2 (\partial_x \phi)^2] \quad (2.31)$$

Note that there is a duality between the density and current representations, if we have worked out one correlation, for instance the density-density corre-

lations, then the corresponding correlation in the other field would be given for free, in this case the current-current correlation. We simply have to take $K \rightarrow \frac{1}{K}$ as we switch the fields.

There is one last trick to perform which although not strictly necessary makes subsequent calculations much easier, particularly those involving finite temperature. By transforming from real time to imaginary time via the Wick rotation, $t \rightarrow -i\tau$, where the imaginary time is now on a finite domain $\tau \in [0, \beta]$ where $\beta = \frac{1}{k_B T}$ is the inverse temperature.

$$S[\theta] = \int dx d\tau \frac{1}{2\pi v K} [(\partial_\tau \theta)^2 + v^2 (\partial_x \theta)^2] \quad (2.32)$$

$$S[\phi] = \int dx d\tau \frac{K}{2\pi v} [(\partial_\tau \phi)^2 + v^2 (\partial_x \phi)^2] \quad (2.33)$$

We have now arrived at the standard form of the fully bosonised Luttinger liquid, as seen in eqs. (2.32) and (2.33). One can see straight away that the Green's function is that of the wave equation, and hence the earlier phenomenological picture of low-energy excitations of one dimensional systems behaving like phonons is an accurate one. Indeed it is possible to think of 1D electron-phonon systems as being a coupled system of two Luttinger liquids, more will be said about this point in chapter 3.

This form of the action will be the foundation of all subsequent calculations, we have reduced a system of interacting fermions to a fully quadratic theory of non-interacting bosons whose properties can be derived rather straightforwardly, this will be the subject of section 2.3.2. Another point to mention is that although everything has thus far been couched in the language of inter-

acting fermions, one can bosonise bosons in a rather similar fashion. Hence the Luttinger liquid action as in eq. (2.32) can describe a wide range of systems, including both fermions and boson as well as phonons.

2.3.2 Correlations and Physical Properties

Now that we are armed with the Luttinger liquid action, eq. (2.26) we are perfectly able to investigate the properties of the Luttinger liquid state, and examine the role of interactions. This will involve the calculation of various correlation functions, the basic building blocks of which are given in appendix B.

The first interesting quantity to look at would be the occupation factor of a Luttinger liquid. We already know that there should be no discontinuity in the single-particle occupation at the Fermi level, as seen by the failure of Fermi liquid theory described in section 2.2, so this makes a good sanity-check calculation. The single-particle occupation is simply given by the Fourier transform (at the Fermi momentum) of the expectation value of finding a particle at a given position.

$$n_\eta(k) = \int dx e^{-i(k_f - k)x} G_\eta(x, \tau = 0^-) \quad (2.34)$$

Where G_η is the single particle Green's function for the η fermion species. This

Green's function can be readily found in terms of the bosonic fields.

$$G_\eta(x, \tau) = - \langle \psi_\eta(x, \tau) \bar{\psi}_\eta(0, 0) \rangle \quad (2.35)$$

$$= \langle \bar{F} F \rangle \langle e^{i(\theta(x, \tau) + \phi(x, \tau) - \theta(0, 0) - \phi(0, 0))} \rangle \quad (2.36)$$

$$= \rho_0 e^{-\frac{1}{2} \langle (\theta(x, \tau) - \theta(0, 0))^2 \rangle} e^{-\frac{1}{2} \langle (\phi(x, \tau) - \phi(0, 0))^2 \rangle} e^{2 \langle \theta(x, \tau) \phi(0, 0) \rangle} \quad (2.37)$$

$$= \rho_0 \frac{\alpha}{\alpha \operatorname{sgn}(\tau) + v\tau + ix} \left(\frac{\alpha}{\sqrt{x^2 + (\alpha \operatorname{sgn}(\tau) + v\tau)^2}} \right)^{\frac{K+K^{-1}}{2} - 1} \quad (2.38)$$

The expressions for the bosonic averages can be found in appendix B. Here we used that the average of the Klein factors just gives the homogeneous part of the fermion density, ρ_0 . Setting the imaginary time to zero from below we can calculate the occupancy factor.

$$n_R(k) = \int dx e^{-i(k-k_f)x} \rho_0 \left(\frac{\alpha}{\sqrt{x^2 + \alpha^2}} \right)^{\frac{K+K^{-1}}{2}} e^{-i \arg(\alpha - ix)} \quad (2.39)$$

$$\sim |k - k_f|^{\frac{K+K^{-1}}{2} - 1} \quad (2.40)$$

At the Fermi momenta the occupancy is perfectly continuous, and hence the Fermi liquid $Z = 0$ as expected. Here α is an ultraviolet cut off, this arises due to our use of point-like interactions, if we were to model the interaction as decaying quickly over some length-scale then the role of α would be taken by that length.

Another interesting quantity to consider is the correlations between the density at two points. The density in terms of the original fermions is given

in eq. (2.42), note that it contains terms with $k \sim 0$ as well as $k \sim 2k_f$.

$$\rho(x, \tau) = \bar{\psi}\psi \quad (2.41)$$

$$= \bar{\psi}_R\psi_R + \bar{\psi}_L\psi_L + e^{2ik_fx}\bar{\psi}_L\psi_R + e^{-2ik_fx}\bar{\psi}_R\psi_L \quad (2.42)$$

$$= +\rho_0 + \frac{1}{\pi}\partial_x\theta + 2\rho_0\cos(2\theta + 2k_fx) \quad (2.43)$$

Using the bosonisation procedure outlined above we arrive at eq. (2.43). The correlation between the density fluctuations can then be readily worked out.

$$\begin{aligned} \langle \delta\rho(x, \tau)\delta\rho(0, 0) \rangle &= \frac{1}{\pi^2} \langle \partial_x\theta(x, \tau)\partial_x\theta(0, 0) \rangle \\ &+ 2\rho_0^2 \cos(2k_fx) e^{-2\langle (\theta(x, \tau) - \theta(0, 0))^2 \rangle} \end{aligned} \quad (2.44)$$

$$\begin{aligned} &\stackrel{T \rightarrow 0}{=} \frac{K}{2\pi^2} \frac{(v\tau + \alpha \operatorname{sgn}(\tau))^2 - x^2}{((v\tau + \alpha \operatorname{sgn}(\tau))^2 + x^2)^2} \\ &+ 2\rho_0^2 \cos(2k_fx) \left(\frac{\alpha}{\sqrt{(v\tau + \alpha \operatorname{sgn}(\tau))^2 + x^2}} \right)^{2K} \end{aligned} \quad (2.45)$$

What is interesting here is that the $k \sim 0$ part of the correlation is relatively boring, it decays as $\sim \frac{1}{r^2}$ just as a Fermi liquid would where the only role of the interaction is to renormalise the amplitude. The $k \sim 2k_f$ part is more unusual, the correlations decay as $\sim \frac{1}{r^{2K}}$ which for repulsive fermionic systems ($K < 1$) decays slower than the $k \sim 0$ part. These correlations tell us that for a repulsive interaction the system is being pushed towards some sort of charge density wave (CDW) ordering. This is an example of the non-universal behaviour exhibited by the Luttinger liquid state, where the exponents are fiercely dependent on the microscopic detail of the theory, in this case the interaction strength. It is worth stating that the inclusion of backscattering ($g_1 \neq 0$) would only enhance these correlations, as backscattering events are

at the nesting wave vector of $2k_f$.

After having looked at the density-density correlations, which are essentially correlations between particle-hole pairs it makes sense to contrast with correlations between pairs of particles. Highly correlated particle pairs would imply something akin to a superconducting state. It can be shown that the dominant contribution to pairing correlations is given by average of creation of both a left and a right mover [20].

$$\bar{\psi}_R \bar{\psi}_L \sim e^{-2i\phi} \quad (2.46)$$

$$\langle \bar{\psi}_R(x, \tau) \bar{\psi}_L(x, \tau) \bar{\psi}_R(0) \bar{\psi}_L(0) \rangle = \rho_0^2 \langle e^{-2i\phi(x, \tau) - 2i\phi(0, 0)} \rangle \quad (2.47)$$

$$= \rho_0^2 e^{-2\langle (\phi(x, \tau) - \phi(0, 0))^2 \rangle} \quad (2.48)$$

$$\stackrel{T \rightarrow 0}{=} \rho_0^2 \left(\frac{\alpha}{\sqrt{(v\tau + \alpha \operatorname{sgn}(\tau))^2 + x^2}} \right)^{\frac{2}{K}} \quad (2.49)$$

Here we have very similar behaviour to the density-density correlation, with a non-universal power law decay, the difference is that the role of the interaction is inverted so for repulsive fermions the superconducting correlations are suppressed more quickly whereas an attractive interaction promotes pairing correlations. This fits well with our earlier qualitative picture of one dimensional Fermi systems, which due to the necessary fulfilment of the nesting condition are on the verge of ordering. The particle-hole susceptibility is in competition with the pairing susceptibility, the role of the interaction is to enhance one set of correlations at the expense of the other. This allows one to draw a ‘phase’ diagram of the Luttinger liquid, as seen in fig. 2.7.

Thus far we have only considered spinless fermions, however adding spin into the formalism is largely problem free. Rather than simply having right

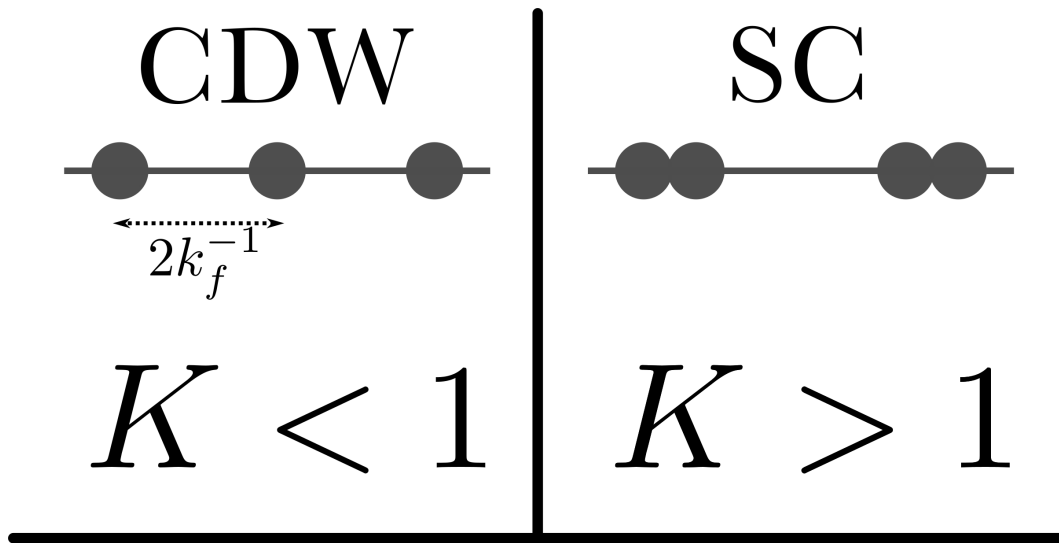


Figure 2.7: The ‘phase’ diagram for a Luttinger liquid derived from a single fermionic species. For attractive interaction ($K > 1$) charge density wave (CDW) wave order is suppressed in favour of slowly decaying superconducting (SC) correlations. For repulsive interactions ($K < 1$) the converse is true and SC correlations are suppressed in favour of CDW correlations. One stresses that these are not long-range order phases as such ordering is prohibited in 1D, the diagram simply shows the power-law correlations which decay slowest for a given interaction.

and left movers we have an additional spin index, hence the bosonic fields will also have an additional index.

$$\psi_{\eta,s} = F_{\eta,s} e^{i\theta_{\eta,s}} \quad (2.50)$$

When switching to the non-chiral representation as in eq. (2.27) the spin index is preserved. As we have fields which are associated with the current and density of a particular spin species, θ_s, ϕ_s , we are free to create new fields associated with the charge and spin degrees of freedom.

$$\theta_\sigma = \theta_\uparrow - \theta_\downarrow \quad (2.51)$$

$$\theta_\rho = \theta_\uparrow + \theta_\downarrow \quad (2.52)$$

Here σ denotes the spin sector and ρ the charge sector. Naturally the ϕ fields can be transformed in the same way. The utility of such a choice of fields is that the action splits cleanly into a charge part and a spin part.

$$S[\theta_s, \phi_s] = S[\theta_\sigma, \phi_\sigma] + S[\theta_\rho, \phi_\rho] \quad (2.53)$$

Where the actions of the spin and charge fields are of the standard Luttinger liquid form (up to a complication which we will come to later), each with their own Luttinger parameters, K_σ, K_ρ and velocities v_σ, v_ρ which are not in general equal. This is somewhat remarkable, the spin and charge degrees of freedom have completely separated, allowing for excitations which carry purely spin or charge which do not even have to travel at the same speed. This is known as spin-charge separation and is one of the wackier phenomena exhibited by 1D

systems.

The wrinkle with spin alluded to previously is that one cannot ignore spin-flip interactions[20]. Although this does not inhibit the bosonisation procedure it does lead to a non-quadratic term.

$$S_1 = 2g_{1\perp} \int dx d\tau \cos(2\sqrt{2}\theta_\sigma) \quad (2.54)$$

This non-linear term is the famous ‘sine-Gordon’ term and can be analysed in a couple of ways. Firstly for weak coupling we can employ renormalisation group methods, this we will not deal with here as very similar calculations are done in sections 2.4.1 and 2.4.2 which are more relevant to the main body of this thesis. It is sufficient to know that for weak coupling the spin Luttinger parameter, K_σ is renormalised due to the spin-flip term. Provided that the spin sector is attractive, $K_\sigma > 1$, weak spin-flip interactions are irrelevant. However if the spin sector is repulsive the coupling grows and we need to consider the opposite limit of large coupling.

For $g_{1\perp} \gg 1$ we can employ classical thinking and assume the cosine would have to be locked into one of its minima, as any large deviation from such a minima would lead to large energetic penalties. One may then expand about one such minima and the resulting action would be much the same as that of a standard Luttinger liquid with the exception that the spin sector has acquired a mass term.

A massive spin sector means spin excitations are gapped, one can see from this that the dominant low energy correlations cannot carry spin. Hence the massive phase diagram would look very similar to the spinless one in fig. 2.7

except where the pairing is of the singlet type, whereas before it was pairing between two identical particles. In the massless phase, $K_\sigma \geq 1$, we would expect dominant spin density wave correlations for a repulsive charge sector and triplet pairing for $K_\rho \geq 1$.

This section has covered some of the physical properties of the Luttinger liquid state, especially when looking at it as arising from interacting fermions. The message to take away here is that attractive interactions lead to a Luttinger liquid that is *like* a superconducting state, and repulsive interactions lead to something *like* a charge/spin density wave.

2.4 Impurities in One Dimension

Thus far we have assumed perfectly clean systems when constructing our Luttinger liquid state, however such cleanliness is experimentally unrealistic. In order to fully assess the stability and physicality of the Luttinger liquid an understanding of the effects of impurities is required. The single impurity problem, first solved by Kane and Fisher[39], is discussed in section 2.4.1, and the problem of many impurities, as dealt with by Giamarchi and Schulz[22], is the subject of section 2.4.2.

In the absence of interactions between particles disorder induced localization is known as Anderson localization[60, 55]. The physical interpretation of this phenomenon is that repeated scattering events between impurities leads to a single particle undergoing self-interference. This is therefore a single particle problem. The work of Giamarchi and Schulz deals with how interactions change this picture for 1D systems.

For a spinless Luttinger liquid there are two types of terms generated by impurities, those which instigate forward scattering and those which bring about backward scattering. The contributions to the Lagrangian are given in eq. (2.56).

$$\mathcal{L}_{imp} = -\eta(x) [\bar{\psi}_R \psi_R + \bar{\psi}_L \psi_L] - \zeta(x) \bar{\psi}_L \psi_R - \bar{\zeta}(x) \bar{\psi}_R \psi_L \quad (2.55)$$

$$= -\eta(x) \frac{1}{\pi} \partial_x \theta - \zeta(x) \rho_0 e^{2i\theta(x,\tau)} - \bar{\zeta}(x) \rho_0 e^{-2i\theta(x,\tau)} \quad (2.56)$$

Here $\eta(x)$ is the forward scattering potential, and $\zeta(x)$ is the complex backward scattering potential. As forward scattering just adds a linear term in the θ field we can simply shift our bosonic field to compensate for it.

$$\theta \rightarrow \theta + \frac{K}{v} \int_{x_0}^x dy \eta(y) \quad (2.57)$$

Here x_0 is an arbitrary point. Although eq. (2.57) does remove the linear term in η it does have an effect upon the backscattering potential.

$$\zeta(x) e^{2i\theta(x,\tau)} \rightarrow \zeta(x) e^{\frac{i2K}{v} \int_{x_0}^x dy \eta(y)} e^{2i\theta(x,\tau)} \quad (2.58)$$

This simply modifies the phase of the backscattering potential and hence just provides a redefinition of ζ . Clearly backscattering introduces highly non-linear terms to the Luttinger liquid action, much in the same way as spin-flip interactions did in section 2.3.2, how to analyse these complications will constitute the remainder of this chapter.

2.4.1 Single Impurity Problem

Here we will give a brief overview of what happens with a single impurity following Kane and Fisher[39]. Although the details of this calculation are not strictly relevant to the main body of the thesis, they do provide a very clean example of how renormalisation group calculations are performed, which will be of use when the mathematics becomes more involved.

We consider a Luttinger liquid within which a solitary impurity is embedded, which for simplicity we take to be at $x = 0$. Let us first have the impurity to be of the backscattering type, forward scattering can be ignored due to the above considerations (eq. (2.57)). As the non-linearity is concentrated on a single point, $\zeta(x) = \zeta\delta(x)$, we are entitled to integrate out the fields at $x \neq 0$.

$$S_0 = \frac{1}{2\beta} \sum_{i\omega_n} \frac{2|\omega_n|}{\pi K} \theta(-i\omega_n) \theta(i\omega_n) \quad (2.59)$$

$$S_{imp} = - \int d\tau \zeta e^{2i\theta(\tau)} + h.c. \quad (2.60)$$

The action in eq. (2.59) can be readily derived by calculating the Green's function at the origin. Remember that we are only really interested in the low energy physics of the system, the renormalisation group method will enable us to assess the importance of a given term at a given energy scale. In order to proceed we split the θ field into fast and slow modes.

$$\theta(\tau) = \frac{1}{\beta} \sum_{0 \leq |\omega_n| < \Lambda'} e^{i\omega_n \tau} \theta(i\omega) + \frac{1}{\beta} \sum_{\Lambda' \leq |\omega_n| < \Lambda} e^{i\omega_n \tau} \theta(i\omega_n) \quad (2.61)$$

$$= \theta^<(\tau) + \theta^>(\tau) + h.c. \quad (2.62)$$

Where Λ is the original ultra-violet cut off of the theory, and Λ' is the new reduced cut off. The idea is that we can integrate out the high energy fast modes, and then rescale our variables so as to compare the new lower energy theory to the original one containing both fast and slow modes. If we see that the impurity term becomes smaller as the energy scale is reduced we know it to be irrelevant to the low energy physics, conversely if the impurity term grows it will clearly have a drastic effect. Note that we still have a non-quadratic action, therefore in order to integrate out the fast modes we will need to treat the impurity perturbatively.

$$Z = \int \mathcal{D}\theta^< \mathcal{D}\theta^> e^{-S_0^<} e^{-S_0^>} e^{-S_{imp}} \quad (2.63)$$

$$= \int \mathcal{D}\theta^< e^{-S_0^<} Z^> \langle e^{-S_{imp}} \rangle_> \quad (2.64)$$

$$\approx Z^> \int \mathcal{D}\theta^< e^{-S_0^<} e^{-\langle S_{imp} \rangle_>} \quad (2.65)$$

The last step is valid only to linear order in the impurity strength, and the factor of $Z^>$ is an irrelevant constant. Averaging the disorder term over the fast fields is done straightforwardly with the help of eq. (B.4).

$$\langle S_{imp} \rangle = \int d\tau \zeta \langle e^{2i\theta^<(\tau) + 2i\theta^>(\tau)} \rangle_> + h.c. \quad (2.66)$$

$$= \int d\tau \zeta e^{2i\theta^<(\tau)} e^{-2\langle \theta^>(\tau) \theta^>(\tau) \rangle} + h.c. \quad (2.67)$$

$$\langle \theta^>(\tau) \theta^>(\tau) \rangle = \int_{\Lambda'}^{\Lambda} \frac{d|\omega|}{2\pi} \frac{\pi K}{|\omega|} \quad (2.68)$$

$$= \frac{K}{2} \log \left(\frac{\Lambda}{\Lambda'} \right) \quad (2.69)$$

$$\langle S_{imp} \rangle = \zeta \left(\frac{\Lambda}{\Lambda'} \right)^{-K} \int d\tau e^{2i\theta^<(\tau)} \quad (2.70)$$

We took the zero temperature limit in the third line to convert ω into a continuous variable. Integrating over the fast modes returns a term of exactly the same form as in eq. (2.60) but with a different impurity strength. In order to properly compare the impurity strength before and after integrating out the high energy scale we need to rescale our variables so that the fields are defined over the same space. In this instance we simply rescale time $\tau \rightarrow \left(\frac{\Lambda}{\Lambda'}\right) \tau$. Here the RG procedure does not produce any new terms, and simply renormalises the impurity strength, we are free to keep repeating this procedure as much as we want. It is therefore useful to consider an infinitesimal change of scale in order to construct a differential equation governing how the parameters flow under successive renormalisations.

$$\Lambda' = \Lambda(1 - \delta l) \tag{2.71}$$

$$\zeta(l + \delta l) = \zeta(l) (1 + (1 - K)\delta l) \tag{2.72}$$

$$\frac{\zeta(l + \delta l) - \zeta(l)}{\delta l} \stackrel{\delta l \rightarrow 0}{=} \frac{d\zeta}{dl} = (1 - K)\zeta \tag{2.73}$$

$$\zeta(l) = \zeta(0)e^{(1-K)l} \tag{2.74}$$

Whether or not the impurity strength grows or shrinks depends highly upon the interactions. For repulsive fermions ζ grows exponentially as one decreases the energy scale, whereas the converse is true for attractive fermions and impurity scattering is exponentially suppressed. Remember that eq. (2.74) is only valid for small ζ and as such says nothing definitive about the fate of repulsively interacting fermions except that single impurities are not irrelevant. In order to make a more concrete statement one would need access to the strong coupling limit, fortunately such a scenario is readily at hand for this problem.

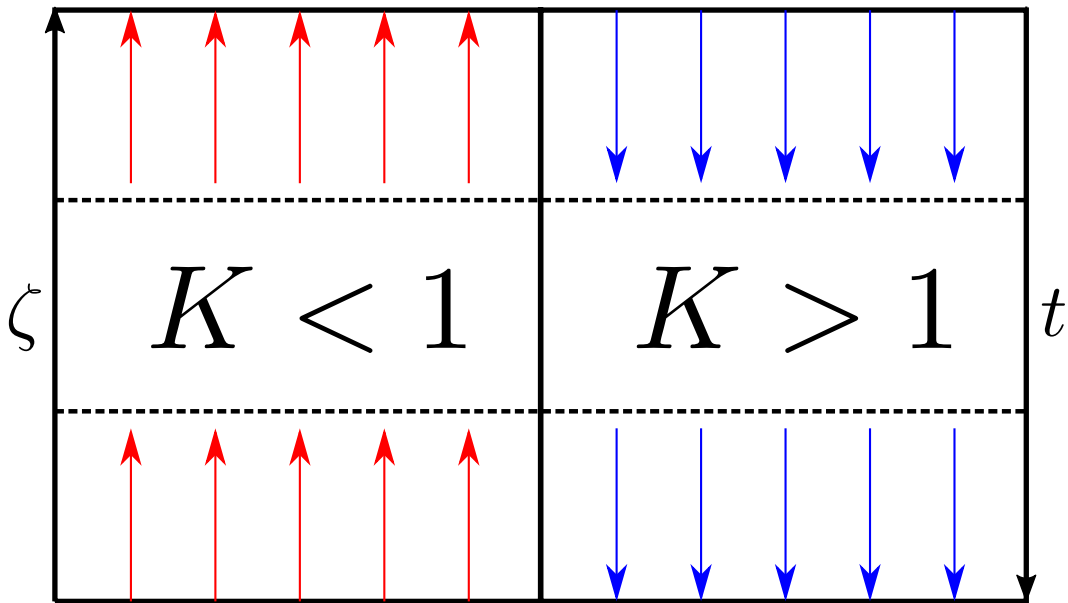


Figure 2.8: The renormalisation group flow for a weak backscattering impurity, with strength ζ and a weak tunnelling impurity with strength t . For repulsive fermions $K < 1$ the scattering strength is enhanced at lower energy scales, and weak tunnelling is suppressed. Whereas for attractive fermions $K > 1$ the opposite is true, scattering is diminished and tunnelling is enhanced. The dashed lines mark out regions where the RG ceases to be valid, however as we have access to both the weak and strong coupling limits in this instance one can safely assume the RG flow continues unabated. As both limits give the same picture we can see that at zero temperature a single impurity completely impedes the conductance of a Luttinger liquid arising from repulsive fermions, whereas attractive fermions do not care about the impurity.

Rather than consider the effect of a weak scatterer, one could start out with two *half* Luttinger liquids, one defined for negative x and the other for positive x , and weakly couple the two at the boundary, with a tunneling amplitude t .

$$S_{tun} = \int d\tau t e^{2i\phi(\tau)} \quad (2.75)$$

Notice that the weak tunnelling action, eq. (2.75), is identical to the weakly backscattering impurity eq. (2.60) except in the current field rather than the density field. We can exploit the duality between the two fields to immediately write down the RG flow for the tunnelling t by taking $K \rightarrow \frac{1}{K}$.

$$t(l) = t(0) e^{(1 - \frac{1}{K})l} \quad (2.76)$$

For attractive interactions the tunnelling term grows with decreasing energy scale, and shrinks for repulsive interactions. This complements the weak scattering flows perfectly and we can infer that single impurities of any strength are irrelevant for attractive fermions, and that they completely kill the conductance of repulsive fermions. This ties in nicely with the physical picture of the Luttinger liquid presented in section 2.3.2, whereby $K > 1$ leads to a superconducting *like* state, for which one would expect perfect conductance, and $K < 1$ a charge density wave *like* order where one would expect the wave to pin on the impurity. The complete RG flow of this system can be seen in fig. 2.8.

2.4.2 Many Impurity Problem

Having dealt with the single impurity problem in section 2.4.1 it is only natural to wonder what happens when we have many impurities. In many experimental systems such disorder would arise naturally and would not be under control. We thus have to perform our calculations for a specific configuration of impurities, and then average the result over all possible configurations. This presupposes self-averaging, whereby a large sample is equivalent to the ensemble of configurations, this is justified as there can be no long range order in 1D.

We still have a backscattering potential as described by eq. (2.56), the only difference being that the scattering potentials are now random variables which we will average over. Here we take the disorder potentials to have a Gaussian distribution, this corresponds to the case of extremely weak, but also extremely dense impurities, which is the opposite limit from the single impurity problem discussed above.

$$\overline{\langle O \rangle} = \frac{\int \mathcal{D}\bar{\zeta} \mathcal{D}\zeta e^{-\frac{1}{2D} \int dx \bar{\zeta}(x) \zeta(x)} \langle O \rangle}{\int \mathcal{D}\bar{\zeta} \mathcal{D}\zeta e^{-\frac{1}{2D} \int dx \bar{\zeta}(x) \zeta(x)}} \quad (2.77)$$

$$\langle O \rangle = \frac{\int \mathcal{D}\theta e^{-S[\theta, \zeta]} O}{\int \mathcal{D}\theta e^{-S[\theta, \zeta]}} \quad (2.78)$$

$$S[\theta, \zeta] = S_0[\theta] - \int dx [\zeta(x) \rho_0 e^{2i\theta(x, \tau)} + \bar{\zeta}(x) \rho_0 e^{-2i\theta(x, \tau)}] \quad (2.79)$$

We denote the averaging over the disorder configurations with a line to differentiate it from standard averaging over the fields as in eq. (2.77). Ideally one would like to take advantage of the fact that the combined action of the

disorder and the Luttinger liquid is quadratic in the backscattering potential and integrate it out, however this is complicated by the presence of $\frac{1}{Z}$ in eq. (2.78). This factor is dealt with using the replica trick[20].

$$\frac{1}{Z} = Z^{n-1} \quad (2.80)$$

$$= \left[\int \mathcal{D}\theta_2 e^{-S[\theta_2, \zeta]} \right] \dots \left[\int \mathcal{D}\theta_n e^{-S[\theta_n, \zeta]} \right] \quad (2.81)$$

Here we have replace the factor of $\frac{1}{Z}$ with $n - 1$ copies of the system. Clearly this is only valid when $n = 0$ but all subsequent analysis will assume $n \geq 1$ and only at the end will we attempt to take the limit $n \rightarrow 0$. We are now in a position to average over the disorder, resulting in an effective action in n fields. As the disorder couples linearly to the bosonic fields, performing the averaging amounts to completing the square. This replica trick therefore amounts to replacing the disorder averaging with interactions between replicas.

$$\overline{\langle O \rangle} = \int \left(\prod_{j=1}^n \mathcal{D}\theta_j \right) O(\theta_1) e^{-S_{eff}} \quad (2.82)$$

$$S_{eff} = \sum_{j=1}^n S_0[\theta_j] - D\rho_0^2 \sum_{i,j=1}^n \int dx \int d\tau d\tau' \cos(2\theta_i(x, \tau) - 2\theta_j(x, \tau')) \quad (2.83)$$

Armed with eq. (2.83) we can now perform RG analysis similar to that in section 2.4.1. One main difference here is that we have fields dependent on two variables, so rather than instituting a straightforward frequency cut off as with a single impurity, we cut off a frequency-momentum shell as shown in fig. 2.9.

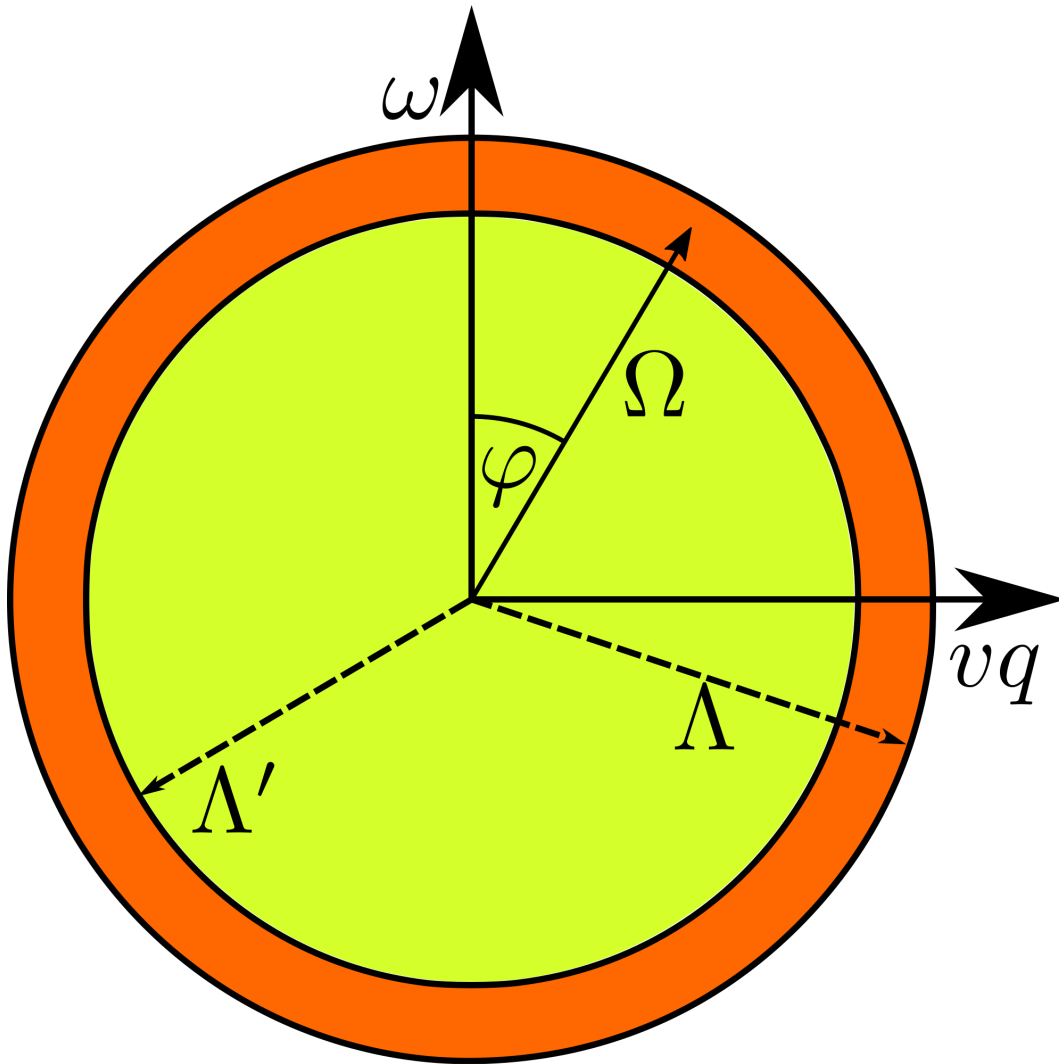


Figure 2.9: The energy-momentum shell renormalisation group scheme. The original ultraviolet cut off is defined as $\omega^2 + v^2 q^2 = \Lambda$ which defines a circular region in energy-momentum space. The new reduced cut off, Λ' , defines a smaller circular region. The RG procedure involves integrating out modes lying in the orange region between the new cut off and the old. Here Ω and φ are the new polar variables in which the scheme can readily be applied.

$$\theta_j^<(x, \tau) = \int_{0 \leq \sqrt{\omega^2 + v^2 q^2} \leq \Lambda'} dx d\tau e^{i\omega\tau + iqx} \theta_j(q, i\omega) \quad (2.84)$$

$$\theta_j^>(x, \tau) = \int_{\Lambda' \leq \sqrt{\omega^2 + v^2 q^2} \leq \Lambda} dx d\tau e^{i\omega\tau + iqx} \theta_j(q, i\omega) \quad (2.85)$$

Just as before we treat the difficult term perturbatively to linear order. We then have to average the disorder term, denoted S_{dis} , over the fast modes and rescale.

$$\langle S_{dis} \rangle = - D\rho_0^2 \sum_{ij} \int dx d\tau d\tau' \cos(2\theta_i^<(x, \tau) - 2\theta_j^<(x, \tau')) e^{-2\langle(\theta_i^>(x, \tau) - \theta_j^>(x, \tau'))\rangle} \quad (2.86)$$

$$= - D\rho_0^2 \sum_{ij} \int dx d\tau d\tau' \cos(2\theta_i^<(x, \tau) - 2\theta_j^<(x, \tau')) (\mathcal{A} + \mathcal{B}) \quad (2.87)$$

$$\mathcal{A} = e^{-2\langle\theta_i^>(x, \tau)\rangle} e^{-2\langle\theta_j^>(x, \tau')\rangle} \quad (2.88)$$

$$\mathcal{B} = e^{-2\langle\theta_i^>(x, \tau)\rangle} e^{-2\langle\theta_j^>(x, \tau')\rangle} \left(e^{2\langle\theta_i^>(x, \tau)\theta_j^>(x, \tau')\rangle} e^{2\langle\theta_j^>(x, \tau')\theta_i^>(x, \tau)\rangle} - 1 \right) \quad (2.89)$$

The logic behind splitting the integral into two parts stems from the replicas. Note that eq. (2.88) gives the same contribution to every combination of replica indices, and hence is a natural candidate to renormalise the disorder strength which is flat in replica space. Equation (2.89), on the other hand, vanishes for the non-diagonal parts of the replica sum and must therefore either introduce a new term or renormalise the quadratic part of the action which is also diagonal in the replicas. The renormalisation of the disorder term can be

calculated rather straightforwardly.

$$\mathcal{A} = \left(\frac{\Lambda}{\Lambda'} \right)^{-2K} \quad (2.90)$$

$$D(\Lambda') = D(\Lambda) \left(\frac{\Lambda}{\Lambda'} \right)^{3-2K} \quad (2.91)$$

Here the three in the exponent comes from the three integrals (two time and one space). The contribution from \mathcal{B} is more difficult and will require extra simplification. Having the RG generate new terms would be inconvenient, so ideally we would like \mathcal{B} to renormalise the quadratic action. If we constrain the two times to be close to one another this would enable us to expand the cosine giving us a term $\sim (\partial_\tau \theta)^2$. However one must take great care in performing this expansion, as the θ field has diverging fluctuations, $\langle \theta^2(x, \tau) \rangle \rightarrow \infty$. In order to safely expand the cosine one must average over the equilibrium fluctuations, this is equivalent to normal ordering in the operator language.

$$\langle \cos(\phi_0 + \phi) \rangle_0 = \langle \cos(\phi_0) \rangle_0 \cos(\phi) - \langle \sin(\phi_0) \rangle_0 \sin(\phi) \quad (2.92)$$

$$= e^{-\frac{1}{2} \langle \phi_0^2 \rangle_0} \left(1 - \frac{1}{2} \phi^2 + O(\phi^4) \right) \quad (2.93)$$

$$\cos(2\theta_j^<(x, \tau) - 2\theta_j^<(x, \tau')) \rightarrow (1 - 2(\partial_\tau \theta^<)^2 \delta\tau^2) e^{-2\langle (\theta_j^<(x, \tau) - \theta_j^<(x, \tau'))^2 \rangle_<} \quad (2.94)$$

The factor stemming from the regularisation pairs neatly with \mathcal{B} , we will denote

this combination $\tilde{\mathcal{B}}$.

$$\tilde{\mathcal{B}} = \mathcal{B} e^{-2 \langle (\theta_j^<(x,\tau) - \theta_j^<(x,\tau'))^2 \rangle_<} \quad (2.95)$$

$$= e^{-2K \int_0^\Lambda \frac{d|\Omega|}{|\Omega|} (1 - J_0(|\Omega|\delta\tau))} \left(1 - e^{-2K \int_{\Lambda'}^\Lambda \frac{d|\Omega|}{|\Omega|} J_0(|\Omega|\delta\tau)} \right) \quad (2.96)$$

$$\approx \left(1 - \left(\frac{\Lambda}{\Lambda'} \right)^{-2K} \right) + O(\delta\tau^2) \quad (2.97)$$

We have taken $|\delta\tau| < \frac{1}{\Lambda}$ to massively simplify the integrals. The correction to the action stemming from $\tilde{\mathcal{B}}$ is then readily calculated.

$$\delta S_{\tilde{\mathcal{B}}} = \frac{\tilde{D}}{2\pi} \int dx d\tau (\partial_\tau \theta)^2 \left(1 - \left(\frac{\Lambda}{\Lambda'} \right)^{-2K} \right) \quad (2.98)$$

The disorder parameter has been redefined here to absorb various irksome constants, $\tilde{D} = \frac{4\pi}{3} \frac{D\rho_0^2}{\Lambda^3}$. By treating the new reduced cut off as being infinitesimally close to the original cut off, $\Lambda' = \Lambda(1 - \delta l)$ we can construct our RG equations governing how the parameters flow under a reduction of energy scale.

$$\frac{d\tilde{D}}{dl} = (3 - 2K)\tilde{D} \quad (2.99)$$

$$\frac{d}{dl} \left(\frac{1}{vK} \right) = 2K\tilde{D} \quad (2.100)$$

$$\frac{d}{dl} \left(\frac{v}{K} \right) = 0 \quad (2.101)$$

We see that disorder not only renormalises itself, but also the defining bulk properties of the Luttinger liquid, the Luttinger parameter K and the characteristic velocity v . A single impurity could not aspire to renormalise the bulk properties of the Luttinger liquid as it is only a local potential. Disorder however can and does renormalise the defining Luttinger liquid parameters,

K and v , as seen in eqs. (2.99) to (2.101) or more explicitly in eqs. (2.102) and (2.103).

$$\frac{dK}{dl} = -vK^3\tilde{D} \quad (2.102)$$

$$\frac{dv}{dl} = -v^2K^2\tilde{D} \quad (2.103)$$

Due to the simplicity of eq. (2.101) one can easily eliminate the velocity from proceedings as $v(l) = \frac{v_0}{K_0}K(l)$ where v_0 & K_0 are the bare parameters. Clearly something special is going on at $K = \frac{3}{2}$, as can be seen from eq. (2.99). If $K < \frac{3}{2}$ then the disorder strength grows, and if $K > \frac{3}{2}$ the disorder strength reduces, however one must remember K is also being renormalised and even if its bare value is above $\frac{3}{2}$ it may pass below this critical threshold before the disorder is eliminated.

The parametric dependence of D on K can be easily figured out by combining eqs. (2.99) and (2.102) to eliminate l , however we will take the not strictly necessary step of zooming in close to the transition point $K = \frac{3}{2}$. We do this in order to draw connections with section 3.4 where such a step helps greatly with the analysis.

$$\begin{aligned} y' &= xy & y(0) &= \left(\frac{3}{2}\right)^2 \sqrt{\frac{v_0}{K_0}D_0} \\ x' &= y^2 & x(0) &= -\delta \end{aligned} \quad (2.104)$$

Where $x = \frac{3}{2} - K$ and $y = \left(\frac{3}{2}\right)^2 \sqrt{\frac{v_0}{K_0}D}$. This particular representation enables one to draw comparisons with the now famous Kosterlitz-Thouless transition[45, 44] in two dimensional statistical mechanics which has exactly the same renormalisation group equations.

Another possible choice of variables allows us to write down a classical Lagrangian and by extension a Hamiltonian. The Lagrangian contains no explicit references to our ‘time’ l and hence the Hamiltonian is conserved. The variables are $y = e^q$ and therefore $\dot{q} = x$, which is the conjugate momentum to q .

$$L = \frac{1}{2}\dot{q}^2 + \frac{1}{2}e^{2q} \quad (2.105)$$

$$H = \frac{1}{2}(x^2 - y^2) = E \quad (2.106)$$

The RG equations thus describe a particle with position q sitting in an exponential potential, $U = -\frac{1}{2}e^{2q}$. Clearly if the particle starts off with no momentum it will just ‘roll down’ the potential hill to $q \rightarrow \infty$ which corresponds to diverging disorder and implies localisation. The particle therefore needs enough momentum, x , to overcome the potential and carry on unbounded to $q \rightarrow -\infty$. In order for the disorder to become irrelevant we need the energy, E to be positive and the initial momentum $\delta > y_0$. The flow diagram for eq. (2.104) is shown in fig. 2.10, for systems where the disorder is irrelevant the Luttinger parameter is still renormalised to a new value $K^* < K_0$ in the effective low energy quadratic theory.

We can use the ‘energy’ of the analogous classical problem to solve for the disorder explicitly. For positive energy the solution, assuming $\delta > 0$ is given by eqs. (2.107) and (2.108) which clearly flows to zero as $l \rightarrow \infty$.

$$D_c = e^{2q} = \frac{k^2}{\sinh^2(kl + \chi)} \quad (2.107)$$

$$k^2 = \delta^2 - D_0 = 2E, \quad \tanh(\chi) = \frac{k}{\delta} \quad (2.108)$$

For negative energy, the solution requires a little bit of tweaking, $E \rightarrow -|E|$ and $k \rightarrow i|k| = i\sqrt{2|E|}$. This solution is given by eqs. (2.109) and (2.110). For this solution the disorder is initially decreasing before diverging at a finite ‘time’ l_K , which is sometimes referred to as the ‘Kondo’ temperature as this problem also maps onto the case of a ferromagnetic Kondo impurity[50].

$$D_i = e^{2q} = \frac{|k|^2}{\sin^2(|k|l + \chi)} \quad (2.109)$$

$$-|k|^2 = \delta_i^2 - D_0, \quad \tan(\chi) = \frac{|k|}{\delta} \quad (2.110)$$

We see that disorder poses far more of a challenge to overcome than a single impurity. For a single impurity all that was required were attractive interactions (in terms of fermions), and then the dominant superconducting correlations were enough to overcome the impurity, for disordered systems the interactions need to be strongly attractive. The strong coupling picture is of a system resembling a charge density wave order, where the wave distorts in order to pin on the impurities.

2.5 Concluding Remarks

This concludes the second chapter, we have seen that interacting fermions in one spatial dimension can be described by a simple quadratic bosonic model.

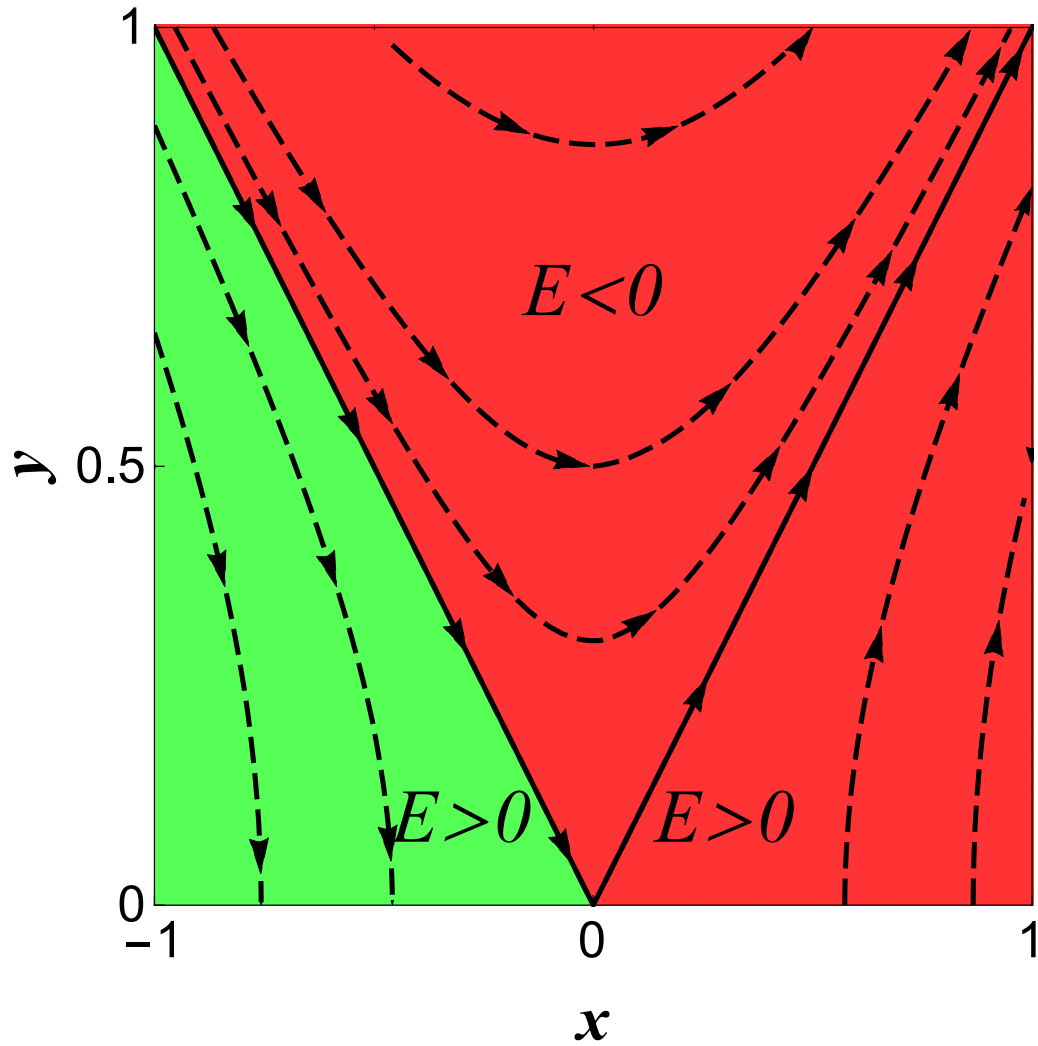


Figure 2.10: Flow diagram of the Berezinskii–Kosterlitz–Thouless renormalisation group equations, eq. (2.104). Green denotes a region where the disorder, $D \propto \sqrt{y}$, becomes irrelevant at low energies, here the energy E is positive. The red regions contain trajectories where disorder grows, and one assumes the disorder precipitates localisation, here the energy could be positive or negative. The variable x characterises how far away from the critical value of $K = \frac{3}{2}$ we are, negative x means $K > \frac{3}{2}$. Taken from ref. [36]

This bosonic representation is known as the Luttinger liquid, and has only two parameters: the Luttinger parameter K which captures the effects of the original interactions and v the effective velocity of the quasi-particles. Such a simple description is possible due to the necessity of collective motion in 1D, particles cannot move out of each other's way.

We have also reviewed some of the strange physical properties of the Luttinger liquid state. Interacting fermions display quasi-long range order, whereby correlations only decay as slow power laws. This is a consequence of the nesting condition always being satisfied, pushing the system towards ordering along a $2k_f$ wave vector but 1D systems cannot order at finite temperature as domain walls are always favoured entropically. This results in a system behaving as if at a phase transition where quantities have power law correlations at zero temperature, except where the exponents are non-universal. For attractive fermions the dominant correlations are of the superconducting type, whereas repulsive interactions promote charge density waves.

If spin is included in one's analysis we see that the spin and charge degrees of freedom completely separate, yielding two types of quasi-particle excitation: those that carry spin and those that carry charge. However, depending upon the spin interaction, spin-flip processes can lead to behaviour where the spin excitations are gapped.

The most relevant piece of physics contained within this chapter is the effects of impurities. We reviewed the Kane & Fischer[39] result that a single impurity either kills conductance for repulsive interactions, or is utterly irrelevant for attractive interactions. We also went over the Giamarchi-Schulz[22] analysis of a disordered Luttinger liquid showing how one arrives at the Kosterlitz-

Thouless RG equations, and under what conditions the system localises.

We are now in a position to tackle what happens when we do not just have a single Luttinger liquid, but more than one which are weakly coupled to one another. This is the focus of chapter 3 which contains the original work of this thesis.

Chapter 3

Multi-Channel Luttinger Liquids

Whereas chapter 2 sought to deal with isolated one dimensional systems, this chapter considers what happens when we have multiple one dimensional channels which are coupled weakly. The weakness of the coupling preserves the validity of the Luttinger liquid description, and hence we refer to such a system as a multi-channel Luttinger liquid (MLL).

This chapter will introduce the types of physical system we aspire to model in section 3.1 before going on to introduce the mathematical framework which describes the MLL with emphasis on the role of the Luttinger matrix, as introduced by ref.[37], in section 3.2 and section 3.3. This sets the scene for the original work of this thesis, in section 3.4, which considers the effect of disorder in the context of MLLs, this work forms the basis of ref. [36].

3.1 What is a Multi-Channel Luttinger Liquid System?

Owing to the generality of the Luttinger liquid description, which accurately describes both fermions and bosons in terms of phonon-like excitations, the MLL can describe a wide range of systems. We have already touched on one of the simpler possibilities in section 2.3.2 when we considered spin. A spin- $\frac{1}{2}$ 1D Fermi system has two channels, one for the spin and another for the charge degree of freedom. As such it makes up the simplest possible MLL where the two channels are completely decoupled.

Its also possible to construct a MLL where the origin of the different channels are extremely distinct. For instance a Bose-Fermi mixture, which is something readily made using cold atoms[25, 58]. This would allow us to have systems with extremely distinct Luttinger parameters as the physical origin of bosonic and fermionic Luttinger parameters are quite different. For fermions the interaction is typically the Coulomb interaction, whereas bosons naturally condense at low temperatures and hence have a ‘natural attraction’. For bosons $K = 1$ corresponds to hard core bosons, $K \ll 1$ the Wigner crystal limit and $K \gg 1$ corresponds to the superfluid limit.

One possibility is in modelling highly anisotropic 2D or 3D materials, such as the Bechgaard salts discussed earlier, where there exists a special axis along which the system behaves like an lattice of 1D wires, each of which could be modelled as a Luttinger liquid. Such a system would exhibit translational symmetry, and hence in many ways would be much easier to treat than a finite number of wires.

Remembering that the whole idea of the Luttinger liquid paradigm is to view one dimensional interacting particles in terms of collective wave-like excitations, one may in turn consider other wave-like excitations as a Luttinger liquid. As hinted at in chapter 2 phonons may be thought of in this way, allowing one to consider electron-phonon interactions present in most solids. Typically phonons will couple to electrons via a deformation potential[1, 53], whereby the density fluctuations of the lattice create a net positive charge which attracts electrons.

$$H_{def} = g_{def} \int dx \rho(x) \nabla \cdot u(x) \quad (3.1)$$

This is described mathematically in eq. (3.1), where ρ is the electronic density and $u(x)$ is the local lattice displacement and g_{def} is the coupling strength. Past work on such a system is covered in ref.[17, 19, 18], with regards to the effect of single impurity scattering in the presence of electron-phonon coupling.

To restate, one can use the multi-channel Luttinger liquid formalism to model a large number of systems. These can be lattices of wires in anisotropic solids, mixtures of bosons and fermions such as in ultra-cold atoms experiments, or even just a humble electron-phonon interaction. The next section will cover how to describe the MLL mathematically in a generic way, which would apply to all these scenarios.

3.2 The Luttinger Matrix

A single Luttinger liquid is written in terms of two scalar bosonic fields, θ and ϕ , whose gradients are associated with the density and current in the liquid

respectively. A multi-channel Luttinger liquid defined by two vector bosonic fields $\vec{\theta}$ and $\vec{\phi}$ whose i^{th} components give the density and current in the i^{th} channel.

$$S[\vec{\theta}, \vec{\phi}] = -\frac{1}{2\pi} \int dx d\tau \begin{pmatrix} \vec{\theta}^T & \vec{\phi}^T \end{pmatrix} \left\{ \begin{pmatrix} 0 & 1 \\ 1 & 0 \end{pmatrix} i\partial_\tau + \begin{pmatrix} \mathbf{V}_+ & 0 \\ 0 & \mathbf{V}_- \end{pmatrix} \partial_x \right\} \partial_x \begin{pmatrix} \vec{\theta} \\ \vec{\phi} \end{pmatrix} \quad (3.2a)$$

$$S[\vec{\theta}] = \frac{1}{2\pi} \int dx d\tau \left[\partial_\tau \vec{\theta}^T \cdot \mathbf{V}_-^{-1} \cdot \partial_\tau \vec{\theta} + \partial_x \vec{\theta} \cdot \mathbf{V}_+ \cdot \partial_x \vec{\theta} \right] \quad (3.2b)$$

$$S[\vec{\phi}] = \frac{1}{2\pi} \int dx d\tau \left[\partial_\tau \vec{\phi}^T \cdot \mathbf{V}_+^{-1} \cdot \partial_\tau \vec{\phi} + \partial_x \vec{\phi} \cdot \mathbf{V}_- \cdot \partial_x \vec{\phi} \right] \quad (3.2c)$$

The full form of the action is given by eq. (3.2a), where the interaction matrices, \mathbf{V}_\pm , encode both the intra- and inter-channel interactions. We omit the possibility of coupling currents to densities as this would break both the inversion and time reversal symmetries of the system. Time reversal symmetry means the system is invariant under $\tau \rightarrow -\tau$ and $\phi \rightarrow -\phi$, remembering the the current field ϕ is in some sense a 1D vector. A system coupling densities to currents would therefore change sign under time-reversal, and as practically all systems have such a symmetry we can justify dropping such a term. We may parametrise the interaction matrices using a generalised g-ology notation, as in eq. (3.3).

$$V_\pm^{ij} = v_f^i \delta_{ij} + \frac{g_4^{ij} \pm g_2^{ij}}{\pi} \quad (3.3)$$

Here v_f^i plays the role of the free Fermi velocity, and the \mathbf{g}_4 and \mathbf{g}_2 matrices define the interactions between left and right movers. The diagonal elements

clearly deal with intra-channel interactions just as with a single liquid, whereas the off diagonal elements characterise the inter-channel coupling. Note that we are free to parametrise any channel in this way, even if it does not have a fermionic origin, as we may reverse the bosonisation procedure and describe the collectivised excitations in terms of interacting fermions. We may use the diagonal elements of the interaction matrices to define the intra-channel Luttinger parameters and velocities.

$$(\mathbf{V}_+)_{ii} = \frac{v_i}{K_i} \quad (3.4)$$

$$(\mathbf{V}_-)_{ii} = v_i K_i \quad (3.5)$$

When calculating MLL correlations, it is prudent to introduce fields which diagonalise the interaction matrices. To this end we introduce the matrix \mathbf{M} .

$$\mathbf{M}^T \mathbf{V}_+ \mathbf{M} = \mathbf{M}^{-1} \mathbf{V}_- (\mathbf{M}^T)^{-1} = \mathbf{u} \quad (3.6)$$

Where the matrix $\mathbf{u} = \text{diag}(\{u_i\})$ gives the effective velocities in the diagonal fields, which are defined by the transformation in eq. (3.7). Note that we require the interaction matrices to be positive definite, or else we would have negative velocities.

$$\vec{\theta} = \mathbf{M} \vec{\tilde{\theta}} \quad \vec{\phi} = (\mathbf{M}^T)^{-1} \vec{\tilde{\phi}} \quad (3.7)$$

In this representation the action is now diagonal in channel-space, as seen in

eqs. (3.8) and (3.9).

$$S = -\frac{1}{2\pi} \int dx d\tau \begin{pmatrix} \vec{\theta}^T & \vec{\phi}^T \end{pmatrix} \left\{ \begin{pmatrix} 0 & 1 \\ 1 & 0 \end{pmatrix} i\partial_\tau + \begin{pmatrix} \mathbf{u} & 0 \\ 0 & \mathbf{u} \end{pmatrix} \partial_x \right\} \partial_x \begin{pmatrix} \vec{\theta} \\ \vec{\phi} \end{pmatrix} \quad (3.8)$$

$$= -\frac{1}{2\pi} \int dx d\tau \sum_j \left[\tilde{\theta}_j i\partial_\tau \partial_x \tilde{\phi}_j + \tilde{\phi}_j i\partial_\tau \partial_x \tilde{\theta}_j + u_j \tilde{\theta}_j \partial_x^2 \tilde{\theta}_j + u_j \tilde{\phi}_j \partial_x^2 \tilde{\phi}_j \right] \quad (3.9)$$

Just as before one is free to integrate out either of the fields, in this case we find the two vector bosons have exactly the same action.

$$S[\vec{\theta}] = \int dx d\tau \sum_j \frac{1}{2\pi u_j} \left[(\partial_\tau \tilde{\theta}_j)^2 + u_j^2 (\partial_x \tilde{\theta}_j)^2 \right] \quad (3.10)$$

$$S[\vec{\phi}] = \int dx d\tau \sum_j \frac{1}{2\pi u_j} \left[(\partial_\tau \tilde{\phi}_j)^2 + u_j^2 (\partial_x \tilde{\phi}_j)^2 \right] \quad (3.11)$$

This is because \mathbf{M} is not just a rotation, it also scales out the Luttinger parameter. The analogous step for a single channel Luttinger liquid is to take $\tilde{\theta} = \frac{\theta}{\sqrt{K}}$ and $\tilde{\phi} = \sqrt{K}\phi$. For this reason we introduce the Luttinger matrix, as in ref. [37].

$$\mathbf{K} = \mathbf{M}\mathbf{M}^T \quad (3.12)$$

As can be seen from eq. (3.12) the Luttinger matrix is a symmetric object, and can be defined purely in terms of the interaction matrices with the help of eq. (3.7).

$$\mathbf{K}\mathbf{V}_+\mathbf{K} = \mathbf{V}_- \quad (3.13)$$

As both \mathbf{V}_\pm are positive definite so too must the Luttinger matrix. Clearly

if there is no inter-channel interaction we have $K_{ij} \rightarrow K_i \delta_{ij}$, which justifies the nomenclature. Although one cannot write down a Lagrangian explicitly containing the Luttinger matrix, it does stand in for the Luttinger parameter in RG equations. To expand upon this point we will very briefly touch on the single impurity problem, as in section 2.4.1, in the context of MLLs. This is covered more exhaustively in ref.[37] using a slightly different methodology.

$$S_{imp} = - \int d\tau \sum_j [\zeta_j e^{i\theta_j(x=0,\tau)} + h.c.] \quad (3.14)$$

Here we have a single backscattering impurity located at $x = 0$, which has the backscattering potential ζ_j in the j^{th} channel. The quadratic part of the action is just that of a MLL as given in eq. (3.2a) where the fields not at the origin have been integrated out as in eq. (2.59). We may perform the RG calculation following exactly the same steps as before, with the only difference being that our free action is the MLL one.

$$\left\langle (\theta_i^>(x=0, \tau))^2 \right\rangle_> = \sum_{mn} M_{im} M_{in} \left\langle \tilde{\theta}_m^> \tilde{\theta}_n^> \right\rangle_> \quad (3.15)$$

$$= \sum_m M_{im} M_{mi}^T \int_{\Lambda'}^{\Lambda} \frac{d|\Omega|}{2\pi} \frac{\pi}{|\Omega|} \quad (3.16)$$

$$= K_{ii} \frac{1}{2} \log\left(\frac{\Lambda}{\Lambda'}\right) \quad (3.17)$$

The only difference between eqs. (2.69) and (3.17) is that $K \rightarrow K_{ii}$. One can then following this through and write down a set of RG equations for the

impurity strength in each channel.

$$\frac{d\zeta_i}{dl} = (1 - K_{ii}) \zeta_i \quad (3.18)$$

As we can see, the role of the intra-channel Luttinger parameter has been usurped by the appropriate diagonal element of the Luttinger matrix. The condition for the irrelevance of a single weak scattering impurity is no longer whether $K_i > 1$ but whether $K_{ii} > 1$ for the i^{th} channel. Depending on the inter-channel interactions the value of K_{ii} can be quite different from K_i . For instance if we take the case of fermions, inter-channel interactions can stabilise the repulsive fermions against the impurity.

In summary we have introduced the concept of a multi-channel Luttinger liquid, which covers a very broad range of physical systems. Whereas single channel LLs are characterised purely by the Luttinger parameter and their velocity, MLLs also have the inter-channel coupling as an important parameter. Each channel now has an ‘effective’ Luttinger parameter given by the appropriate diagonal element of the Luttinger matrix, as defined in eq. (3.12), which governs the properties of the liquid. Although one cannot write down an action in terms of \mathbf{K} , it appears straightforwardly in RG equations. This section has been somewhat generic, however in section 3.3 we will focus on the case of two-channel liquids with specific examples.

3.3 Two-Channel Luttinger Liquids

In this section we restrict ourselves to considering just two coupled Luttinger liquids. The reason for this is twofold: firstly this is an accessible experimen-

tal set-up, especially when the two channels are very distinct, whether it be electron-phonon interactions in a single 1D wire, a Bose-Fermi mixture of cold atoms or even edge states in a topological insulator[40, 7, 56]; the second, and perhaps more honest reason, is that the Luttinger matrix takes a particularly simple form for just two channels, as seen in eq. (3.19).

$$\mathbf{K} = \sqrt{\frac{\kappa}{ac - b^2}} \begin{pmatrix} a & b \\ b & c \end{pmatrix}, \begin{cases} a = V_-^{11} + \kappa V_+^{22} \\ b = V_-^{12} - \kappa V_+^{12} \\ c = V_-^{22} + \kappa V_+^{11} \end{cases} \quad (3.19)$$

$$\kappa = \det(\mathbf{K}) = \sqrt{\frac{\det(\mathbf{V}_-)}{\det(\mathbf{V}_+)}} \quad (3.20)$$

The interaction matrices can also be rather conveniently parametrised in this instance, where the positive definite property is ensured by having the coupling strengths $|\alpha_{\pm}| \leq 1$.

$$\mathbf{V}_+ = \begin{pmatrix} \frac{v_1}{K_1} & \sqrt{\frac{v_1 v_2}{K_1 K_2}} \alpha_+ \\ \sqrt{\frac{v_1 v_2}{K_1 K_2}} \alpha_+ & \frac{v_2}{K_2} \end{pmatrix} \quad (3.21)$$

$$\mathbf{V}_- = \begin{pmatrix} v_1 K_1 & \sqrt{v_1 K_1 v_2 K_2} \alpha_- \\ \sqrt{v_1 K_1 v_2 K_2} \alpha_- & v_2 K_2 \end{pmatrix} \quad (3.22)$$

If we were in the situation where either of the couplings $|\alpha_{\pm}| > 1$ one of the velocities will go negative. This signifies an instability in the system which the MLL model cannot accurately capture, for the case of electrons and phonons this is the Wentzel-Bardeen instability[64]. The velocities in the new system

can be obtained through eqs. (3.12) and (3.13).

$$\det(\mathbf{u}^2) = \det\left((\mathbf{M}^T \mathbf{V}_+ \mathbf{M})^2\right) \quad (3.23a)$$

$$u_1^2 + u_2^2 = \det(\mathbf{V}_+ \mathbf{K} \mathbf{V}_+ \mathbf{K}) \quad (3.23b)$$

$$= \det((\mathbf{V}_+ \mathbf{V}_-)) \quad (3.23c)$$

$$\text{tr}(\mathbf{u}) = u_1 + u_2 = \text{tr}(\mathbf{V}_+ \mathbf{K}) \quad (3.23d)$$

One can solve eq. (3.23) for the effective velocities, $u_{1,2}$.

$$u_{1,2}^2 = \frac{v_1^2 + v_2^2 + 2v_1 v_2 \alpha_+ \alpha_-}{2} \pm \frac{1}{2} \sqrt{(v_1^2 + v_2^2 + 2v_1 v_2 \alpha_+ \alpha_-)^2 - 4v_1^2 v_2^2 (1 - \alpha_+^2)(1 - \alpha_-^2)} \quad (3.24)$$

If one writes the Luttinger matrix using this parametrisation, seen in eq. (3.25), one can see something curious happens when $\alpha_+ = \alpha_- = \alpha$. In this limit the Luttinger matrix becomes diagonal, with the diagonal entries K_1 and K_2 just as if there were no inter-channel interactions at all. One can infer from this that density-density interactions are in competition with current-current ones.

$$\mathbf{K} = \frac{1}{u_1 + u_2} \begin{pmatrix} K_1 \left(v_1 + v_2 \sqrt{\frac{1 - \alpha_-^2}{1 - \alpha_+^2}} \right) & \sqrt{v_1 K_1 v_2 K_2} \left(\alpha_- - \sqrt{\frac{1 - \alpha_-^2}{1 - \alpha_+^2}} \alpha_+ \right) \\ \sqrt{v_1 K_1 v_2 K_2} \left(\alpha_- - \sqrt{\frac{1 - \alpha_-^2}{1 - \alpha_+^2}} \alpha_+ \right) & K_2 \left(v_2 + v_1 \sqrt{\frac{1 - \alpha_-^2}{1 - \alpha_+^2}} \right) \end{pmatrix} \quad (3.25)$$

We can think of the diagonal element K_{ii} as an *effective* Luttinger parameter. The ratios of this effective Luttinger parameter to the original intra-channel K_i are shown in figs. 3.1 and 3.2 for a variety of coupling strengths.

We see that the role of density-density interactions is to enhance the effective Luttinger parameter such that $K_{ii} > K_i$, whereas current-current interactions diminish it. This opens up interesting possibilities, for instance thinking back to the single impurity problem, especially eq. (3.14), we have the possibility of inter-channel interactions stabilising repulsive fermions against weak back-scattering.

This can be connected with previous work done in ref.[19] which considered electron-phonon coupling. For this scenario we would have only interactions of the α_+ type, which arise from the deformation potential as in eq. (3.1). The velocities are given by eq. (3.26) where c is the speed of sound and v the effective electronic velocity.

$$u_{1,2}^2 = \frac{1}{2} \left(v^2 + c^2 \pm \sqrt{(v^2 - c^2)^2 + 4v^2c^2\alpha_+^2} \right) \quad (3.26)$$

As we can see from figs. 3.1 and 3.2 pure density-density interactions can only enhance the Luttinger parameter. Hence coupling to phonons makes the electronic channel more attractive and hence increases the superconducting fluctuations as to be expected from analogy with Bardeen-Cooper-Schrieffer (BCS) theory[12, 5, 4].

We have now introduced the two-channel Luttinger matrix, which helps us to see the effect of inter-channel interactions. The general rule is that density-density interactions push the system to behave more like attractive fermions, whereas current-current interactions favour repulsive fermion-like behaviour. We are now in a position to tackle the meat of this thesis in section 3.4.

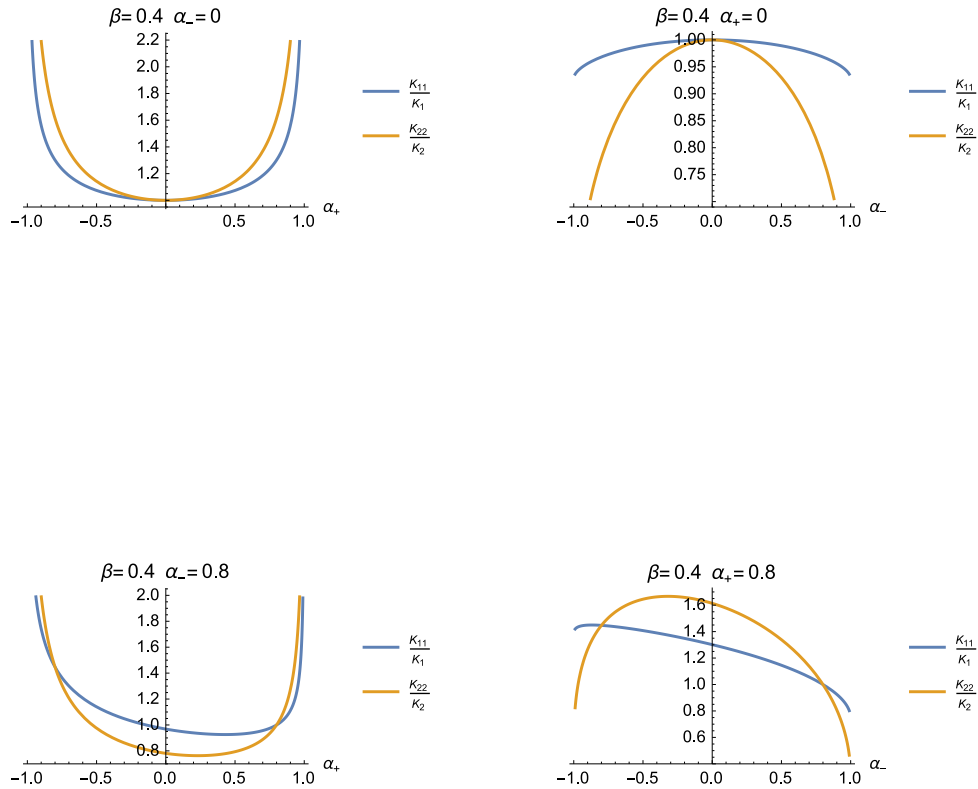


Figure 3.1: Graphs showing how the effective Luttinger parameter of a two channel system, K_{jj} is modified with respect to the uncoupled Luttinger parameter, K_j . Here $\beta = \frac{v_2}{v_1}$ and serves only to separate the the two channels. Top-left: Density-density interactions only, here we see α_+ on its own only enhances the Luttinger parameter. Top-Right: Current-current interactions only, α_- , we see they only decrease the Luttinger parameter. Bottom: Both current-current and density-density couplings. Having both types of coupling introduces asymmetries.

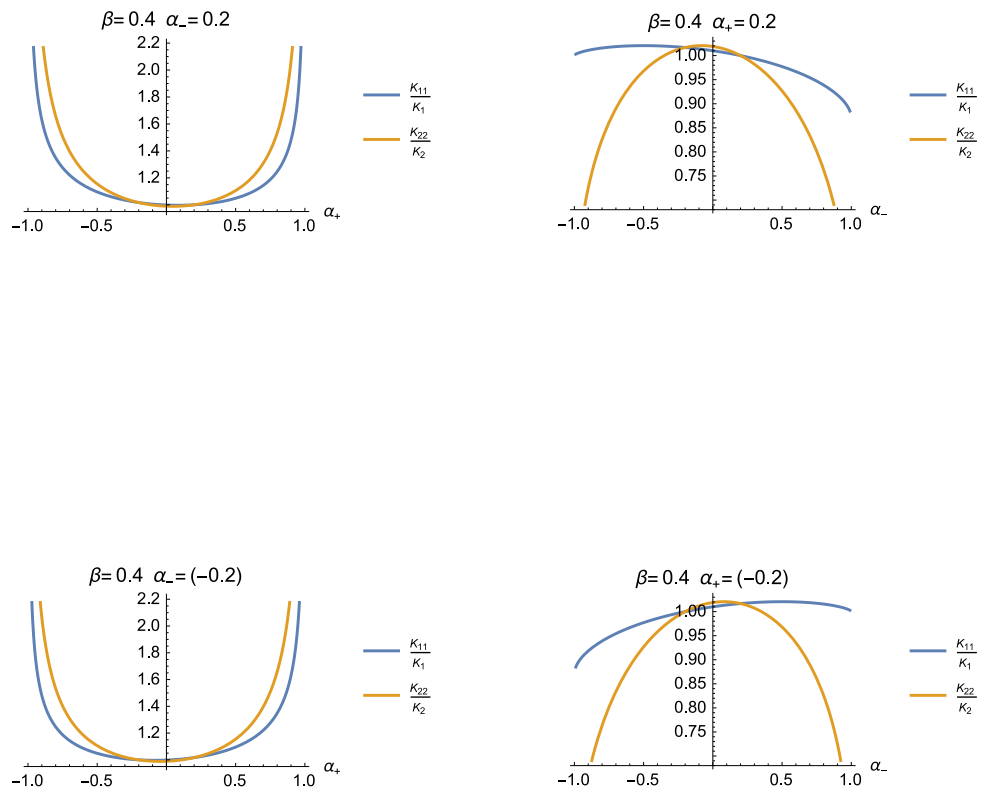


Figure 3.2: Similar to fig. 3.1, changing the sign of the coupling just serves to flip the asymmetry.

3.4 Multi-Channel Disorder

This section is devoted to the problem of disorder in a Multi-Channel Luttinger liquid. This section is the original contribution to this thesis, whose results are contained within ref. [36]. We will start by deriving the action and subsequent renormalisation group equations for a generic MLL with embedded continuous disorder, before specialising the analysis to two cases. The first case is simply a lattice of identical channels whereas the second will be that of a two channel system, as in 3.3 but with the addition of disorder.

The quadratic part of the action is naturally the same as in eq. (3.2b), we now embed into each channel a static backscattering potential $\zeta_j(x)$ just as in section 2.4.2. The contribution to the action is given in eq. (3.27), note we still do not allow backscattering between channels, the channels only talk to each other through the quadratic action.

$$S_{dis} = - \sum_j \int dx d\tau [\zeta_j(x)\rho_0 e^{2i\theta_j(x,\tau)} + \bar{\zeta}_j(x)\rho_0 e^{-2i\theta_j(x,\tau)}] \quad (3.27)$$

As before we are not interested in solving the physics of a specific configuration of impurities, but in solving the problem for a random configuration. Hence we have to average over the backscattering potentials, just as in section 2.4.2, using the replica trick. Replicas will be distinguished using Greek indices.

$$p(\vec{\zeta}, \vec{\bar{\zeta}}) = e^{-\int dx \bar{\zeta}_i D_{ij}^{-1} \zeta_j} \quad (3.28a)$$

$$\langle \zeta_i(x) \bar{\zeta}_j(x') \rangle = D_{ij} \delta(x - x') \quad (3.28b)$$

We take the random backscattering potentials to be point correlated as in

eq. (3.28), where the disorder strength is given by the matrix \mathbf{D} . After averaging over the disorder we arrive at eq. (3.29).

$$S_{dis} = - \int dx d\tau d\tau' \sum_{\alpha\beta} \sum_{ij} \rho_0^2 D_{ij} \cos\left(2\theta_i^\alpha(x, \tau) - 2\theta_j^\beta(x, \tau')\right) \quad (3.29)$$

The above has the same form as eq. (2.83) except with the addition of summing over channel indices. This term is highly non-linear and hence we will need the help of RG techniques to analyse its effect as before. We split the fields into fast and slow modes using an energy-momentum shell scheme as in fig. 2.9, where we take each field to have the same ultra-violet cut-off. The disorder is then treated perturbatively to first order, leaving us having to calculate $\langle S_{dis} \rangle_>$ as before.

Following the same logic as in the single channel disorder problem, we split the integral into two parts, one that is flat in replica space, \mathcal{A} and another which is diagonal in the replicas, \mathcal{B} , as seen in eq. (3.30).

$$\mathcal{A} + \mathcal{B} = \left\langle e^{2i\theta_i^\alpha(x, \tau) - 2i\theta_j^\beta(x, \tau')} \right\rangle_> \quad (3.30a)$$

$$\mathcal{A} = e^{-2\langle \theta_i^\alpha(x, \tau) \theta_j^\alpha(x, \tau) \rangle_>} e^{-2\langle \theta_i^\beta(x, \tau') \theta_j^\beta(x, \tau') \rangle_>} \quad (3.30b)$$

$$\mathcal{B} = e^{-2\langle \theta_i^\alpha(x, \tau) \theta_j^\alpha(x, \tau) \rangle_>} e^{-2\langle \theta_i^\beta(x, \tau') \theta_j^\beta(x, \tau') \rangle_>} \left(e^{4\langle \theta_i^\alpha(x, \tau) \theta_j^\beta(x, \tau') \rangle_>} - 1 \right) \quad (3.30c)$$

We are therefore required to calculate correlations of the form given in eq. (3.31)

which is done straightforwardly at zero temperature.

$$\left\langle \theta_i^\alpha(x, \tau) \theta_j^\beta(x, \tau') \right\rangle_{>} = \int \frac{dq}{2\pi} \frac{d\omega}{2\pi} e^{i\omega(\tau-\tau')} \left\langle \theta_i^\alpha(-q, -\omega) \theta_j^\alpha(q, \omega) \right\rangle_{>} \delta^{\alpha\beta} \quad (3.31a)$$

$$= \frac{1}{2} \delta^{\alpha\beta} K_{ij} \int_{\Lambda'}^{\Lambda} \frac{d|\Omega|}{|\Omega|} J_0(|\Omega|(\tau - \tau')) \quad (3.31b)$$

$$\stackrel{\tau \rightarrow \tau'}{=} \frac{1}{2} \delta^{\alpha\beta} K_{ij} \log \left(\frac{\Lambda}{\Lambda'} \right) \quad (3.31c)$$

We thus arrive at \mathcal{A} in eq. (3.32), which has the same form as for the single channel case, except where $K \rightarrow K_{ij}$.

$$\mathcal{A} = \left(\frac{\Lambda}{\Lambda'} \right)^{-2K_{ij}} \quad (3.32)$$

Calculating the contribution diagonal in the replicas is somewhat more challenging. For the case where $i = j$ we can perform the same expansion for $|\tau - \tau'| \ll \frac{1}{\Lambda}$ that proved successful in the single channel problem. This involved carefully expanding out the ‘normal ordered’ cosine, in order to get a correction to $(\partial_\tau \theta_i^\alpha)^2$, this is given in eq. (3.33) where the disorder has been rescaled as in eq. (2.98).

$$\delta S_{\mathcal{B}}^{ii} = \sum_{\alpha} \frac{\tilde{D}_{ii}}{2\pi} \int dx d\tau (\partial_\tau \theta_i^\alpha)^2 \left(1 - \left(\frac{\Lambda}{\Lambda'} \right)^{-2K_{ii}} \right) \quad (3.33)$$

Alas the small time expansion has no utility when dealing with the off diagonal case, $i \neq j$: the RG simply generates new terms. For this reason we restrict ourselves to the case of ‘uncorrelated disorder’ by which we mean

$D_{ij} = D_j \delta_{ij}$. This is not too unreasonable a simplification, for instance if the system comprises of two coupled nano-wires there is no reason for the impurity potentials in either channel to be correlated.

$$\frac{d\tilde{D}_i}{dl} = (3 - 2K_{ii}) \tilde{D}_{bi} \quad (3.34)$$

$$\frac{d(\mathbf{V}_-^{-1})_{ij}}{dl} = 2K_{ii} \tilde{D}_i \delta_{ij} \quad (3.35)$$

$$\frac{d\mathbf{V}_+}{dl} = 0 \quad (3.36)$$

Taking the new reduced cut-off to be infinitesimally small we arrive at the RG equations given in eqs. (3.34) to (3.36). These equations have the same structure as for the single channel case, given in eqs. (2.99) and (2.102), where the diagonal elements of the Luttinger matrix play the role of the Luttinger parameter, as in the case of the single impurity problem. The fact that the density interaction matrix, \mathbf{V}_+ , does not renormalise tells us that density-density interactions are unaffected by disorder as well as the combination $\frac{v_i}{K_i}$ in each channel. Care should also be taken with eq. (3.35), where it should be stressed that it is the diagonal elements of the inverse current interaction matrix and not the inverse of the diagonal elements that are renormalised, hence as well as renormalisation of the intra-channel Luttinger parameters and velocities the current-current interactions are also affected.

We have now derived the RG equations for the problem of a multi-channel Luttinger liquid with a random disorder potential in each channel. This has been done for a generic system for which the MLL appropriately describes the physics, provided the disorder is only correlated inside the channel. In order

to solve the RG equations we need to consider more specific systems, the rest of this chapter will be dedicated to solving these equations in two disparate limits: a periodic lattice of identical channels; and just two generic channels.

3.4.1 Lattice of Identical Channels

This section considers an periodic array of channels, this allows us to use the translational symmetry of the problem to greatly simplify the equations. The physical situation this model pertains to would be a highly anisotropic 3D solid, which would be comprised of a 2D lattice of 1D systems, it would work equally well for an artificial bundle of wires. This work is contained within ref. [36].

One might be tempted to wonder whether this weak coupling between channels means the system is no longer 1D. The stability of such a system is analysed in ref. [16]. The conclusions of which are that a lattice of Luttinger liquids is stable provided inter-wire tunnelling, of both the single and two particle type is suppressed.

The first step is to take advantage of the translational symmetry which the lattice model provides. This allows us not to think of matrices but of scalar fields defined on the lattice. We will denote the lattice as \mathcal{L} , and the position as $\vec{R} \in \mathcal{L}$. Provided the system forms a Bravais lattice we can take $\mathbf{V}_{\pm} \rightarrow V_{\pm}(\vec{R} - \vec{R}')$. If we did not have a Bravais lattice, but for example a periodic array with two inequivalent sites, we would instead have another matrix whose size was determined by the number of inequivalent sites inside the unit cell. This representation has drastic effects on eq. (3.13), which becomes

a scalar equation.

$$\sum_{\vec{R}_l, \vec{R}_m \in \mathcal{L}} K(\vec{R}_i - \vec{R}_l) V_+(\vec{R}_l - \vec{R}_m) K(\vec{R}_m - \vec{R}_j) = V_-(\vec{R}_i - \vec{R}_j) \quad (3.37)$$

Note that what was hitherto referred to as a diagonal element of the Luttinger matrix now corresponds to $K(\vec{r} = 0)$. One can easily solve for this Luttinger ‘matrix’ with the help of a lattice Fourier transform.

$$F(\vec{R}) = \int_{BZ} \frac{d^d q}{(2\pi)^d} F(\vec{q}) e^{i\vec{q} \cdot \vec{R}} \quad (3.38a)$$

$$F(\vec{q}) = \sum_{\vec{R} \in \mathcal{L}} F(\vec{R}) e^{-i\vec{q} \cdot \vec{R}} \quad (3.38b)$$

Here d denotes dimensionality of the lattice, typically 2D, and BZ is the Brillouin zone. The Luttinger matrix is given in eq. (3.39).

$$K(\vec{r}) = \int_{BZ} \frac{d^d q}{(2\pi)^d} \sqrt{\frac{V_-(\vec{q})}{V_+(\vec{q})}} e^{i\vec{q} \cdot \vec{r}} \quad (3.39)$$

Remembering that the channels are all identical, we take $D_i(l) \rightarrow D(l)$ in each channel. The RG equations reduce to eqs. (3.40) and (3.41).

$$\frac{dD(l)}{dl} = (3 - 2K_{r=0})D, \quad D(0) = D_0 \quad (3.40)$$

$$\frac{dV_-^{-1}(q)}{dl} = 2K_{r=0}D, \quad V_-^{-1}(0) = V_0^{-1} \quad (3.41)$$

Just as in the single channel case, the point $K_{r=0} = \frac{3}{2}$ is clearly special, and governs the metal-insulator transition. We therefore attempt to zoom into the transition, by linearising $K_{r=0}$ about its critical value. To this end we

re-parametrise $V_-^{-1}(q; l)$ as in eq. (3.42).

$$V_-^{-1}(q; l) = V_0^{-1}(q) + c(l) \quad c(l=0) = 0 \quad (3.42)$$

There is a critical value of $c = c^*$ at which the transition takes place, namely $K(c^*) = \frac{3}{2}$, if we take the system to start close to the transition it follows that $c^* \ll 1$ and we may expand $K_{r=0}$ for small c , as seen in eq. (3.43).

$$K_{r=0} \approx K_{r=0}^0 - \kappa c \quad (3.43)$$

$$\kappa = - \left. \frac{dK_{r=0}(c)}{dc} \right|_{c=0} = \frac{1}{2} \int \frac{d^d q}{(2\pi)^d} \frac{V_0^{-3/2}(\vec{q})}{V_+^{1/2}(\vec{q})} \quad (3.44)$$

We now introduce the parameter $\delta = K_{r=0}^0 - \frac{3}{2}$ which is simply the initial detuning from the transition, and it is assumed small. The equations can now be cast into the Berezinskii–Kosterlitz–Thouless form as for the single channel problem in terms of the variables $x = \kappa c - \delta$ and $y = \sqrt{3D}$.

$$x' = \kappa y^2, \quad x(l=0) = -\delta \quad (3.45)$$

$$y' = xy, \quad y(l=0) = \sqrt{3D_0} \quad (3.46)$$

These equations are the same as in section 2.4.2 and yield to the exact same analysis. There is hence an integral of motion corresponding to the energy of a particle in an exponential potential.

$$E = \frac{1}{2} \left(\frac{x^2}{\kappa} - y^2 \right) \quad (3.47)$$

$$= \frac{1}{2} \left(\frac{\delta^2}{\kappa} - 3D_0 \right) \quad (3.48)$$

Whether the disorder grows under RG depends upon whether the energy is positive or negative just as with a single channel (see fig. 2.10). If the energy is negative the disorder blows up, however if it is positive and if the initial detuning is positive, $\delta > 0$, the disorder will become irrelevant leading to a conducting solution. The conditions for the various possibilities are summarised in eq. (3.49).

$$\delta > \sqrt{3\kappa D_0} > 0 \quad \mathbf{Conducting} \quad (3.49a)$$

$$\delta < \sqrt{3\kappa D_0} > 0 \quad \mathbf{Insulating} \quad (3.49b)$$

$$\delta < 0 \quad \mathbf{Insulating} \quad (3.49c)$$

What makes this problem different to the single channel disorder problem is contained within the parameters κ and δ . Inter-channel interactions will increase κ and hence shrink the conducting region in x, y space, however one should remember δ gives the detuning from the Luttinger matrix, $K_{r=0} = \frac{3}{2}$, and not the intra-channel Luttinger parameter. Inter-channel interactions may allow the Luttinger matrix to be close to the transition even if the original Luttinger parameter is well below it.

This concludes our treatment of disorder in a lattice of identical wires. We have derived the full RG equations, eqs. (3.40) and (3.41), which describe a metal-insulator transition when the lattice analogue of the Luttinger matrix $K_{r=0} = \frac{3}{2}$. The RG flow can be solved in the vicinity of this transition and is found to be of the Berezinskii-Kosterlitz-Thouless type, where inter-channel interactions shift the boundary between the conducting and insulating phases.

3.4.2 Two Disordered Channels

We will now turn our gaze upon the problem of a two channel MLL in the presence of disorder. Here we generalise the work of Crépin, Zaránd and Simon[14, 15] which focused on disordered Bose-Fermi mixtures with density-density interactions only. The Luttinger matrix formalism allows us to easily consider current-current interactions, as well as to greatly simplify the equations in the vicinity of the metal-insulator transition. Again this work is published in ref. [36].

The RG equations are those given earlier in eqs. (3.34) to (3.36) where the form of the interaction matrices and Luttinger matrix are those of the two-channel Luttinger liquid, eqs. (3.19), (3.21) and (3.22). An explicit expression for the inverse current interaction matrix is given in eq. (3.50).

$$\mathbf{V}_-^{-1} = \frac{1}{1 - \alpha_-^2} \begin{pmatrix} \frac{1}{v_1 K_1} & \frac{-\alpha_-}{\sqrt{v_1 K_1 v_2 K_2}} \\ \frac{-\alpha_-}{\sqrt{v_1 K_1 v_2 K_2}} & \frac{1}{v_2 K_2} \end{pmatrix} \quad (3.50)$$

As we know from the RG equations disorder precipitates the renormalisation of the diagonal elements of \mathbf{V}_- only. This means that as well as the velocities and Luttinger parameters in each channel undergoing renormalisation the current-current interaction, α_- also renormalises. Note that the density-density interaction, α_+ does not renormalise. The full RG equations in terms

of these parameters are given in eq. (3.51).

$$\frac{dD_1}{dl} = (3 - 2K_{11})D_1, \quad \frac{dD_2}{dl} = (3 - 2K_{22})D_2 \quad (3.51a)$$

$$\frac{dv_1}{dl} = \frac{v_1}{K_1} \frac{dK_1}{dl}, \quad \frac{dv_2}{dl} = \frac{v_2}{K_2} \frac{dK_2}{dl} \quad (3.51b)$$

$$\frac{dK_1}{dl} = -v_1 K_1^2 K_{11} D_1 - \alpha_-^2 v_2 K_1 K_2 K_{22} D_2 \quad (3.51c)$$

$$\frac{dK_2}{dl} = -v_2 K_2^2 K_{22} D_2 - \alpha_-^2 v_1 K_2 K_1 K_{11} D_1 \quad (3.51d)$$

$$\frac{d\alpha_-}{dl} = -\alpha_- (1 - \alpha_-^2) (v_1 K_1 K_{11} D_1 + v_2 K_2 K_{22} D_2) \quad (3.51e)$$

$$\frac{d\alpha_+}{dl} = 0 \quad (3.51f)$$

As one can see, these equations are highly non-linear, and as such there are only a few routes available to us. For one, we can try to analyse these equations numerically, or else we can attempt to zoom into the transition as with the single channel case, section 2.4.2, and the identical many-channel case, section 3.4.1. However, let us first attempt to get a qualitative idea of what the equations are telling us.

Clearly $K_{ii} = \frac{3}{2}$ marks a transition in the i^{th} channel. If $K_{ii} > \frac{3}{2}$ then the disorder is decreasing just as with the other realisations of the disorder problem. The velocities can be solved for with ease, and their values are simply slaved to that of the corresponding Luttinger parameter, as in eq. (3.52).

$$v_i(l) = \frac{v_i(l=0)}{K_i(l=0)} K_i(l) \quad (3.52)$$

We should also remember that $K_i > 0, D_i > 0$ and $\alpha_-^2 > 0$, hence the RG

equations for K_1, K_2 and α_- can only bring the values of these parameters closer to zero. The disorder therefore makes the two channels behave more like repulsive fermions by reducing the intra-channel Luttinger parameters, as in the single channel case, and it also strives to reduce the current-current interaction strength regardless of its sign whilst leaving the density-density interactions unaffected.

Each solution to eq. (3.51) is defined by seven parameters and whatever scale we choose to stop the renormalisation at. These parameters are initial conditions $K_1^0, K_2^0, y_1^0, y_2^0, \beta_0, \alpha_-^0$ and α_+ , where we have defined the ratio of velocities $\beta = \frac{v_2}{v_1}$. The thought of dealing with a seven-dimensional space is somewhat unappealing, however we are fortunate in that three of these parameters are relatively boring.

The results of numerically analysing the RG equations can be seen in figs. 3.3 to 3.10. The algorithm works as follows: for a given initial value of the parameters the system is solved up to $l = 80$ or once either of the disorders becomes too large, the gradient of the disorder is then checked just before the endpoint of the solution to see if it is growing or shrinking, depending upon the gradient the solution is assigned a numerical value. We have four possible outcomes: insulating in both channels, (ii)-phase; insulating in one channel and conducting in the other, (ic)- and (ci)-phases; conducting in both channels, (cc)-phase. The figures show the phases as a function of the two bare intra-channel Luttinger parameters, K_1^0 and K_2^0 .

The ratio of velocities simply biases one channel in favour of the other, as can be seen in fig. 3.4. The higher the initial values of disorder, y_1^0 and y_2^0 , the higher the Luttinger parameter has to be in order for the disorder to become

irrelevant. We can therefore think of the initial disorder values as simply setting a scale, see fig. 3.5. We therefore only need to vary four parameters in order to get a good picture of what the physics is.

As expected for no inter-channel interactions we simply have flat boundaries showing the four possible phases, see fig. 3.3. When density-density interactions are switched on, fig. 3.6, the picture becomes more interesting. We know from eq. (3.19) that the higher the density-density interaction the lower the relevant Luttinger parameter can be for $K_{ii} = \frac{3}{2}$, the effect of this can be seen as a large enhancement of the (cc)-phase. However what is more interesting is the suppression of the mixed phases close to the simultaneous transition in both channels, more will be said about this later. If one looks at a point where one channel is deep inside its insulating phase, for example $K_2^0 < 1$, the boundary between the (ii)- and (ci)-phases is at $K_1^0 = \frac{3}{2}$ as if the density-density interactions were not there. This can be understood from looking at the RG equations, if we are in a situation where the disorder is relevant in one channel, the corresponding Luttinger parameter (and therefore velocity) is being made increasingly small. In this limit the diagonal element of the Luttinger matrix in the other channel reverts to being the Luttinger parameter once again. Hence far away from the simultaneous transition, density-density interactions are irrelevant.

Current-current interactions affect the system in a somewhat different way, see fig. 3.7. For starters α_- reduces rather than enhances the (cc)-phase, however the mixed phases are still suppressed close to the simultaneous transition here also. The fact that the current-current interaction is renormalised as well means the behaviour far away from the simultaneous transition is a little dif-

ferent than in the density-density case. Even if one channel is fairly firmly localised the current-current interactions still effect the value at which the other channel has its metal-insulator transition.

When both types of interaction are present, figs. 3.8 and 3.10, we see that they are in competition with one another. This leaves the (cc)-region largely unaffected, however the boundaries of the mixed phases are severely altered. Close to the simultaneous transtion they are once again suppressed, and far way from this point the system behaves as if the density-density interactions are not there.

Regardless of which parameters we pick, provided there are inter-channel interactions we see a suppression of the mixed (ci)- and (ic)-phases. In order to understand this we will now simplify the RG equations, eq. (3.51), close to the simultaneous transition, $K_{11} = K_{22} = \frac{3}{2}$, in order to make analytic progress. To do so we will introduce the matrix \mathbf{c} which parametrises the deviation of the current-current matrix from its starting value.

$$\mathbf{V}_{-}^{-1}(l) = \mathbf{V}_{-}^{-1}(l=0) + \mathbf{c}(l) \quad (3.53)$$

Where $\mathbf{c} = \text{diag}(c_1, c_2)$ is diagonal with the initial values $c_i(l=0) = 0$. Introducing the diagonal disorder matrix $\mathbf{D} = \text{diag}(D_1, D_2)$ and $\tilde{\mathbf{K}} = \text{diag}(K_{11}, K_{22})$ to simplify notations we arrive at eqs. (3.54) and (3.55).

$$\frac{d}{dl} \mathbf{D} = (3 - 2\tilde{\mathbf{K}}) \mathbf{D} \quad (3.54)$$

$$\frac{d}{dl} \mathbf{c} = 2\tilde{\mathbf{K}} \mathbf{D} \quad (3.55)$$

We can now parametrise the Luttinger matrix in terms of the c variables, which

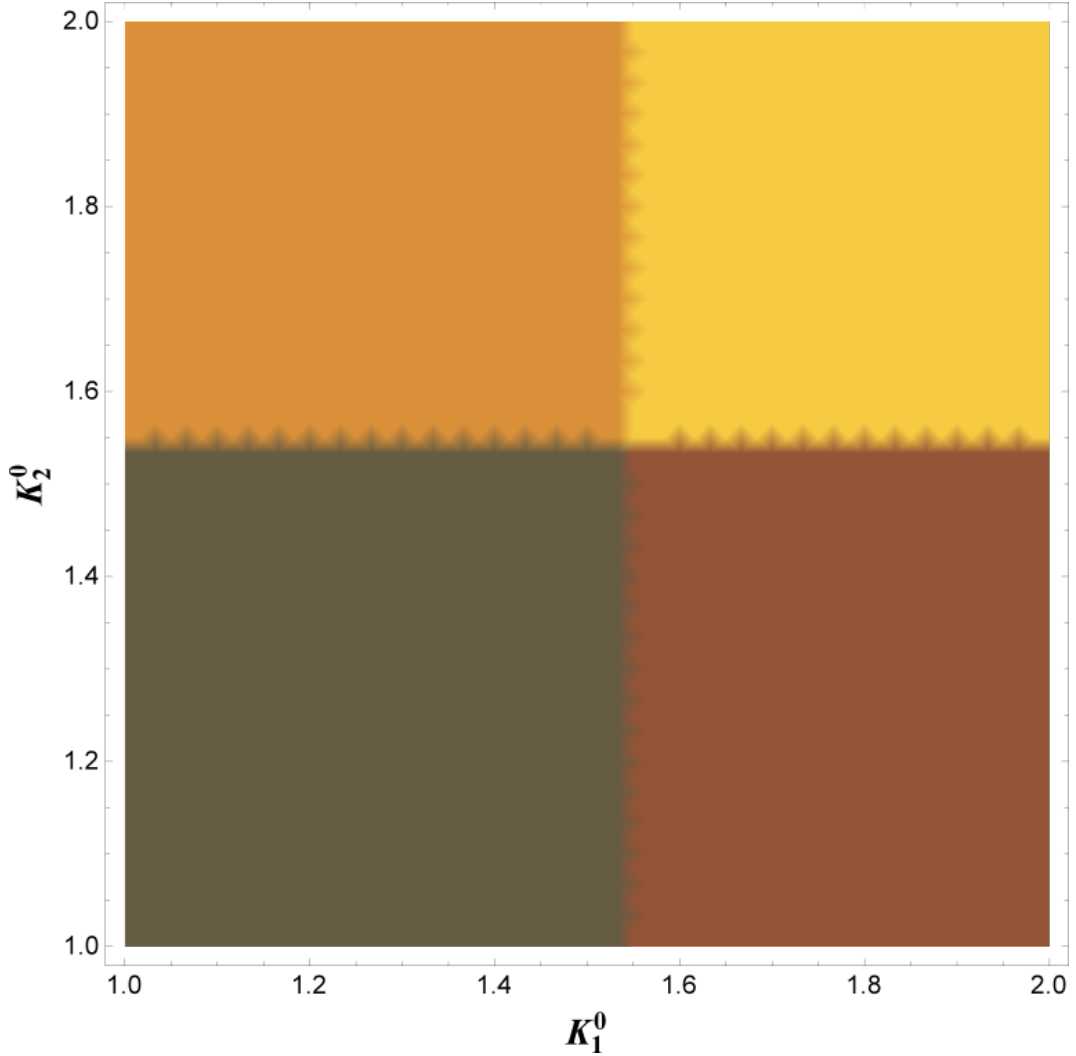


Figure 3.3: Numerical analysis of eq. (3.51). Here we show the fate of disorder as a function of the two initial values of the intra-channel Luttinger parameters, K_1^0, K_2^0 . The yellow region: disorder is irrelevant in both channels. Dark region: disorder is relevant in both channels. Muddy region: disorder is irrelevant in the first channel only. Orange region: the disorder survives in the second channel only. The relevance of the disorder is determined by looking at the gradient of the disorder after a long time, $y_i(l_f)$. Here the initial ratio of velocities, $\beta_0 = 1$ and the initial inter-channel interactions are $\alpha_-^0 = 0$ and $\alpha_+ = 0$. This shows the expected uncoupled behaviour.

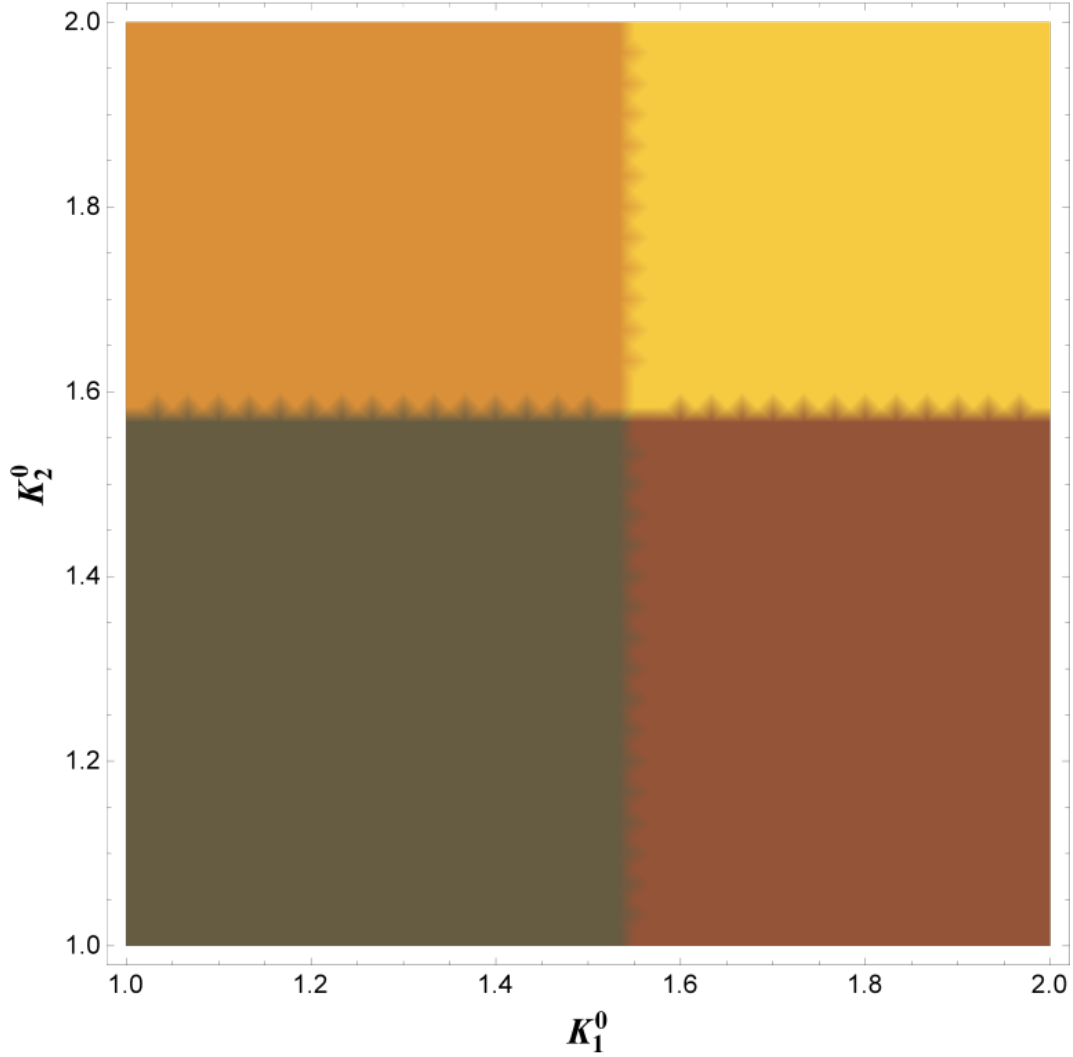


Figure 3.4: Same as in fig. 3.3 except for here the initial ratio of velocities, $\beta_0 = 2$ and the initial inter-channel interactions are $\alpha_-^0 = 0$ and $\alpha_+ = 0$. The boundaries between conducting and insulating behaviour are shifted by changing the ratio of velocities between the channels. The higher β is the larger the value of K_2^0 required to have conducting behaviour.

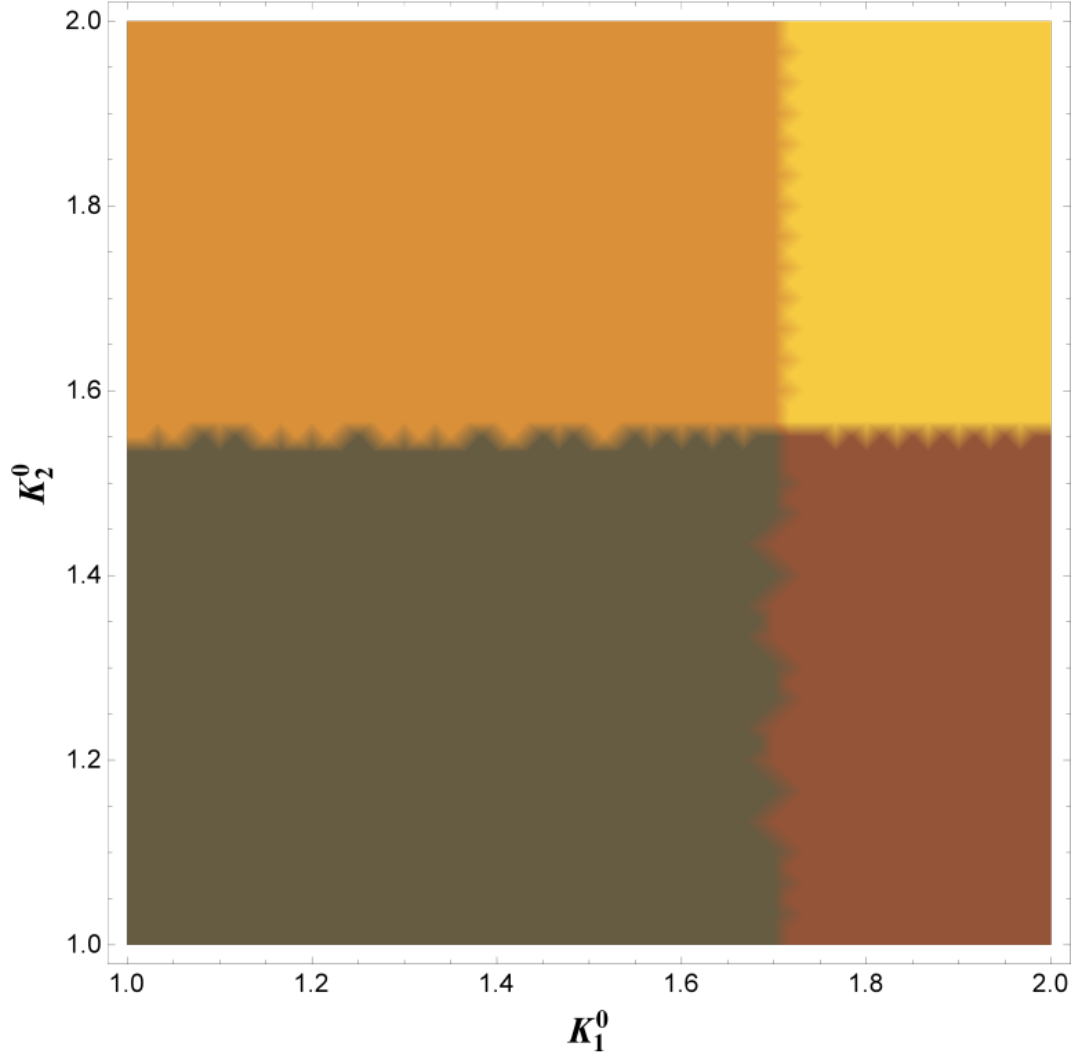


Figure 3.5: Same as in fig. 3.3 except for here the initial ratio of velocities, $\beta_0 = 1$ and the initial inter-channel interactions are $\alpha_-^0 = 0$ and $\alpha_+ = 0$. However the initial disorder in the two channels is different, $D_1^0 = 0.01v_1^0$ and $D_2^0 = 0.001v_1^0$. The effect of this is to shift the boundaries at which the metal-insulator transitions occur.

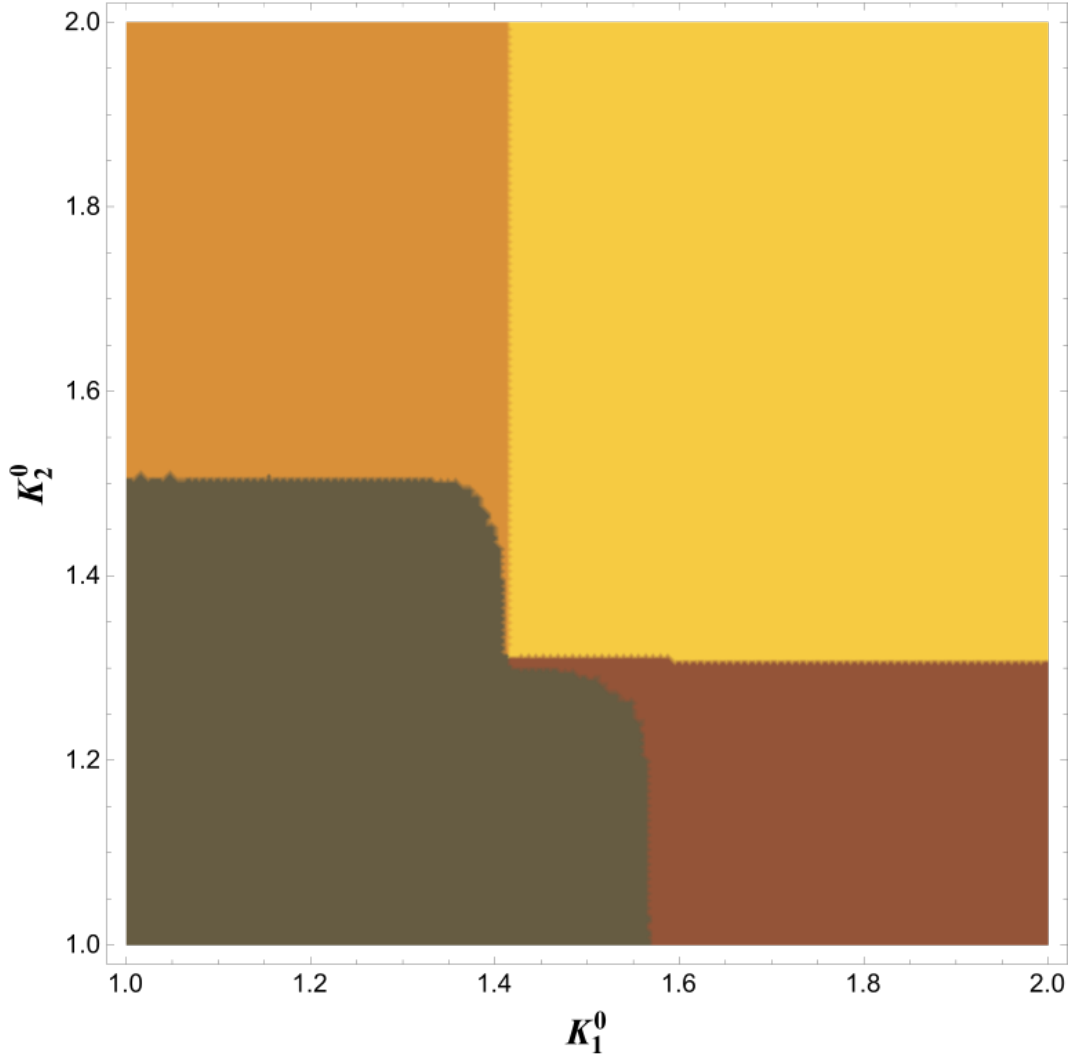


Figure 3.6: Same as in fig. 3.3 except for here the initial ratio of velocities, $\beta_0 = 1$ and the initial inter-channel interactions are $\alpha_-^0 = 0$ and $\alpha_+ = 0.6$. Positive density-density interactions lower the required value of both Luttinger parameters to arrive at a conducting solution. However the mixed phase is affected quite strongly, once one channel becomes insulating, the other channels begins to behave as if the interactions are switched off. Note the suppression of the mixed phase close to the simultaneous transition, this will be picked up on later.

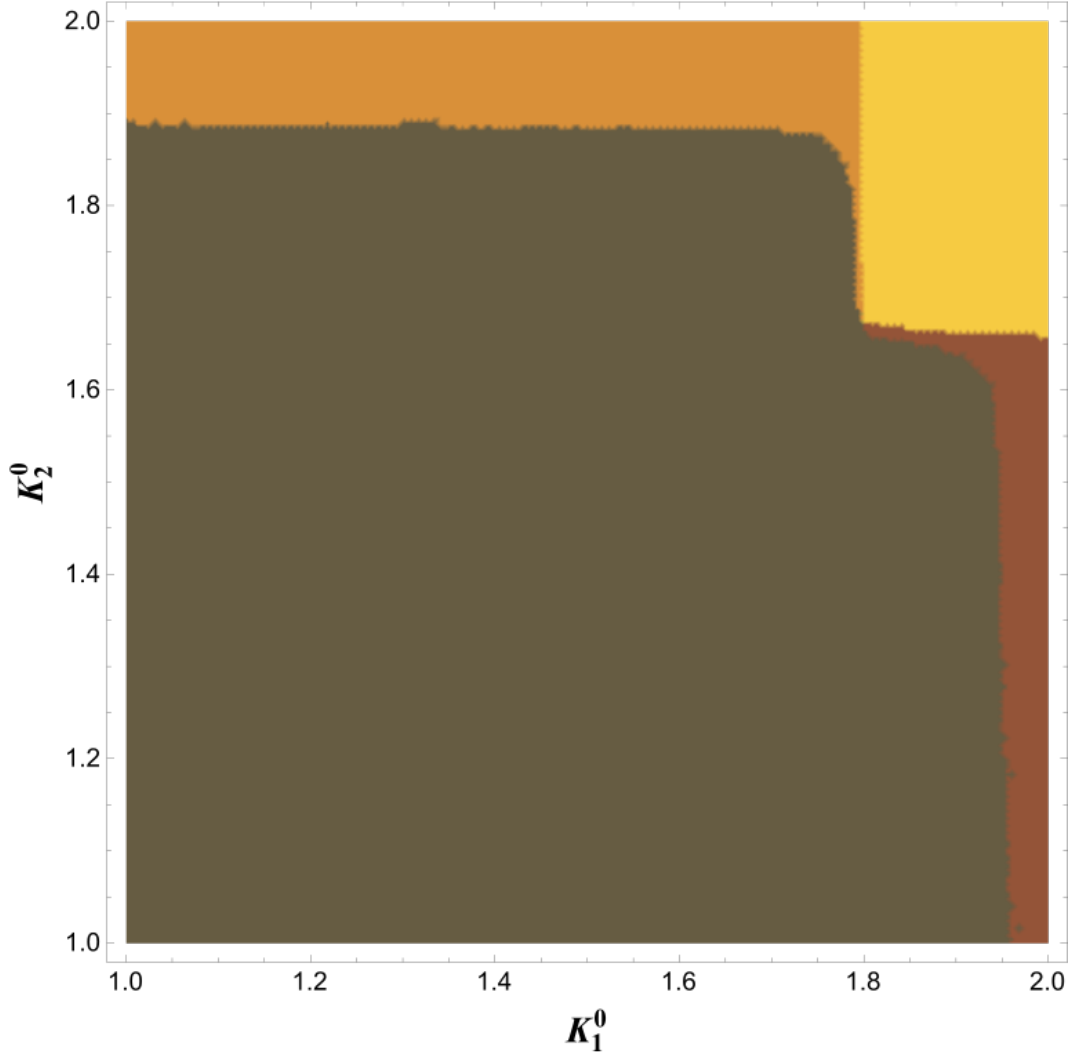


Figure 3.7: Same as in fig. 3.3 except for here the initial ratio of velocities, $\beta_0 = 1$ and the initial inter-channel interactions are $\alpha_-^0 = 0.6$ and $\alpha_+ = 0$. Positive current-current interactions have the opposite effect to density-density interactions close to the transition: the conducting region is suppressed. The fact that α_- is renormalised plays a significant effect on the mixed region. When one channel is deep inside its localised phase, the current-current interaction can still suppress the conductivity in the other channel. Hence the mixed-insulating boundary does not occur at $K_i = \frac{3}{2}$ as in the density-density case.

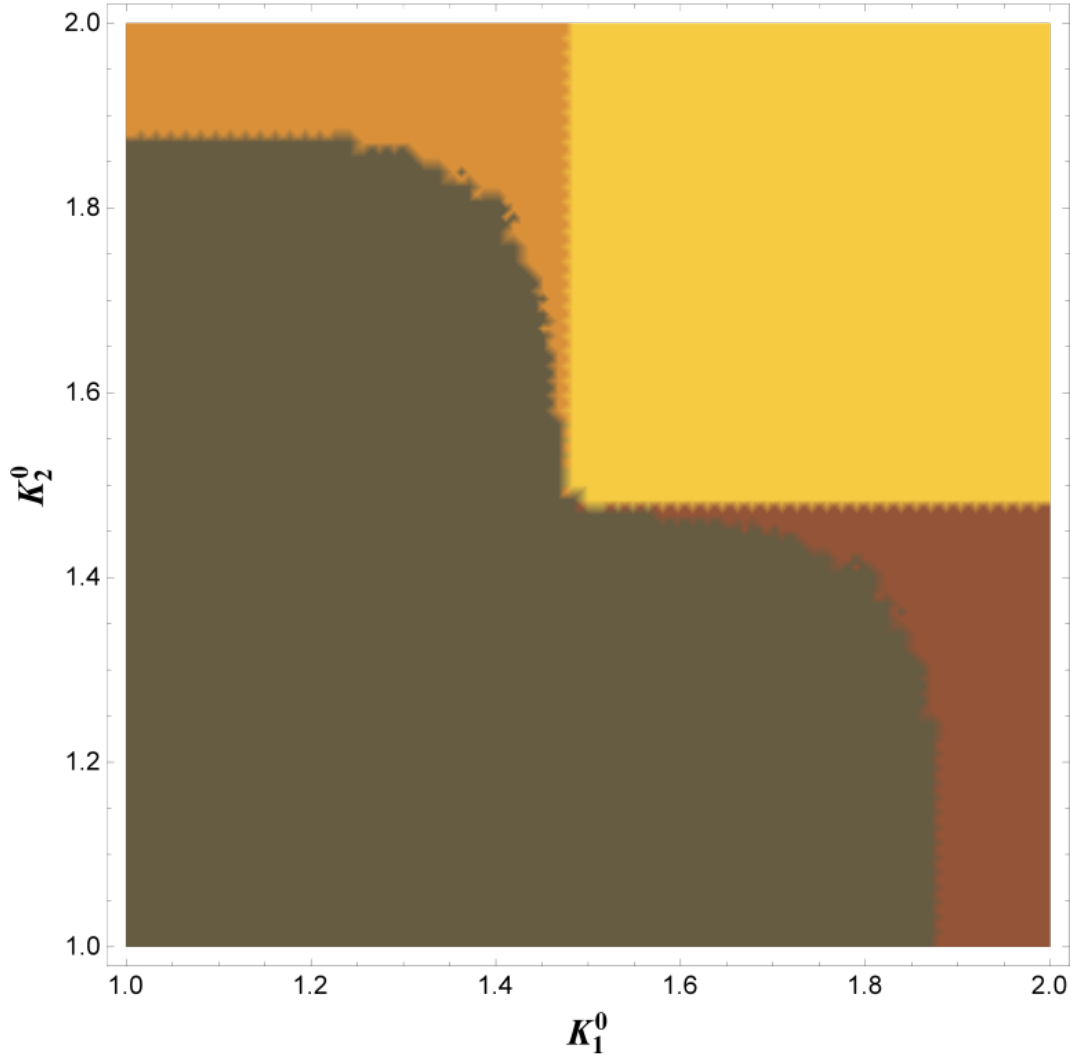


Figure 3.8: Same as in fig. 3.3 except for here the initial ratio of velocities, $\beta_0 = 1$ and the initial inter-channel interactions are $\alpha_-^0 = 0.6$ and $\alpha_+ = 0.6$. This is the special case of equal current-current and density-density interactions. Close to the simultaneous transition the interactions are in competition, and the size of the conducting region is largely unaffected, however the mixed phase is suppressed as before. Away from the transition the density-density interactions behave as if switched off, and the boundaries are defined by the current-current interactions as in fig. 3.7.

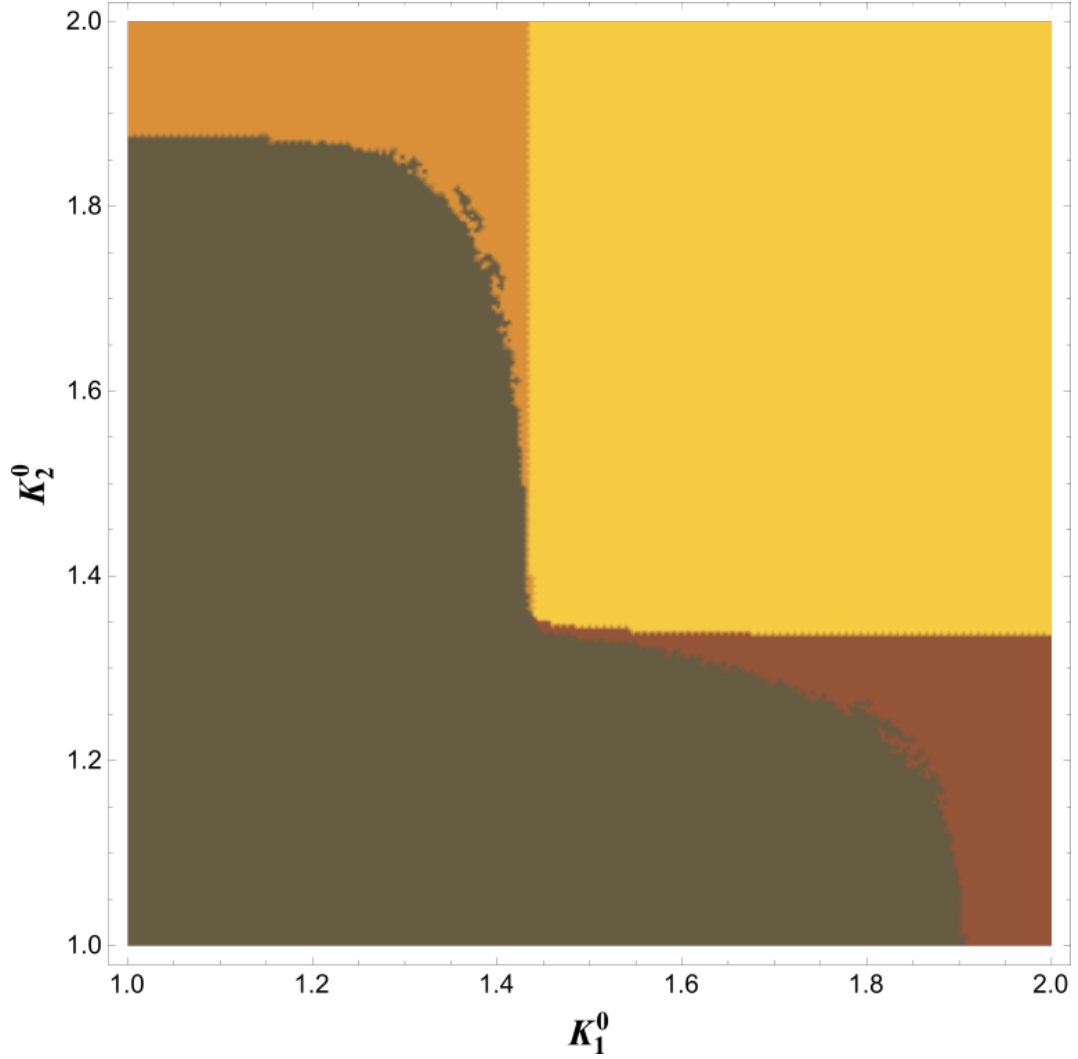


Figure 3.9: Same as in fig. 3.3 except for here the initial ratio of velocities, $\beta_0 = 1$ and the initial inter-channel interactions are $\alpha_-^0 = -0.6$ and $\alpha_+ = 0.6$. Current-Current and density-density interactions of opposite sign reinforce one another, in this case expanding the conducting region. Away from the simultaneous transition the density-density interaction plays little role, as in figs. 3.7 and 3.8.

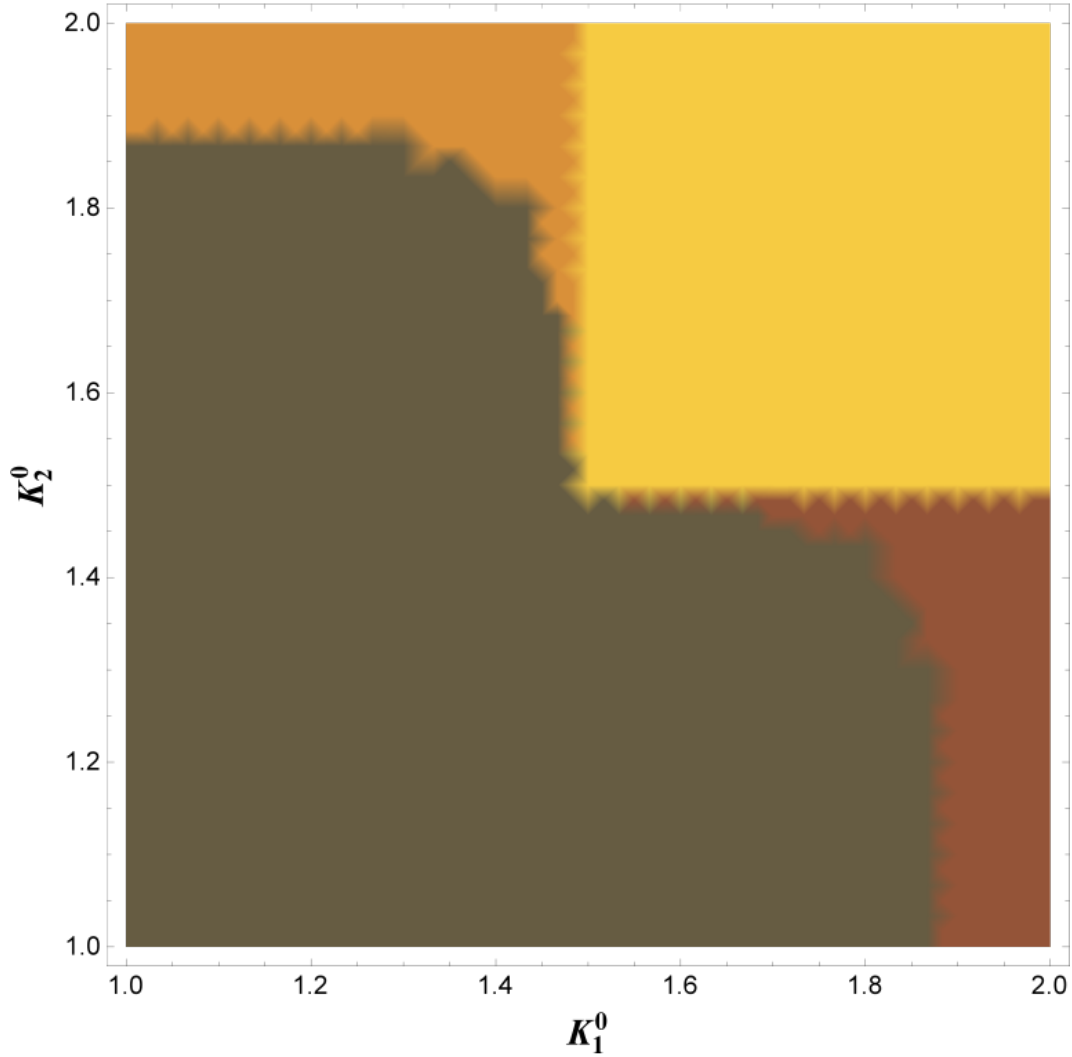


Figure 3.10: Same as in fig. 3.3 except for here the initial ratio of velocities, $\beta_0 = 1$ and the initial inter-channel interactions are $\alpha_-^0 = 0.6$ and $\alpha_+ = -0.4$. Current-Current and density-density interactions of opposite sign reinforce one another, in this case expanding the conducting region. Away from the simultaneous transition the density-density interaction plays little role, as in figs. 3.7 and 3.8.

is advantageous as we know the transition will take place at $K_{ii} = \frac{3}{2}$, and hence it is the Luttinger matrix itself which we wish to linearise in. We thus now have $K_{ii}(c_1, c_2)$, which we are free to expand for small c . We justify the expansion by assuming we start close to the transition, $|K_{ii}(c_1 = 0, c_2 = 0) - \frac{3}{2}| \ll 1$ and therefore neither of the c_i 's will be able to deviate very far from their original values.

$$K_{ii}(c_1, c_2) = K_{ii}^{(0)} - \sum_j \kappa_{ij} c_j \quad (3.56)$$

$$\kappa_{ij} = - \left. \frac{\partial K_{ii}}{\partial c_j} \right|_{c_1=c_2=0} \quad (3.57)$$

All details of the inter-channel interactions are now included within the κ_{ij} parameters. The best way to get an expression for these parameters is to go back to eq. (3.13), and linearise in the Luttinger matrix.

$$\mathbf{K} = \mathbf{K}_0 + \delta\mathbf{K} \quad (3.58)$$

$$\mathbf{K}_0 = \frac{3}{2} \begin{pmatrix} 1 & k \\ k & 1 \end{pmatrix} \quad (3.59)$$

We naturally take the diagonal elements of the Luttinger matrix as being close to $\frac{3}{2}$ however the only restriction on the off-diagonal element is that the Luttinger matrix remains positive-definite, $|k| \leq 1$. We may now combine eqs. (3.13), (3.53) and (3.58) to arrive at a convenient equation for $\delta\mathbf{K}$, eq. (3.60).

$$\mathbf{V}_0^{-1} \delta\mathbf{K} \mathbf{K}_0^{-1} + \mathbf{K}_0^{-1} \delta\mathbf{K} \mathbf{V}_0^{-1} = -\mathbf{c} \quad (3.60)$$

The correction to the Luttinger matrix which solves this equation is given in eq. (3.61) where $\boldsymbol{\tau} = i\hat{\sigma}_y$.

$$\boldsymbol{\delta K} = -\frac{1}{2}\mathbf{V}_0[\mathbf{c} + \omega\boldsymbol{\tau}]\mathbf{K}_0 \quad (3.61)$$

The unknown parameter ω can be straightforwardly found using the condition that the correction to the Luttinger matrix must be symmetric, $\text{tr}(\boldsymbol{\tau}\boldsymbol{\delta K}) = 0$.

$$\omega = \frac{1}{T} \text{tr}(\boldsymbol{\tau}\mathbf{V}_0\mathbf{c}\mathbf{K}) \quad (3.62)$$

$$T = -\text{tr}(\boldsymbol{\tau}\mathbf{V}_0\boldsymbol{\tau}\mathbf{K}) \quad (3.63)$$

$$= \frac{3}{2} (V_-^{11} + V_-^{22} - 2kV_-^{12}) > 0 \quad (3.64)$$

We need simply take the derivative of eq. (3.61) with respect to the appropriate c_j to arrive at κ_{ij} , the results of which are in eqs. (3.65) and (3.67).

$$\kappa_{ii} = \frac{1}{T} [(1 - k^2)V_{ii}^2 + \det(V)] \geq 0 \quad (3.65)$$

$$\kappa = \kappa_{12} = \kappa_{21} \quad (3.66)$$

$$= \frac{1}{T} [(1 - k^2)V_{12}^2 + k^2 \det(V)] \geq 0 \quad (3.67)$$

These parameters are all positive, and contain all the information about the inter-channel interactions. We are now in a position to rewrite the RG equations in a form similar to the single channel case, eq. (2.104).

$$\frac{dy_i}{dl} = x_i y_i, \quad y_i(l=0) = \sqrt{\frac{3}{2}D_i^0} \quad (3.68)$$

$$\frac{dx_i}{dl} = \sum_{j=1,2} \kappa_{ij} y_j^2, \quad x_i(l=0) = -\delta_i \quad (3.69)$$

Where x_i is given in eq. (3.70), $y_i = \sqrt{\frac{3}{2}D_i}$, and δ_i is the detuning from the transition in the i^{th} channel, eq. (3.71).

$$x_i = \sum_j \kappa_{ij} c_j - \delta_i \quad (3.70)$$

$$\delta_i = K_{ii}^{(0)} - \frac{3}{2} \quad (3.71)$$

One should stress that eqs. (3.68) and (3.69) are only valid for a system where both channels are close to the metal-insulator transition, that is to say both $\delta_1, \delta_2 \ll 1$. We have now recast the two-channel disorder problem into a set of coupled BKT equations, as such the analysis on these BKT equations done previously will be of some use. It is worth stating that the correspondence to the BKT transition is largely mathematical and a detailed discussion of the BKT transition is beyond the scope of this thesis.

When inter-channel interactions are switched off we were able to map the RG equations onto a particle in an attractive one dimensional exponential potential. The effect of the interactions is to firstly put the particle into a two dimensional potential, but also to couple the velocities such that we have a ‘tensor mass’, \mathbf{m} . This can be seen in eqs. (3.72) to (3.74), where the positions are related to the disorder by $y_i = e^{q_i}$.

$$L = \frac{1}{2} \dot{\vec{q}} \cdot \mathbf{m} \cdot \dot{\vec{q}} - U(\vec{q}) \quad (3.72)$$

$$U(\vec{q}) = -\frac{1}{2} \sum_i e^{2q_i} \quad (3.73)$$

$$\mathbf{m} = \begin{pmatrix} m_1 & -m \\ -m & m_2 \end{pmatrix} = \boldsymbol{\kappa}^{-1} \quad (3.74)$$

This Lagrangian has an associated Hamiltonian which is conserved. Note that in the uncoupled scenario, the Lagrangian decomposes into one for each channel, $L = \sum_i L_i$, each with their own conserved energy E_i . The coupling therefore reduces the number of integrals of motion from two to one, vastly complicating things. The conserved total energy, E , is given by eq. (3.75) and the no longer conserved ‘energies’ of the individual channels, E_i , by eq. (3.76).

$$E = \frac{1}{2} \dot{\vec{q}} \cdot \mathbf{m} \cdot \dot{\vec{q}} - \frac{1}{2} \sum_i e^{2q_i} \quad (3.75)$$

$$E_i = \frac{1}{2} m_i \dot{q}_i^2 - \frac{1}{2} e^{2q_i} \quad (3.76)$$

As the number of conserved quantities is reduced, we are unable to construct analytic solutions as with the uncoupled system, (eqs. (2.107) and (2.109)), however if we assume weak inter-channel coupling, $m \ll 1$, we can get a perturbative picture in which the individual channel energies change adiabatically.

This adiabatic solution is given by eq. (3.77).

$$D_i(l) = e^{2q_i(l)} = \frac{m_i k_i^2(l)}{\sinh^2(\theta(l))} \quad (3.77)$$

$$\theta_i(l) = \int_0^l dl' k_i(l') + \chi_i \quad (3.78)$$

$$E_i = \frac{1}{2} m_i k_i^2(l) \quad (3.79)$$

Where the definition of χ follows eqs. (2.108) and (2.110). Clearly the sign of the energy has a massive effect upon the character of the solution, and as the energy is no longer conserved we have to be careful. For instance if we start off with positive energy in a particular channel, the energy change may be significant enough for the channel energy to become negative forcing us to switch to the insulating solution.

We can use the conservation of the total energy to construct equations for how the energy changes in each channel, given in eq. (3.80).

$$\dot{E}_i = m \dot{q}_i \ddot{q}_{-i} \quad (3.80)$$

Here the notation $-i$ is to be read as not i . As the change in channel energy is already linear in the inter-channel coupling, m we may simply use the non-interacting solutions of eqs. (2.107) and (2.109) and still be accurate to linear order in the coupling.

One can see from the Lagrangian that $\ddot{q}_i = \kappa_{ij} e^{2q_j} \geq 0$ for all classes of solution. Therefore the sign of \dot{q}_i will give us valuable clues as to what is happening in the weak coupling regime. When dealing with the positive energy conducting solution, we have $\dot{q}_i \leq 0$, whereas the negative energy insulating

solution also starts with $\dot{q}_i \leq 0$ before turning positive as it begins to diverge.

Let us start by first analysing the insulating solutions. In this case both channels will start with negative energy, and $\dot{q}_i \leq 0$ until the minimum is reached. In the particle language the minima correspond to when the particle's momentum in each direction runs out, leaving the particle nowhere to go but down the potential resulting in localisation. Negative energy solutions therefore acquire a negative energy shift, meaning insulating solutions remain stable in the face of inter-channel coupling. This can be seen in fig. 3.11.

Positive energy solutions also acquire a negative energy shift, this can be seen in fig. 3.12. Even if both channels start with positive energy, which would naively mean a conducting solution, the negative energy shift could be sufficient enough to force one or both channels into the insulating phase. Hence the boundary of the (cc)-phase is shrunk due to the inter-channel coupling.

The mixed (ic)- and (ci)-phases are also of interest. We have thus far ignored the role of \ddot{q}_{-i} in eq. (3.80) thinking of it only as positive, however its effects are significant when considering the mixed phase. Let us take an example where channel two starts in the insulating phase, and channel one in the conducting phase, we know initially both channels acquire a negative energy shift. This on its own may be enough to force both channels into the insulating phase as discussed above, however something interesting happens even if this initial shift is not enough. As $\ddot{q}_{-i} \propto e^{2q-i}$ as channel two begins to diverge the second derivative is enhanced exponentially, and as such the negative energy shift in channel one also grows exponentially. This can be seen in figs. 3.12 and 3.13 where as soon as one channel starts to diverge, the other is dragged along into the insulating phase. For this reason the mixed

phases do not survive, which is in good agreement with the numerics as seen in figs. 3.3 to 3.10 where we saw the suppression of the mixed phase close to the simultaneous transition.

This concludes our analysis of disorder in multi-channel Luttinger liquids. We derived the RG equations, eqs. (3.34) to (3.36), using the Luttinger matrix formalism to capture the effects of inter-channel interactions. These equations were analysed in two realisations of the MLL: a bravais lattice of identical channels, and two distinct channels. The identical channel case reduced to a BKT transition just as with a single channel where the inter-channel coupling shifts the boundary between the conducting and insulating phases.

The distinct two-channel model proved more varied. We arrived at the somewhat complicated RG equations in terms of the intra-channel parameters, eq. (3.51), which we analysed numerically. Inter-channel interactions of the density-density type reduce the required values of the intra-channel Luttinger parameters to arrive at the (cc)-phase. This was to be expected from looking at the definition of the Luttinger matrix, eq. (3.19), as it is the diagonal elements of this matrix which appear in the RG equations rather than the intra-channel parameters. The behaviour of the mixed (ci)- and (ic)-phases is more unusual, close to the simultaneous transition the mixed phases are highly suppressed, whereas away from the simultaneous transition the mixed phase boundary behaved as if there were no density-density interactions at all.

Current-current interactions result in rather different behaviour, the boundary of the (cc)-phase takes place when both $K_i > \frac{3}{2}$ and hence the system has to behave more like attractive fermions in order to not localise. Away from the simultaneous transition, unlike with density-density interactions, current-

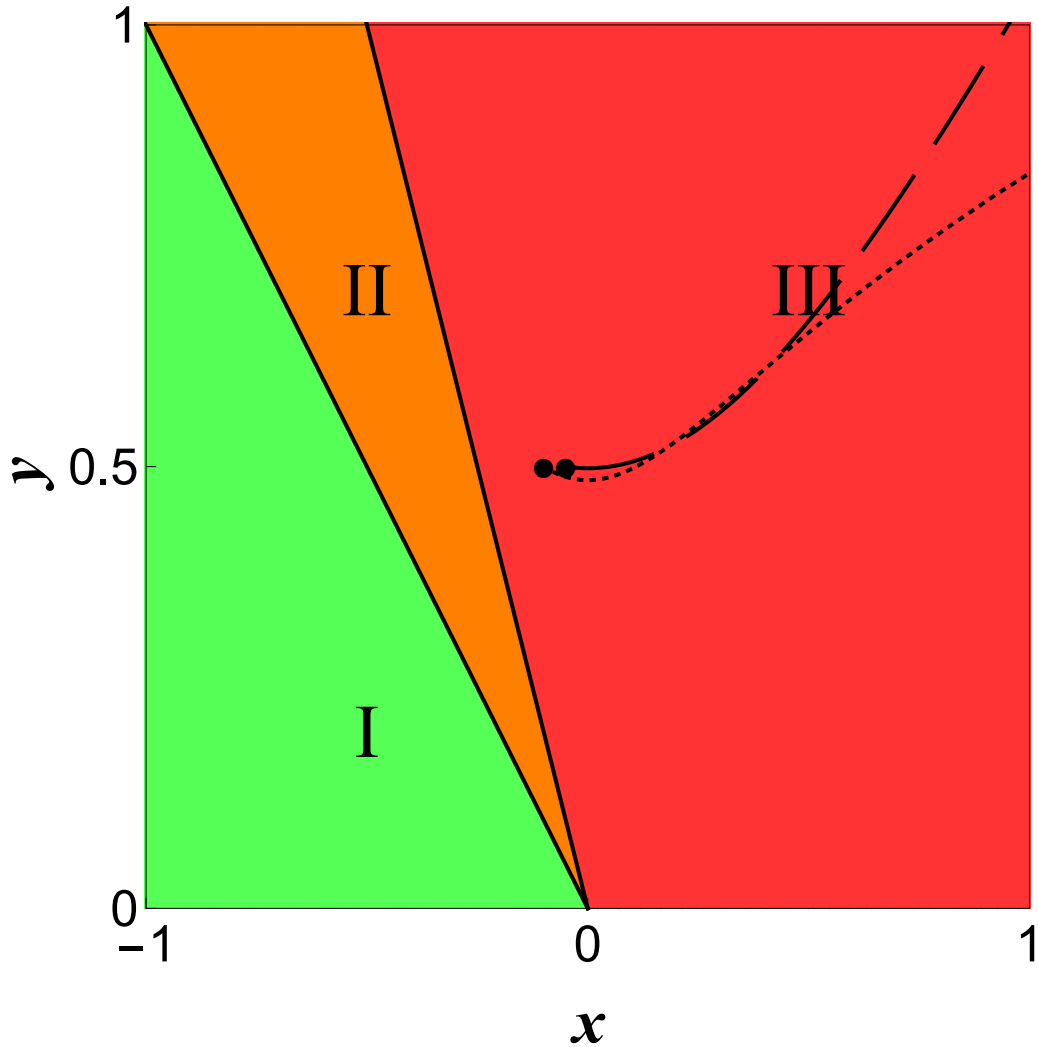


Figure 3.11: Diagram showing the different phases of a two-channel Luttinger liquid. The colours correspond to the three different possibilities in the uncoupled case. Green (I): (cc)-phase, both channels having positive energy. Amber (II): (ic)-phase, where energy is positive in one channel, but negative in the other. Red (III): (ii)-phase, energy is negative in both channels. The trajectories are numerical solutions to the coupled BKT RG equations. Dashed and dotted lines correspond to channel 1 and 2 respectively. Trajectories starting in the (ii)-phase remain in the (ii)-phase. Adapted from ref. [36].

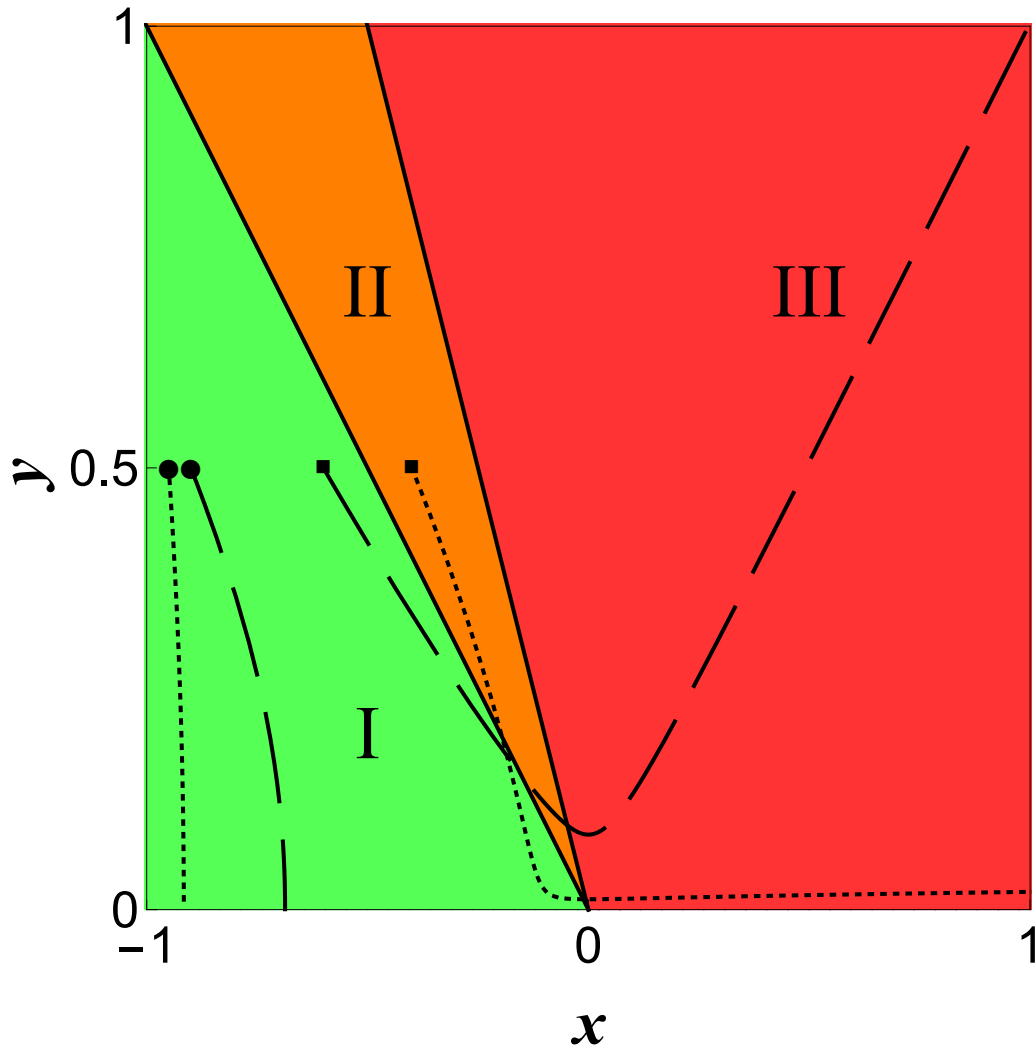


Figure 3.12: See fig. 3.11 for details. Two pairs of trajectories are shown here: those starting with circles are deep in the conducting phase, and the negative energy shift from the coupling is insufficient to change the system qualitatively; the square trajectories also both start with positive energy, however they are much closer to the boundary and the negative energy shift drags channel 1 into the insulating phase, which in turn forces channel 2 to go insulating as well. Adapted from ref. [36]

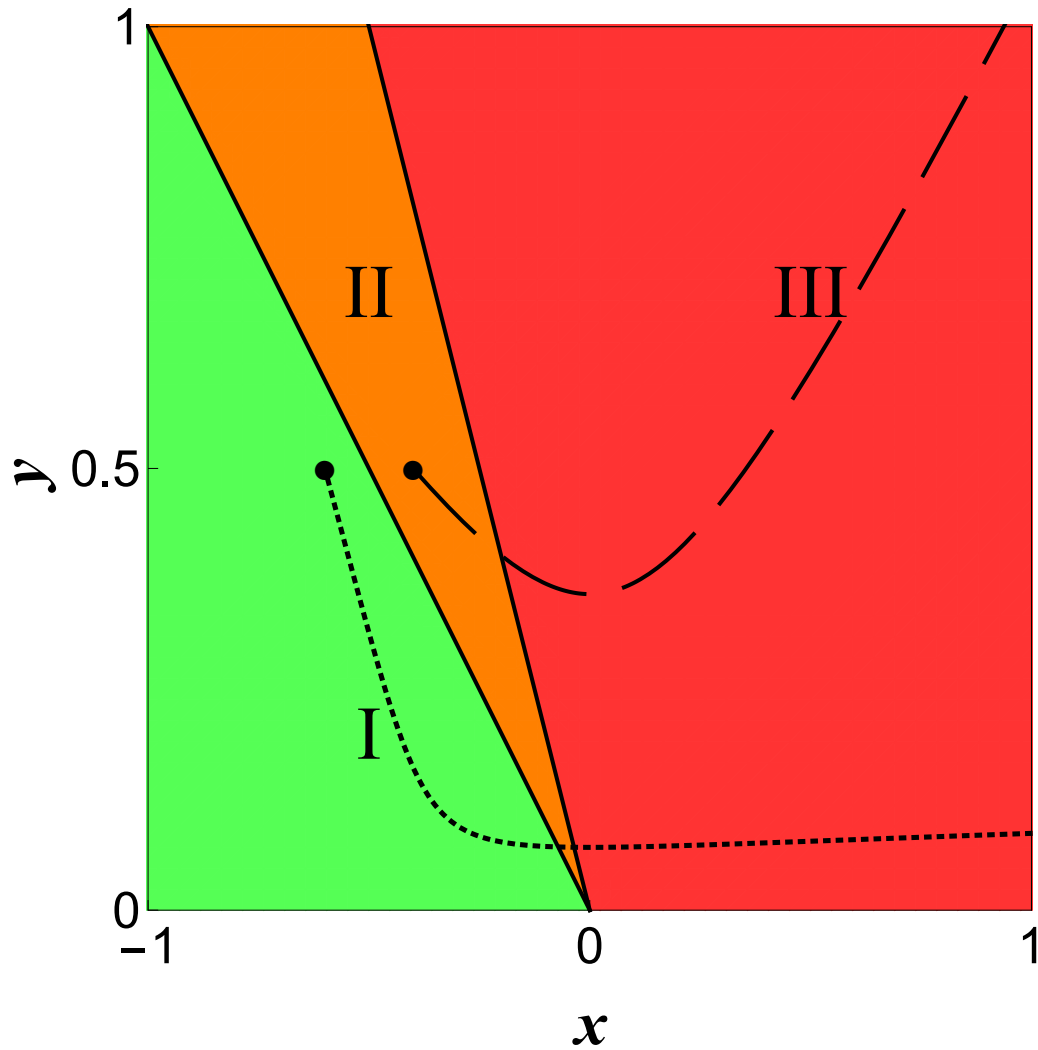


Figure 3.13: See fig. 3.11 for details. The trajectories here start in the non-interacting mixed phase, channel 1 has negative energy but channel two positive. As channel 1 begins to diverge, channel 2 is taken into the insulating region as well. This shows how the mixed (ic)-phase is suppressed close to the simultaneous transition. Adapted from ref. [36]

current interactions still take effect, this is due to the fact that they too are renormalised. However, close to the simultaneous transition the mixed phase is suppressed in this instance as well.

We analysed the system close to the simultaneous transition, where the RG equations reduced to a coupled set of BKT equations, eqs. (3.68) and (3.69). The individual channel ‘energy’ is no longer conserved due to the coupling. Both channels were found to acquire a negative energy correction when starting in the conducting phase, as well as initially in the insulating phase. This negative energy correction causes the (cc)–phase to shrink with respect to the uncoupled version, and to destroy the mixed (ic)– and (ci)–phases in agreement with the numerics.

Chapter 4

Conclusions

In this thesis we have given an overview of the one dimensional physics covered by Luttinger liquid theory. The scope of the Luttinger liquid to describe one dimensional systems is vast; whether we are dealing with fermions, bosons or phonons all can be described in terms of a Luttinger liquid. We showed that repulsive fermions, with Luttinger parameters $K < 1$ favour a charge density wave (CDW) quasi-order and these waves tend to pin on impurities, blocking conductivity. When dealing with continuous disorder this threshold interaction strength is pushed into the attractive fermion regime, $K < \frac{3}{2}$.

The prevailing question in this thesis was ‘how do many coupled Luttinger liquids respond to disorder’. Using the standard disorder averaging technique we arrived at a generic set of renormalisation group (RG) equations, eqs. (3.34) to (3.36), which describe a multi-channel Luttinger liquid where the interactions could be of a density-density type or, more novelly, a current-current type. We find that as well as the usual renormalisation of disorder strength, Luttinger parameters, and effective velocities, interactions of the current-current

type are also renormalised.

The RG equations were analysed with two specific models in mind. The first, covered in section 3.4.1, was the case of a Bravais lattice of identical channels. As the channels were identical, the metal-insulator transition would take place at the same Luttinger parameter in each channel. Zooming into this simultaneous transition the RG equations could be cast into a Berezinskii–Kosterlitz–Thouless (BKT) form, and solved exactly. The interactions between channels do indeed move the position of the metal-insulator transition, with density-density interactions pushing the transition to lower values of the Luttinger parameter, and current-current interactions forcing K to be higher.

The second case was of two distinct channels, which could have any physical origin. We derived explicit RG equations in terms of the original intra-channel parameters, eq. (3.51), which were analysed numerically. The numerics showed how density-density interactions expanded the phase where both channels were metallic, the (cc)–phase, and how current-current interactions shrunk this phase. They also showed how away from the boundary of the (cc)–phase the density-density interactions had minimal effect, and each channel behaves as if independent. Current-current interactions do, however, survive away from this boundary so even if one channel is firmly insulating the metal-insulator transition in the other channel will still have a shifted boundary.

Interestingly close to the simultaneous transition in both channels, the mixed (ic)– and (ci)–phases were heavily suppressed. We again zoomed into this point, this time allowing the problem to be cast as a coupled set of BKT equations. In the absence of coupling each channel has an associated conserved integral of motion, analogous with the energy of a particle in an exponential

well. The coupling destroys this integrability in each channel, leaving only a single global conserved ‘energy’ insufficient to solve the problem. We demonstrated that the coupling between channels generates a negative ‘energy’ shift in each channel, this shift favours the insulating phase. Once one channel goes insulating, the ‘energy’ shift in the other channel is enhanced, resulting in a suppression of the mixed phase. These results are presented in ref. [36].

An obvious extension to this work would be to combine the two cases considered. That is to say, rather than considering a lattice of identical sites, have a periodic array of two inequivalent channels. In this case we would have a two by two Luttinger matrix indexed by a lattice momentum \vec{q} . Examples of such a system could be a bundle of nanowires where each wire has two spin species or a situation where each channel has an electronic and a phononic degree of freedom.

Another potentially interesting path would be to consider correlated disorder, the present considerations explicitly exclude correlations between the disorder in differing channels. This is justified when thinking about disorder in, for instance, separate nanowires brought close to one another. However, if the two channels concerned were something akin spin and charge degrees of freedom it is not hard to envisage something which backscatters both charge and spin excitations.

As a final extension, one could consider different types of coupling rather than just density-density, and current-current couplings. This is definitely possible in the context of electron-phonon interactions, for instance magnetic fields couple the transverse phonons of a nano-wire to the current in the wire through the Lorentz force[2, 65]. Rather than coupling the gradient of the lat-

tice displacement to the current such a system couples the lattice displacement directly to current field. In the MLL language such a coupling would be of the form given in eq. (4.1).

$$S_{ext} = \int d\xi g_{ext} \phi_i \partial_x \phi_j \quad (4.1)$$

Such a coupling would require some sort of mass term, in the case of magnetic field coupling, this would originate from the back-reaction of the field generated by the induced current, namely the cyclotron frequency. It may be possible to generalise this to include capacitive coupling, which is a highly accessible experimental scenario in the form of carbon nanotube electro-mechanical resonators[57, 62]. Coupling the mechanical and electrical degrees of freedom of a nanotube has also proved to be highly tunable[6], if this could be combined with considerations of disorder it raises the possibility of applications in the field of nano-electronics.

Appendices

Appendix A

Jacobian

This appendix is dedicated to deriving the expression for the Jacobian used in section 2.3 when deriving the bosonised form of the Luttinger liquid action.

The action we start off with is that of the Tomonaga Luttinger model for right and left moving fermions,

$$S[\bar{\psi}, \psi, \varphi] = \sum_{\eta=R,L} [\bar{\psi}_\eta \circ i\partial_\eta \psi_\eta + \varphi_\eta \circ \bar{\psi}_\eta \psi_\eta], \quad (\text{A.1})$$

$$\partial_\eta = \partial_t + v_f \partial_x. \quad (\text{A.2})$$

The notation \circ is shorthand for integrating over the variables. Here φ_η is a bosonic field coupled to the chiral density. This bosonic field can be thought of as a density source field, which is taken to zero at the end of the calculation, or else as a Hubbard-Stratonovich field which removes the interaction term. Either way, the purpose of φ is simply to show how the density operator behaves

under the bosonisation procedure. We perform the gauge transformation:

$$\psi_\eta \rightarrow \psi_\eta^{i\theta_\eta}, \quad (\text{A.3})$$

$$\bar{\psi}_\eta \rightarrow \bar{\psi}_\eta e^{-i\theta_\eta}. \quad (\text{A.4})$$

Here θ_η are the gauge fields. The action naively transforms into

$$S[\bar{\psi}, \psi, \varphi, \theta] = \sum_\eta [\bar{\psi}_\eta \circ (i\partial_\eta - \partial_\eta \theta_\eta) \psi_\eta + \varphi \circ \bar{\psi}_\eta \psi_\eta]. \quad (\text{A.5})$$

However the partition functions must be equal after the transformation, we use this equality to solve for the Jacobian, $J[\theta]$,

$$\int \mathcal{D} [\bar{\psi}, \psi] e^{iS[\bar{\psi}, \psi, \varphi]} = \int \mathcal{D} [\bar{\psi}, \psi] J[\theta] e^{iS[\bar{\psi}, \psi, \varphi, \theta]}. \quad (\text{A.6})$$

As the integrals on both sides of the equation are perfectly Gaussian they can be readily performed. This leads to,

$$\prod_\eta \det(i\partial_\eta + \varphi_\eta) = \prod_\eta J_\eta[\theta_\eta] \det(i\partial_\eta - \partial_\eta \theta_\eta + \varphi_\eta), \quad (\text{A.7})$$

where we have decomposed the Jacobian into a product of two Jacobii, one for each chirality. We can use the identity $\log \det(M) = \text{tr} \log(M)$ to arrive at the expression:

$$J_\eta(\theta_\eta) = e^{\text{tr} \log(i\partial_\eta + \varphi_\eta) - \text{tr} \log(i\partial_\eta - \partial_\eta \theta_\eta + \varphi_\eta)} \quad (\text{A.8})$$

$$= e^{\text{tr} \log(1 + g_\eta \circ \phi_\eta) - \text{tr} \log(1 + g_\eta(\varphi_\eta - \partial_\eta))}, \quad (\text{A.9})$$

where we have introduced the Green's function defined by $i\partial_\eta g_\eta(\xi - \xi') = \delta(\xi - \xi')$. We can expand the logarithms, this is useful as this particular Green's function has the useful property that,

$$\text{tr}((g_\eta \vartheta)^n) = 0, \quad \text{if } n > 2. \quad (\text{A.10})$$

The $n = 1$ contribution is a global one, and as such is cancelled by the ionic background coming from the lattice. We therefore only need to consider the $n = 2$ terms leading to:

$$\log(J_\eta) = -i\frac{\eta}{4\pi}\partial_\eta\theta_\eta \circ \partial_x\theta_\eta + i\varphi \circ \frac{\eta}{2\pi}\partial_x\theta_\eta. \quad (\text{A.11})$$

This gives the term quadratic in the gauge fields, which is essentially the bosonic form of the Luttinger liquid action, the term linear in φ tells us how the chiral densities transform under the bosonisation procedure.

Appendix B

List of Correlations

The purpose of this appendix is to provide a list of the basic Luttinger liquid correlation functions. The correlators will be given in the Matsubara formalism, however one can analytically continue using $\tau \rightarrow it + \delta \operatorname{sgn}(t)$. The correlations of the bosonic fields are given by eqs. (B.1) to (B.3).

$$\langle \theta(q, i\omega_n) \theta(k, i\epsilon_n) \rangle = \frac{\pi v K}{\omega_n^2 + v^2 q^2} 2\pi \beta \delta_{i\omega_n, -i\epsilon_n} \delta_{k-q} \quad (\text{B.1})$$

$$\langle \phi(q, i\omega_n) \phi(k, i\epsilon_n) \rangle = \frac{\pi \frac{v}{K}}{\omega_n^2 + v^2 q^2} 2\pi \beta \delta_{i\omega_n, -i\epsilon_n} \delta_{k-q} \quad (\text{B.2})$$

$$\langle \theta(q, i\omega_n) \phi(k, i\epsilon_n) \rangle = - \frac{\pi \frac{i\omega_n}{q}}{\omega_n^2 + v^2 q^2} 2\pi \beta \delta_{i\omega_n, -i\epsilon_n} \delta_{k-q} \quad (\text{B.3})$$

As the fermionic fields are related to the bosonic fields via an exponential, $\psi \sim e^{i\theta}$, we often need the average of the exponential of the field. For fields averaged with respect to a Gaussian action there is a tremendously useful identity given by eq. (B.4) which is derived using Wick's theorem.

$$\langle e^{i(\theta_i - \theta_j)} \rangle = e^{-\frac{1}{2} \langle (\theta_i - \theta_j)^2 \rangle} \quad (\text{B.4})$$

Hence it is useful to have the following to hand.

$$\langle (\theta(x, \tau) - \theta(0, 0))^2 \rangle = \frac{1}{\beta} \sum_{i\omega_n} \int \frac{dq}{2\pi} (2 - 2 \cos(xq + \tau\omega_n)) \frac{\pi v K}{\omega_n^2 + v^2 q^2} \quad (\text{B.5})$$

$$= 2\pi v K \int \frac{dq}{2\pi} \left[\frac{2f_B(vq)(1 - \cos(qx) \cosh(\tau vq))}{2vq} + \frac{1 - \cos(qx)e^{-|\tau|vq}}{2vq} \right] \quad (\text{B.6})$$

$$= K \int_0^\infty dq e^{-\alpha q} \left[\frac{2f_B(vq)(1 - \cos(qx) \cosh(\tau vq))}{q} + \frac{1 - \cos(qx)e^{-|\tau|vq}}{q} \right] \quad (\text{B.7})$$

$$= \frac{K}{2} \log \left(\frac{\beta^2 v^2}{\pi^2 \alpha^2} \left(\sinh^2 \left(\frac{\pi x}{\beta v} \right) + \sin^2 \left(\frac{\pi \tau}{\beta} \right) \right) \right) \quad (\text{B.8})$$

$$\stackrel{T \rightarrow 0}{=} \frac{K}{2} \log \left(\frac{x^2 + (v|\tau| + \alpha)^2}{\alpha^2} \right) \quad (\text{B.9})$$

Where we introduced the ultraviolet cut-off $\alpha \ll \sqrt{x^2 + v^2 \tau^2}$. The corresponding ϕ correlation can be obtained by the usual $K \rightarrow \frac{1}{K}$. The mixed correlator is given by:

$$\langle \theta(x, \tau) \phi(0, 0) \rangle = - \frac{i}{2} \int_0^\infty \frac{dq}{q} e^{-\alpha q} [\sin(qx \operatorname{sgn}(\tau)) e^{-vq|\tau|} - 2f_B(vq) \sin(qx \operatorname{sgn}(\tau)) \sinh(vq|\tau|)] \quad (\text{B.10})$$

$$= -i \arg \left(\frac{\beta v}{\pi} \left(\tan \left(\frac{\pi(v|\tau| + \alpha)}{\beta v} \right) + i \tanh \left(\frac{\pi x}{\beta v} \right) \right) \right) \quad (\text{B.11})$$

$$\stackrel{T \rightarrow 0}{=} - \frac{i}{2} \arg(\alpha \operatorname{sgn}(\tau) + v\tau + ix) \quad (\text{B.12})$$

$$\stackrel{T \rightarrow 0}{=} - \frac{1}{2} \log \left(\frac{(\alpha \operatorname{sgn}(\tau) + v\tau) + ix}{\sqrt{(\alpha + v|\tau|)^2 + x^2}} \right) \quad (\text{B.13})$$

Bibliography

- [1] A. A. Abrikosov, L. P. Gorkov, I. E. Dzyaloshinski, and R. A. Silverman. *Methods of Quantum Field Theory in Statistical Physics*. Dover Books on Physics. Dover Publications, 2012. ISBN 9780486140155. URL <http://books.google.co.uk/books?id=JYTCAgAAQBAJ>. 5, 8, 53
- [2] K.-H. Ahn and H. Yi. Elementary excitations in one-dimensional electromechanical systems; transport with back-reaction. *Europhysics Letters (EPL)*, 67(4):641–647, aug 2004. ISSN 0295-5075. doi: 10.1209/epl/i2004-10106-9. URL <http://iopscience.iop.org/article/10.1209/epl/i2004-10106-9><http://stacks.iop.org/0295-5075/67/i=4/a=641?key=crossref.f998c3cb4148743901c4bb854f9be9c1>. 99
- [3] A. Altland and B. Simons. *Condensed Matter Field Theory*. Cambridge University Press, 2006. ISBN 9780521845083. URL <http://books.google.co.uk/books?id=0KMkfAMe3JkC>. 5
- [4] J. Bardeen, L. N. Cooper, and J. R. Schrieffer. Theory of Superconductivity. *Physical Review*, 108(5):1175–1204, dec 1957. ISSN 0031-899X. doi: 10.1103/PhysRev.108.1175. URL <https://link.aps.org/doi/10.1103/PhysRev.108.1175>. 61

- [5] J. Bardeen, L. N. Cooper, and J. R. Schrieffer. Microscopic Theory of Superconductivity. *Physical Review*, 106(1):162–164, apr 1957. ISSN 0031-899X. doi: 10.1103/PhysRev.106.162. URL <https://link.aps.org/doi/10.1103/PhysRev.106.162>. 61
- [6] a. Benyamini, a. Hamo, S. V. Kusminskiy, F. V. Oppen, S. Ilani, F. von Oppen, E.-p. Coupling, and S. Ilani. Real-space tailoring of the electron–phonon coupling in ultraclean nanotube mechanical resonators. *Nature Physics*, 10(2):151–156, 2014. ISSN 1745-2473. doi: 10.1038/nphys2842. URL <http://www.nature.com/doi/10.1038/nphys2842>. 100
- [7] D. Bernard, E. A. Kim, and A. Leclair. Edge states for topological insulators in two dimensions and their Luttinger-like liquids. *Physical Review B - Condensed Matter and Materials Physics*, 86(20), 2012. ISSN 10980121. doi: 10.1103/PhysRevB.86.205116. URL <https://journals.aps.org/prb/pdf/10.1103/PhysRevB.86.205116>. 59
- [8] B. A. Bernevig, T. L. Hughes, and S.-C. Zhang. Quantum spin Hall effect and topological phase transition in HgTe quantum wells. *Science (New York, N.Y.)*, 314(5806):1757–61, dec 2006. ISSN 1095-9203. doi: 10.1126/science.1133734. URL <http://www.ncbi.nlm.nih.gov/pubmed/17170299><http://arxiv.org/abs/cond-mat/0611399><http://dx.doi.org/10.1126/science.1133734><http://www.sciencemag.org/cgi/doi/10.1126/science.1133734>. 3
- [9] I. Bloch, J. Dalibard, and W. Zwerger. Many-body physics with ultracold gases. *Reviews of Modern Physics*, 80(3):885–964, jul 2008.

ISSN 0034-6861. doi: 10.1103/RevModPhys.80.885. URL <https://journals.aps.org/rmp/pdf/10.1103/RevModPhys.80.885><https://link.aps.org/doi/10.1103/RevModPhys.80.885><http://arxiv.org/abs/0704.3011><http://dx.doi.org/10.1103/RevModPhys.80.885>.
2

[10] M. Bockrath, D. H. Cobden, J. Lu, A. G. Rinzler, R. E. Smalley, L. Balents, and P. L. McEuen. Luttinger-liquid behaviour in carbon nanotubes. *Nature*, 397(6720):4–7, 1999. 2

[11] S. T. Carr. STRONG CORRELATION EFFECTS IN SINGLE-WALL CARBON NANOTUBES. *International Journal of Modern Physics B*, 22(30):5235–5260, dec 2008. ISSN 0217-9792. doi: 10.1142/S0217979208049455. URL <http://www.worldscientific.com/doi/abs/10.1142/S0217979208049455>. 2

[12] L. N. Cooper. Bound Electron Pairs in a Degenerate Fermi Gas. *Physical Review*, 104(4):1189–1190, nov 1956. ISSN 0031-899X. doi: 10.1103/PhysRev.104.1189. URL <https://link.aps.org/doi/10.1103/PhysRev.104.1189>. 61

[13] P. Courteille, R. S. Freeland, D. J. Heinzen, F. A. van Abeelen, and B. J. Verhaar. Observation of a Feshbach Resonance in Cold Atom Scattering. *Physical Review Letters*, 81(1):69–72, jul 1998. ISSN 0031-9007. doi: 10.1103/PhysRevLett.81.69. URL <https://journals.aps.org/prl/pdf/10.1103/PhysRevLett.81.69><https://link.aps.org/doi/10.1103/PhysRevLett.81.69>. 2

- [14] F. Crépin, G. Zaránd, and P. Simon. Disordered one-dimensional bose-fermi mixtures: the Bose-Fermi glass. *Physical review letters*, 105(11):115301, sep 2010. ISSN 1079-7114. doi: 10.1103/PhysRevLett.105.115301. URL <http://dx.doi.org/10.1103/PhysRevLett.105.115301>. 72
- [15] F. Crépin, G. Zaránd, and P. Simon. Mixtures of ultracold atoms in one-dimensional disordered potentials. *Physical Review A*, 85(2):023625, feb 2012. ISSN 1050-2947. doi: 10.1103/PhysRevA.85.023625. URL <http://link.aps.org/doi/10.1103/PhysRevA.85.023625>. 72
- [16] V. Fleurov, V. Kagalovsky, I. V. Lerner, and I. V. Yurkevich. Instability of sliding Luttinger liquid. nov 2017. URL <http://arxiv.org/abs/1711.01639>. 68
- [17] A. Galda, I. V. Yurkevich, and I. V. Lerner. Effect of electron-phonon coupling on transmission through Luttinger liquid hybridized with resonant level. *EPL (Europhysics Letters)*, 17009(1):6, jan 2010. ISSN 0295-5075. doi: 10.1209/0295-5075/93/17009. URL <http://arxiv.org/abs/1011.3934><http://stacks.iop.org/0295-5075/93/i=1/a=17009>. 19, 53
- [18] A. Galda, I. V. Yurkevich, and I. V. Lerner. Impurity scattering in a Luttinger liquid with electron-phonon coupling. *Physical Review B*, 83(4):041106, jan 2011. ISSN 1098-0121. doi: 10.1103/PhysRevB.83.041106. URL <http://link.aps.org/doi/10.1103/PhysRevB.83.041106>. 19, 53
- [19] A. Galda, I. V. Yurkevich, and I. V. Lerner. Impurity scattering in a Luttinger liquid with electron-phonon coupling. *Physical Review B*, 83(4):041106, jan 2011. ISSN 1098-0121. doi:

- 10.1103/PhysRevB.83.041106. URL <http://arxiv.org/abs/1008.3270><http://link.aps.org/doi/10.1103/PhysRevB.83.041106><http://iopscience.iop.org/1742-6596/286/1/012049>. 53, 61
- [20] T. Giamarchi. *Quantum Physics in One Dimension*. International Series of Monographs on Physics. Clarendon Press, 2003. ISBN 9780198525004. URL <http://books.google.co.uk/books?id=0CGVxiyUZYC>. 11, 12, 18, 27, 30, 39
- [21] T. Giamarchi. One-dimensional physics in the 21st century. *Comptes Rendus Physique*, 17(3-4):322–331, mar 2016. ISSN 16310705. doi: 10.1016/j.crhy.2015.11.009. URL https://ac.els-cdn.com/S1631070515002261/1-s2.0-S1631070515002261-main.pdf?{}_tid=2517eece-a35b-11e7-8795-00000aacb361{&}acdnat=1506499932{ }528e982da6130b57e944b9e75ef9e2ee<http://linkinghub.elsevier.com/retrieve/pii/S1631070515002261>. 2
- [22] T. Giamarchi and H. J. Schulz. Anderson localization and interactions in one-dimensional metals. *Physical Review B*, 37(1):325–340, jan 1988. ISSN 0163-1829. doi: 10.1103/PhysRevB.37.325. URL <http://link.aps.org/doi/10.1103/PhysRevB.37.325>. 31, 48
- [23] M. Greiner, O. Mandel, T. Esslinger, T. W. Hänsch, and I. Bloch. Quantum phase transition from a superfluid to a Mott insulator in a gas of ultracold atoms. *Nature*, 415(6867):39–44, jan 2002. ISSN 00280836. doi: 10.1038/415039a. URL <https://www.nature.com/nature/journal/v415/n6867/pdf/415039a.pdf><http://www.nature.com/doifinder/10.1038/415039a>. 2

- [24] A. Grishin, I. V. Yurkevich, and I. V. Lerner. Functional integral bosonization for an impurity in a Luttinger liquid. *Physical Review B - Condensed Matter and Materials Physics*, 69(16):1–7, 2004. ISSN 01631829. doi: 10.1103/PhysRevB.69.165108. 19
- [25] K. Günter, T. Stöferle, H. Moritz, M. Köhl, and T. Esslinger. Bose-Fermi Mixtures in a Three-Dimensional Optical Lattice. *Physical Review Letters*, 96(18):180402, may 2006. ISSN 0031-9007. doi: 10.1103/PhysRevLett.96.180402. URL <https://link.aps.org/doi/10.1103/PhysRevLett.96.180402>. 52
- [26] D. B. Gutman, Y. Gefen, and a. D. Mirlin. Bosonization of one-dimensional fermions out of equilibrium. *Phys. Rev. B*, 81(8):85436, feb 2010. doi: 10.1103/PhysRevB.81.085436. URL <http://link.aps.org/doi/10.1103/PhysRevB.81.085436><http://arxiv.org/abs/0911.4559>. 19
- [27] F. D. M. Haldane. Coupling between charge and spin degrees of freedom in the one-dimensional Fermi gas with backscattering. *Journal of Physics C: Solid State Physics*, 12(22):4791, nov 1979. ISSN 0022-3719. doi: 10.1088/0022-3719/12/22/020. URL <http://stacks.iop.org/0022-3719/12/i=22/a=020?key=crossref.55609ca5545b39b809bec1f25b779834><http://iopscience.iop.org/0022-3719/12/22/020>{%}5Cnpapers3://publication/doi/10.1088/0022-3719/12/22/020. 18
- [28] F. D. M. Haldane. Effective harmonic-Fluid approach to low-energy properties of one-dimensional quantum fluids. *Physical Review Letters*, 47(25):

- 1840–1843, dec 1981. ISSN 00319007. doi: 10.1103/PhysRevLett.47.1840.
URL <http://link.aps.org/doi/10.1103/PhysRevLett.47.1840>. 8, 18
- [29] F. D. M. Haldane. 'Luttinger liquid theory' of one-dimensional quantum fluids. I. Properties of the Luttinger model and their extension to the general 1D interacting spinless Fermi gas. *Journal of Physics C: Solid State Physics*, 14(19):2585–2609, jul 1981. ISSN 0022-3719. doi: 10.1088/0022-3719/14/19/010. URL <http://stacks.iop.org/0022-3719/14/i=19/a=010?key=crossref.da6c355b9e483430f11a2dd5c2d10eb4>. 18
- [30] M. Z. Hasan and C. L. Kane. Topological Insulators. *Physics*, 82(4):23, 2010. ISSN 0034-6861. doi: 10.1103/RevModPhys.82.3045. URL <http://arxiv.org/abs/1002.3895>. 3
- [31] S. Inouye, M. R. Andrews, J. Stenger, H.-J. Miesner, D. M. Stamper-Kurn, and W. Ketterle. Observation of Feshbach resonances in a Bose–Einstein condensate. *Nature*, 392(6672):151–154, mar 1998. ISSN 0028-0836. doi: 10.1038/32354. URL http://rleweb.mit.edu/cua/_pub/ketterle/_group/Projects_1998/Pubs_98/inou98.pdf
<http://www.nature.com/doifinder/10.1038/32354>. 2
- [32] H. Ishii, H. Kataura, and H. Shiozawa. Direct observation of Tomonaga – Luttinger-liquid state in carbon nanotubes at low temperatures. *Nature*, 426(December):1–5, 2003. doi: 10.1038/nature02199. Published. 2
- [33] D. Jerome. Organic Superconductors: A Survey of Low Dimensional Phenomena. *Molecular Crystals and Liquid Crystals*, 79(1):511–538, jan

1982. ISSN 0026-8941. doi: 10.1080/00268948208070997. URL <http://www.tandfonline.com/doi/abs/10.1080/00268948208070997>. 2
- [34] D. Jérôme. Organic conductors: from charge density wave TTF-TCNQ to superconducting (TMTSF)₂PF₆. *Chemical reviews*, 104(11):5565–92, nov 2004. ISSN 0009-2665. doi: 10.1021/cr030652g. URL <http://pubs.acs.org/doi/abs/10.1021/cr030652g><http://www.ncbi.nlm.nih.gov/pubmed/15535660>. 2
- [35] D. Jérôme, A. Mazaud, M. Ribault, and K. Bechgaard. Superconductivity in a synthetic organic conductor (TMTSF)₂PF₆. *Journal de Physique Lettres*, 41(4):95–98, feb 1980. ISSN 0302-072X. doi: 10.1051/jphyslet:0198000410409500. URL <http://www.edpsciences.org/10.1051/jphyslet:0198000410409500>. 2
- [36] M. Jones, I. V. Lerner, and I. V. Yurkevich. Berezinskii-Kosterlitz-Thouless transition in disordered multichannel Luttinger liquids. *Physical Review B*, 96(17):174210, sep 2017. ISSN 2469-9950. doi: 10.1103/PhysRevB.96.174210. URL <https://link.aps.org/doi/10.1103/PhysRevB.96.174210>. 4, 47, 51, 64, 68, 72, 92, 93, 94, 99
- [37] V. Kagalovsky, I. V. Lerner, and I. V. Yurkevich. Local impurity in a multichannel Luttinger liquid. *Physical Review B*, 95(20):205122, may 2017. ISSN 2469-9950. doi: 10.1103/PhysRevB.95.205122. URL <http://dx.doi.org/10.1103/PhysRevB.95.205122>. 51, 56, 57
- [38] A. Kamenev. *Field Theory of Non-Equilibrium Systems*. Cambridge Uni-

- versity Press, 2011. ISBN 9781139500296. URL <http://books.google.co.uk/books?id=CwlrUepnla4C>. 5, 19
- [39] C. L. Kane and M. P. A. Fisher. Transport in a one-channel Luttinger liquid. *Physical Review Letters*, 68(8):1220–1223, feb 1992. ISSN 0031-9007. doi: 10.1103/PhysRevLett.68.1220. URL <http://link.aps.org/doi/10.1103/PhysRevLett.68.1220>. 31, 33, 48
- [40] C. L. Kane and M. P. A. Fisher. Edge-State Transport. In *Perspectives in Quantum Hall Effects*, pages 109–159. Wiley-VCH Verlag GmbH, Weinheim, Germany, 1997. ISBN 9783527617258. doi: 10.1002/9783527617258.ch4. URL <http://doi.wiley.com/10.1002/9783527617258.ch4>. 59
- [41] C. L. Kane and E. J. Mele. Quantum Spin hall effect in graphene. *Physical Review Letters*, 95(22), 2005. ISSN 00319007. 3
- [42] L. V. Keldysh. Diagram technique for nonequilibrium processes. *Jetp*, 20(5):1080, 1964. ISSN 0393-697X. doi: 10.1007/BF02724324. URL http://www.jetp.ac.ru/cgi-bin/dn/e{}_020{}_04{}_1018.pdf. 19
- [43] P. Kopietz. *Bosonization of Interacting Fermions in Arbitrary Dimensions*, volume 48 of *Lecture Notes in Physics Monographs*. Springer Berlin Heidelberg, Berlin, Heidelberg, 1997. ISBN 978-3-540-62720-3. doi: 10.1007/978-3-540-68495-4. URL <http://link.springer.com/10.1007/978-3-540-68495-4>. 20
- [44] J. M. Kosterlitz. The critical properties of the two-dimensional xy model. *Journal of Physics C: Solid State Physics*, 7(6):1046–1060, mar 1974. ISSN 0022-3719. doi: 10.1088/0022-3719/7/6/005. URL

<http://iopscience.iop.org/article/10.1088/0022-3719/7/6/005/meta><http://stacks.iop.org/0022-3719/7/i=6/a=005><http://stacks.iop.org/0022-3719/7/i=6/a=005?key=crossref>.
bc07cf0ade9b842a8c6626e279e39a20. 44

- [45] J. M. Kosterlitz and D. J. Thouless. Ordering, metastability and phase transitions in two-dimensional systems. *Journal of Physics C: Solid State Physics*, 6(7):1181–1203, apr 1973. ISSN 0022-3719. doi: 10.1088/0022-3719/6/7/010. URL <http://stacks.iop.org/0022-3719/6/i=7/a=010?key=crossref.f2d443370878b9288c142e398ad429b1>. 44
- [46] L. D. Landau. The Theory of a Fermi Liquid. *Soviet Phys. JETP*, 3(6): 920, 1957. ISSN 0038-5646. doi: 10.1016/B978-0-08-010586-4.50095-X. URL <http://www.jetp.ac.ru/files/Landau1en.pdf><http://scholar.google.com/scholar?hl=en&btnG=Search&q=intitle:The+theory+of+a+fermi+liquid{#}0.6>
- [47] L. D. Landau. Oscillations in a Fermi Liquid. *Soviet Phys. JETP*, 5(1):101, 1957. ISSN 0038-5646. doi: 10.1016/B978-0-08-010586-4.50096-1. URL <http://www.jetp.ac.ru/files/Landau2en.pdf><http://www.jetp.ac.ru/cgi-bin/e/index/e/5/1/p101?a=list>. 6
- [48] L. D. Landau. ON THE THEORY OF THE FERMI LIQUID. *Soviet Phys. JETP*, 35(35):97–103, 1959. URL http://www.jetp.ac.ru/cgi-bin/dn/e/_008_{_}01_{_}0070.pdf. 6
- [49] L. D. Landau, E. M. Lifshitz, L. P. Pitaevskii, J. B. Sykes, and M. J.

- Kearsley. *Statistical physics. Part 1*. Elsevier Butterworth Heinemann, 1980. ISBN 9780080570464. 11
- [50] K. Le Hur. Coulomb Blockade of a Noisy Metallic Box: A Realization of Bose-Fermi Kondo Models. *Physical Review Letters*, 92(19):196804, may 2004. ISSN 0031-9007. doi: 10.1103/PhysRevLett.92.196804. URL <https://link.aps.org/doi/10.1103/PhysRevLett.92.196804>. 46
- [51] I. V. Lerner and I. V. Yurkevich. Impurity in the Tomonaga-Luttinger model: a Functional Integral Approach. *eprint arXiv:cond-mat/0508223*, 81(C):109–127, aug 2005. ISSN 09248099. doi: 10.1016/S0924-8099(05)80043-5. 19
- [52] J. M. Luttinger. An Exactly Soluble Model of a Many-Fermion System. *Journal of Mathematical Physics*, 4(9):1154–1162, sep 1963. ISSN 0022-2488. doi: 10.1063/1.1704046. URL <http://aip.scitation.org/doi/10.1063/1.1704046>. 16
- [53] G. D. Mahan. *Many-Particle Physics*. Physics of Solids and Liquids. Springer, 2000. ISBN 9780306463389. URL <http://books.google.co.uk/books?id=xzSgZ4-yyMEC>. 5, 8, 9, 53
- [54] D. C. Mattis and E. H. Lieb. Exact Solution of a Many-Fermion System and Its Associated Boson Field. *Journal of Mathematical Physics*, 6(2):304–312, 1965. ISSN 00222488. doi: <http://dx.doi.org/10.1063/1.1704281>. URL <http://scitation.aip.org/content/aip/journal/jmp/6/2/10.1063/1.1704281>. 16
- [55] P. Phillips. Anderson Localization and the Exceptions. *Annual Review of*

- Physical Chemistry*, 44(1):115–144, oct 1993. ISSN 0066-426X. doi: 10.1146/annurev.pc.44.100193.000555. URL <http://www.annualreviews.org/doi/10.1146/annurev.pc.44.100193.000555>. 31
- [56] R. A. Santos, C. W. Huang, Y. Gefen, and D. B. Gutman. Fractional topological insulators: From sliding Luttinger liquids to Chern-Simons theory. *Physical Review B - Condensed Matter and Materials Physics*, 91(20), 2015. ISSN 1550235X. doi: 10.1103/PhysRevB.91.205141. URL <https://journals.aps.org/prb/pdf/10.1103/PhysRevB.91.205141>. 59
- [57] V. Sazonova, Y. Yaish, H. Ustünel, D. Roundy, T. A. Arias, and P. L. McEuen. A tunable carbon nanotube electromechanical oscillator. *Nature*, 431(7006):284–7, sep 2004. ISSN 1476-4687. doi: 10.1038/nature02905. URL <http://dx.doi.org/10.1038/nature02905>. 100
- [58] F. Schreck, L. Khaykovich, K. L. Corwin, G. Ferrari, T. Bourdel, J. Cubizolles, and C. Salomon. Quasipure Bose-Einstein Condensate Immersed in a Fermi Sea. *Physical Review Letters*, 87(8):080403, aug 2001. ISSN 0031-9007. doi: 10.1103/PhysRevLett.87.080403. URL <https://link.aps.org/doi/10.1103/PhysRevLett.87.080403>. 52
- [59] A. Schwartz, M. Dressel, G. Grüner, V. Vescoli, L. Degiorgi, and T. Giamarchi. On-chain electrodynamic of metallic (TMTSF)₂X salts: Observation of Tomonaga-Luttinger liquid response. *Physical Review B*, 58(3):1261–1271, jul 1998. ISSN 0163-1829. doi: 10.1103/PhysRevB.58.1261. URL <https://link.aps.org/doi/10.1103/PhysRevB.58.1261>. 2
- [60] D. J. Thouless. Anderson’s theory of localized states. *Journal of Physics*

- C: Solid State Physics*, 3(7):1559–1566, jul 1970. ISSN 0022-3719. doi: 10.1088/0022-3719/3/7/012. URL <http://stacks.iop.org/0022-3719/3/i=7/a=012?key=crossref.b1c1664938c4bab8ba04c851efae92e5>. 31
- [61] S.-i. Tomonaga. Remarks on Bloch’s Method of Sound Waves applied to Many-Fermion Problems. *Progress of Theoretical Physics*, 5(4): 544–569, apr 1951. ISSN 0033-068X. doi: 10.1143/PTP.5.544. URL <https://academic.oup.com/ptp/article-lookup/doi/10.1143/ptp/5.4.544><http://ptp.oxfordjournals.org/content/5/4/544>. [shorthhttp://ptp.ipap.jp/link?PTP/5/544/](http://ptp.ipap.jp/link?PTP/5/544/). 15
- [62] H. Ustünel, D. Roundy, and T. a. Arias. Modeling a suspended nanotube oscillator. *Nano letters*, 5(3):523–526, 2005. ISSN 1530-6984. doi: 10.1021/nl0481371. URL <http://www.ncbi.nlm.nih.gov/pubmed/15755107>. 100
- [63] J. von Delft and H. Schoeller. Bosonization for beginners - refermionization for experts. *Annalen der Physik*, 7(4):225–305, nov 1998. ISSN 00033804. doi: 10.1002/(SICI)1521-3889(199811)7:4<225::AID-ANDP225>3.0.CO;2-L. URL <http://doi.wiley.com/10.1002/{%}28SICI{%}291521-3889{%}28199811{%}297{%}3A4{%}3C225{%}3A{%}3AAID-ANDP225.0.CO{%}3B2-L>. 18
- [64] G. Wentzel. The interaction of lattice vibrations with electrons in a metal [7], jul 1951. ISSN 0031899X. URL <http://link.aps.org/doi/10.1103/PhysRev.83.168>. 59
- [65] H. Yi and K.-H. Ahn. Dynamical electron transport through a nano-

electromechanical wire in a magnetic field. *The European Physical Journal B*, 76(2):283–287, jun 2010. ISSN 1434-6028. doi: 10.1140/epjb/e2010-00187-1. URL <http://www.springerlink.com/index/10.1140/epjb/e2010-00187-1>. 99

- [66] I. Yurkevich. Bosonisation as the Hubbard-Stratonovich Transformation. *eprint arXiv:cond-mat/0112270*, 0(5):1–8, dec 2001. URL <http://arxiv.org/abs/cond-mat/0112270>. 19